



UNIVERSITY OF THE PELOPONNESE
Ourania Kordali
(R.N. 1012201502014)

DIPLOMA THESIS:
A Study of Corrosion Patterns in Ancient Glass

SUPERVISING COMMITTEE:

- Assoc. Prof. N. Zacharias
- Dr. A. Lagoyiannis

EXAMINATION COMMITTEE:

- Assoc. Prof. N. Zacharias
- Dr. A. Lagoyiannis
- Assoc. Prof. E.Zimi

KALAMATA, SEPTEMBER 2016

“Because they had only a few precious stones
(our afflicted empire was extremely poor)
they wore artificial ones: numerous pieces of glass,
red, green, or blue. I find
nothing humiliating or undignified
in those little pieces of coloured glass.”

C.P. Cavafy, *Of Colored Glass*

Acknowledgements

The corrosion mechanism of glass is an issue that is trying to be determined systematically for more than 30 years. The complex nature of the material and the variation of corrosion mechanisms have created many questions that need to be answered. The interest for the study of ancient glass objects has increased significantly in the last years. Issues about the technology, provenance and recycling of glass are still under investigation.

This master thesis could not have been written without the assistance or support of a number of other people. Associate professor and Director at the Laboratory of Archaeometry of the University of Peloponnese, Nikolaos. Zacharias has provided supervision and guidance. He inspired me during my graduate studies to take an interest on glass analysis and especially to glass corrosion.

I am thankful to Dr Anastasios Lagoyiannis, Researcher from the Institute of Nuclear and Particle Physics, National Scientific Research Center Demokritos, for his invaluable support, advice and sense of humor. He was very patient in instructing me during the experimental part of the RBS technique.

Dr. Artemios Oikonomou has provided me with tons of papers and data from his previous study at the samples.

I have been very lucky to undertake my studies in University of Peloponnese, Kalamata. The assistance of PhD candidate Eleni Palamara was very important during the SEM/EDS analysis. I also would like to thank Post Doc Researcher George Provatas from Tandem Accelerator Laboratory NSRC Demokritos, for his patience and assistance during the RBS technique.

And to my sister, Anna, who has morally supported me during my graduation studies, I am forever grateful.

Contents

| | |
|---|----|
| 1. Abstract..... | 8 |
| 2. Introduction..... | 9 |
| 3. Theoretical Part..... | 12 |
| 3.1. The Nature of Glass | 12 |
| 3.1.1. Raw Materials and Main Compounds..... | 13 |
| 3.2. Glass Coloration and Opacification | 15 |
| 3.3. Technology Production and Decoration of Glass | 15 |
| 3.3.1. Beads..... | 15 |
| 3.3.2. Core Formed Vessels | 20 |
| 3.4. Corrosion of Glass | 21 |
| 3.5. Archaeological and Historic Background and the Material Studied..... | 24 |
| 3.5.1. The Region..... | 24 |
| 3.5.2. The Material Studied..... | 26 |
| 4. Methods..... | 27 |
| 4.1. Scanning Electron Microscopy / Energy-Dispersive X-Ray Spectroscopy (SEM/EDS)..... | 27 |
| 4.2. Ion Beam Analytical Techniques (RBS)..... | 28 |
| Depth Profiling using RBS | 29 |
| 5. Experimental Part..... | 32 |
| 5.1. Introduction..... | 32 |
| 5.2. The samples | 32 |
| 5.3. Macroscopic Examination..... | 34 |
| 5.4. Microscopic Examination | 34 |
| 5.5. LED-OM Examination of the Beads..... | 35 |
| 5.6. LED-OM Examination of Core Form Vessel Fragments | 42 |
| 5.7. Surface Analysis Using SEM-EDS..... | 44 |
| Pitting and Micropitting:..... | 45 |
| Lamination and Iridescence: | 47 |
| Gel Layer Formation..... | 49 |
| Semi-Opaque Milky Effect | 51 |
| 5.8. Corrosion Depth Analysis..... | 52 |
| 5.8.1. Line Scanning measurements SEM-EDS..... | 52 |
| 5.8.2. RBS Ion Beam Analysis | 58 |
| 6. Discussion:..... | 63 |

| | |
|---|----|
| <i>Corrosion Depth Analysis</i> | 67 |
| 7. Conclusions..... | 72 |
| Bibliography | 73 |
| 8. Appendix..... | 76 |
| 8.1. The Analytical Data of the Beads | 76 |
| 8.2. The Analytical Data of The Core Formed Vessels | 79 |
| 8.3. Line Scanning Data..... | 81 |
| 8.4. Graphs of Concentration profiles by RBS | 85 |

Table of Figures

| | |
|---|----|
| Figure 3.1 The rod forming technique | 17 |
| Figure 3.2 The two ways of mould pressing technique, for the bead formation | 18 |
| Figure 3.3 The two ways of filling the mould, above with crushed glass, below by pouring molten glass | 18 |
| Figure 3.4 Techniques of bead making: (a) threading soft glass around a wire;(b) folding soft glass around a wire; (c) perforating a lump of soft glass; (d) perforating and drawing out a lump of glass; (e) fusing powdered glass in an open mould and drilling holes through the corners; (f) drilling through a cold lump of glass; (g) forming a mosaic glass bead. (Davinson, 2003) | 19 |
| Figure 3.5 Map of the ancient Boeotia | 25 |
| Figure 4.1 A simplified schematic diagram of a scanning electron microscope (Sharma, 2014) | 27 |
| Figure 4.2 The SEM/EDS equipment of Laboratory of Archaeometry, which was used in this study. Photo taken at University of Peloponnese, Kalamata, Greece. | 28 |
| Figure 4.3 schematic figure of the analytical techniques an ion beam accelerator can apply. | 29 |
| Figure 4.4 The RBS setup at NSRC Democritos | 30 |
| Figure 4.5 The special holder of the RBS | 31 |
| Figure 5.1 Different glass areas of sample T23 under x100 and x300 magnification | 45 |
| Figure 5.2 SEM images of sample T31, left the polished area right the corroded (magnification x300) | 46 |
| Figure 5.3 Lamination formation on initial stage | 47 |
| Figure 5.4 Initial iridescence phenomenon and crust formation of spongy texture | 48 |
| Figure 5.5 Top left image pristine glass area, Top right image round initial formation of hydrated silica rich layer, down left image crust formation and down right image flakes, craters and hollows at the crustation Sample T45 | 49 |
| Figure 5.6 The semi opaque milky effect ,pits, lamellae, local crust | 51 |
| Figure 5.7 Line scanning Sample Man7 Blue area | 54 |
| Figure 5.8 Line scanning Sample Man7 yellow area | 55 |
| Figure 5.9 5.10 Line scanning Sample Man7 white area | 57 |
| Figure 5.11 RBS Analysis of Sample T45, the red line represent the experimental and the blue the simulated spectrum respectively. | 59 |
| Figure 5.12 Concentration graph of sample T45 | 60 |
| Figure 5.13 SEM-BSE image of sample Man 11.Lamellae 50 μm thick at the decoration edge. | 66 |
| Figure 5.14 Micropitting and light iridescence patterns under LED-OM and SEM | 67 |
| Figure 5.15 RBS Graph of sample T2 | 68 |
| Figure 5.16 sample T16 images of SEM showing pristine and corroded areas (x 70, x 330) | 69 |
| Figure 5.17 RBS Graph showing the concentration profile of sample T16 | 70 |
| Figure 8.1Man 1 Blue area line scanning | 81 |
| Figure 8.2 Man 1 yellow area line scanning | 82 |
| Figure 8.3Man 11 blue area line scanning | 83 |
| Figure 8.4Figure 8.3Man 11 white area line scanning | 84 |
| Figure 8.5 Concentration profile for sample T1 by RBS | 85 |
| Figure 8.6 Concentration profile for sample T2 by RBS | 85 |
| Figure 8.7 Concentration profile for sample T16 by RBS | 86 |
| Figure 8.8Concentration profile for sample T45 by RBS | 86 |

Table of Tables

| | |
|--|----|
| Table 3.1.1 Compositional Characteristics related to the time period. (Freestone 1991) | 14 |
| Table 3.1.2 Mean percent concentrations and standard deviation range (Sayre and Smith, 1965) | 14 |
| Table 5.2.1 The list of the samples | 33 |
| Table 5.4.1 LED Images of samples T1 and T2 under magnification x50 and x200 | 36 |
| Table 5.4.2 LED Images of samples T16 and T45 under magnification x50 and x200. | 37 |
| Table 5.4.3 Table 5.4.1 LED Images of samples T22 and T23 under magnification x50 and x200 | 38 |
| Table 5.4.4 LED Images of samples T11 and T50 under magnification x50 and x200 | 39 |
| Table 5.4.5 LED Images of samples T31 and T34 under magnification x50 and x200 | 40 |
| Table 5.4.6 LED Images of samples T15 and T26 under magnification x50 and x200 | 41 |
| Table 5.4.7 LED Images of sample T 50 under magnification x50 and x200 | 41 |
| Table 5.7.1 The bulk analysis of the pristine glass areas from the beads and the vessels. | 44 |
| Table 5.7.2 Chemical composition of major oxides present on the pristine glass and the iridescent areas of sample T31 (determined by SEM/EDS, in wt%, normalised to 100%) | 46 |
| Table 5.7.3 Chemical composition of major oxides present on the pristine glass and the iridescent areas of sample T22 (determined by SEM/EDS, in wt%, normalised to 100%) | 48 |
| Table 5.7.4 Chemical composition of major oxides present on the pristine glass and the corroded areas of sample T 45 (determined by SEM/EDS, in wt%, normalised to 100%) | 50 |
| Table 5.7.5 Chemical composition of major oxides present on the pristine glass and the corroded areas of sample T 26 (determined by SEM/EDS, in wt%, normalised to 100%) | 52 |
| Table 5.8.1 Depth profiling, chemical compositional analysis of Sample T45. (Atomic Concentration of the oxides at %) | 60 |
| Table 5.8.2 Depth profiling, chemical compositional analysis of Sample T16. (Atomic Concentration of the oxides at %) | 61 |
| Table 5.8.3 Depth profiling, chemical compositional analysis of Sample T2. (Atomic Concentration of the oxides at %) | 61 |
| Table 5.8.4 Depth profiling, chemical compositional analysis of Sample T1. (Atomic Concentration of the oxides at %) | 62 |
| Table 6.1 The percentage loss of alkalis of the beads. The seven color groups are presented: white, light blue, blue, green, black, brown, colorless samples | 64 |
| Table 6.2 The percentage loss of alkalis of the core formed vessels. Samples Man 7, Man 1 and Man11 for blue, white and yellow colored glass areas | 65 |
| Table 6.3c Chemical composition of major oxides present on the corroded area of sample T2 (determined by SEM/EDS, in wt. %, normalized to 100%) | 68 |
| Table 6.4 Na ₂ O values determined by RBS | 69 |
| Table 6.5 Chemical composition of major oxides present on the pristine glass and the iridescent areas of sample T16 (determined by SEM/EDS, in wt. %, normalized to 100%) | 69 |
| Table 6.6 Sample T 16 Ca profile with RBS | 70 |
| Table 43.1.1 EDS compositional analysis of major elements of green glass beads. The standard deviation (σ) is presented for each sample n.d.: not determined. | 76 |
| Table 43.1.2 EDS compositional analysis of major elements of dark blue glass beads. The standard deviation (σ) is presented for each sample n.d.: not determined | 76 |
| Table 43.1.3 EDS compositional analysis of major elements of light blue glass beads. The standard deviation (σ) is presented for each sample n.d.: not determined | 77 |
| Table 43.1.4 EDS compositional analysis of major elements of colorless glass beads. The standard deviation (σ) is presented for each sample n.d.: not determined | 77 |
| Table 43.1.5 EDS compositional analysis of major elements of brown glass beads. The standard deviation (σ) is presented for each sample n.d.: not determined | 78 |

| | |
|---|----|
| Table 43.1.6 EDS compositional analysis of major elements of black glass beads. The standard deviation (σ) is presented for each sample n.d.: not determined | 78 |
| Table 43.1.7 EDS compositional analysis of major elements the white glass bead. The standard deviation (σ) is presented for each sample n.d.: not determined | 79 |
| Table 43.2.1 Table 8. EDS compositional analysis of major elements of the blue glass areas of core formed vessels.n.d. not determined | 79 |
| Table 43.2.2 Table 8. EDS compositional analysis of major elements of the yellow glass areas of core formed vessels.n.d. not determined | 79 |
| Table 43.2.3 EDS compositional analysis of major elements of the white glass areas of core formed vessels.n.d. not determined | 80 |

1. Abstract

The corrosion mechanisms of ancient glasses is a complex process. The objects which have been exposed to the burial environments, usually lack of coherency and transparency. The examination of excavated corroded glasses, often concludes to alkalis loss and the formation of different corrosion patterns on the surface.

In this study a collection of soda lime silica glasses is examined, aiming to the identification of the corrosion mechanism and its effects. The under study samples originated from the mainland Greece, Thebes. Since the composition of the examined samples have already determined this work is focusing to the different corrosion patterns which have formed.

This research has a number of objectives: determination of the morphology of the surface of leached layer in glasses with different surface finishes, examination and correlation of the decay rate in different colored glasses, analysis of the concentration profiles of highly and slightly corroded samples and investigation of the burial environment based on the corrosion evidence.

A combination of scientific analytical tools, such as SEM/EDS, LED-OM and RBS technique was used to completely characterize the corrosion mechanism. Destructive and non-destructive techniques were applied. The analytical data provided useful information about the decay rate and determined the corrosion patterns, occurred at the surfaces of the samples. Clear statements about the alkalis leaching and the surface homogeneity were resulted. Also, suggestions about the effects of different colorants at the deterioration process, have been stated.

2. Introduction

The complexity of the glass as a material had attracted many scientist the last 30 years to focus on its analysis and develop new theories about it. The Archaeometry studies until now are mostly focused on the analysis of ancient and historic glass for technology and provenance purposes. The social and economic correlation of glass and society is strong.

However, as complex is the glass nature the more complex is its corrosion mechanism. In the recent years more detailed and focused studies have been aiming to determine the deterioration process. The two factors we have to take into consideration about the glass corrosion is the chemical composition and the environment which is exposed to. Another factors influence the deterioration are the pH, the presence of water, the crafting technique of the object etc. Most of the times the factors affect the glass simultaneously and activate many different alteration processes which taking place at the outer surface but even on the inner layers of the glass.

For that reason this study has state clear questions about the corrosion mechanism and attempt to extract an answer.

Overview of the research:

The aim of this research is the identification of corrosion mechanisms of the archaeological colored glasses. A collection of glass beads, beads fragments, glass waste and core formed vessel fragments is under study. All the samples have been analyzed and determined as soda lime silica glass using natron as the main flux. The fragments originated from the same region, Thebes, in mainland Greece. Thebes was a city with significant power at the ancient world. It was in contact to different other areas and was influenced by different ancient societies. The samples are dated from Archaic to Hellenistic period, their chemical composition characterize them as soda lime silica glasses.

The usage of analytical tools SEM/EDS, LED-OM and RBS technique was used to completely characterize the corrosion mechanism

Aim of the Research:

This project attempted to answer important questions about the chemical degradation of glass. How the composition and the colorants affect the corrosion process? How the environment

affects the degradation trend? What are the differences between corrosion patterns that are formed on the outer and inner layers of the glasses?

Furthermore, the study was focused on:

- the determination of the morphology of the surface of leached layer in glasses with different surface finishes
- examination and correlation of the decay rate in different colored glasses,
- analysis of the concentration profiles of highly and slightly corroded samples and investigation of the burial environment based on the corrosion evidence

Methodology of the Research:

The stages of this study are presented below.

- a) A macroscopic examination for the selection of the beads Through macroscopic examination
- b) The photographic documentation of the selected samples
- c) Initial characterization of the preservation state.
- d) Microscopic examination and documentation using LED_OM
- e) Microtopography examination and identification of the different corrosion patterns formed at the surface.
- f) Composition analysis of bulk and weathered samples.
- g) Comparison of the alkalis percentage loss
- h) Line scanning and RBS application for the analysis of corrosion depth profile.
- i) Discussion of the results and comparison between them

Structure:

The main body of the text can be divided into three parts.

- The first part includes Chapters 3 and 4 provides a background to both the material which is studied but also for the analytical techniques which have been applied. Chapter 2 includes the theoretical background for the nature of glass, historic context of the material, the production techniques of the analyzed samples and the theoretical part of the corrosion mechanisms. Chapter 4 refers to the analytical tools which have been used and their main function

- The Chapter 5 includes the experimental part of the study. The analytical data are presented accomplished to an initial commendation of the results.
- The third and last part of the study includes the discussion and conclusions. At the Chapter 6 the data are explained in comparison to results from the literature search. Diagrams and graphs are also showed to support or to un-justify the initial hypothesis. The final Chapter of conclusions summarizes the results and statements of discussion Chapter.

3. Theoretical Part

3.1. The Nature of Glass

Glass is a non-crystalline amorphous solid, often transparent and has widespread practical and technological usage. The characterization of glass as an amorphous solid refers to the absence of widespread class (long range order) or periodicity of the individual components (Doremus, 1994). However, despite the absence of a strict, periodic structure which distinguishes it from a crystalline solid, glass has a well-defined local structure. It consists of silica, alkali metal oxides and lime. The alkali metal oxides can be soda, potash, or in some cases both (Davinson, 2003). It is formed from a melt by cooling to rigidity without crystallization.

Glasses can be distinguished into two main categories; the *natural glasses* and the *man-made glasses* or *technical glasses*. Natural glasses have been used since prehistoric times, before even man developed the expertise of glass making. Their usage as weapons or tools begun in about 3000 BC (Davinson, 2003). One of the most well-known natural glasses is *obsidian*, which is formed by rapidly cooling of lava. Other natural glasses are the *tektites* and the *fulgurites*, which have meteoritic origin and are formed by light striking to sandy areas respectively.

Technical glasses can be categorized in four products: *glass*, *glaze*, *enamel* and *faience* (also called Egyptian). Glass, glaze and enamel always contain large quantities of soda oxides (Na_2O) or another alkali metal oxide, such as potash (K_2O), and sometimes both. Faience contains only quite small amounts of alkali metal oxide. Silicate glass is formed from silica, lime and metal oxides that have been heated and melted to give a homogenous structure. Chemically, glass, glaze and enamel can all be identical in composition, the fundamental difference being their method of use in antiquity. Glaze was applied as a coating before or in some cases after firing to make the object impermeable (Davinson, 2003). Faience was composed from fritted (frit is a fused and granulated ceramic composition) silica with water addition as the bonding agent. The formation of faience was shaped exclusively with bear hands (Davinson, 2003).

Glass is described as having a complex network, silica is the network former and the network modifiers were usually added to reduce the melting temperature. Silica (Si), the network former, forms SiO_4 tetrahedra, but not all of the molecules' corners are filled, so the empty space is filled with the network modifiers.

3.1.1. Raw Materials and Main Compounds

Natural materials like rocks and minerals were used for glass production. Silica, alkalis and lime were mixed, heated and melted to about 1000C°-900C° in order to form glass. However, the ancient recipes include only two ingredients. The main compounds of glass are:

Silica

Silica is the main component of glass; its main source were sand, pebbles and flints. Sand was prepared by sifting, washing, heating and grinding (Ignatiadou & Antonaras, 2008) and pebbles were collected, grounded and mixed with plant ash. Impurities differ, depending on where the sand was collected from. Egyptian sand, for example, has low percentage of iron (Fe), so the objects did not have the greenish effect than others manufactured by sand of different provenance (Henderson, 2000).

Alkalis:

- a) ***Sodium Oxide (Na₂O)*** -a network modifier- was added to glass through natron and plant ash; their usage was to reduce the melting point. Natron was collected from dried and evaporated lakes, in crystal form. Plants like seaweeds and saltmarsh were burned and their ashes were added to the glass mixture.
- b) ***Potassium Oxide (K₂O)***, which was also reducing the melting point during manufacturing process, was found in forest plant ashes.

Lime:

In the ancient world, ***soda-lime-silica glass*** was used for the longest period (Henderson, 2000). The addition of too much alkalis resulted in a more soluble glass, calcium oxide was added and worked as a network stabilizer. It was introduced to the glass through shells, when the raw material was beach sand (Pliny, N.H. XXXVI) or by adding dolomite sandstone. The raw material that was used for the glass manufacture is associated with impurities at the ancient glasses. For example, dolomite was a source of magnesium oxide (MgO) and calcium oxide (CaO). (Lambert, 1997)

Depending on the period and the area, the minor elements from the impurities are different. However, it had to be taken into consideration that the dominant recipes remain the

same. The broad compositional characteristics with the main components related to the time period are shown in Table 3.1.1 Compositional Characteristics related to the time period. (Freestone 1991). (Freestone, 1991)

Table 3.1.1 Compositional Characteristics related to the time period. (Freestone 1991)

| | Egyptian 15th century BC | Roman 1st century AD | European 13th century AD | Syrian 14th century AD |
|--|--|---------------------------------|-------------------------------------|--|
| Silica, SiO₂ (wt. %) | 65 | 68 | 53 | 70 |
| Soda, Na₂O (wt. %) | 20 | 16 | 3 | 12 |
| Potash, K₂O (wt. %) | 2 | 0.5 | 17 | 2 |
| Lime, CaO (wt. %) | 4 | 8 | 12 | 10 |
| Magnesia, MgO (wt. %) | 4 | 0.5 | 7 | 3 |
| Alkalis and Silica source | Plant ash/ Quartz | Natron/ Sand | Wood Ash Sand/Quartz | Plant ash/ Sand/Quartz |

Sayre and Smith investigated the variation of the oxides, trace elements, and associated the mean concentration with the chronological period they appeared. This categorization is presented in Table 3.1.2. (Sayre & Smith, 1965)

Table 3.1.2 Mean percent concentrations and standard deviation range (Sayre and Smith, 1965)

| Glass group | Magnesium MgO | Potassium K₂O | Manganese MnO | Antimony Sb₂O₅ | Lead PbO |
|---|--------------------------|-------------------------------------|--------------------------|---|---------------------|
| Second millennium B.C.(1500- 700B.C) | 4.6-2.9 | 1.89-0.69 | 0.046-0.021 | 0.32-0.011 | 0.048-0.0010 |
| Antimony-rich (600- 400 B.C) | 1.24-0.60 | 0.47-0.17 | 0.035-0.014 | 1.93-0.53 | 0.077-0.0047 |
| Roman (400- 900A.D.) | 1.47-0.73 | 0.63-0.22 | 1.60-0.10 | 0.089-0.018 | 0.057-0.0033 |
| Early Islamic (800-1000 A.D) | 6.5-3.6 | 2.2-0.94 | 1.07-0.21 | 0.035-0.012 | 0.047-0.0016 |
| Islamic lead | 0.47-0.24 | 0.051-0.013 | 0.031-0.016 | 0.19-0.035 | 40-33 |

3.2. Glass Coloration and Opacification

Other compounds that were also inserted to the glass are the *colorants*. The coloration process can be associated with the absorption bands of the added elements, the chemical reactions inside the glass and the condition inside the furnace. The colorants that are added to the glass mixture can be minerals, oxides or an already colored glass object.

Some of the most important colorants are **Copper (Cu)**, **Iron (Fe)**, **Cobalt (Co)** and **Manganese (Mn)**. The oxides are usually dissolved in small quantities inside the glass and result in a vivid coloration. Cobalt oxides have a deep dark blue effect only in 0.1% quantity (Brill, 1992). Copper oxides can give glass a blue, green, orange and light red color. Iron oxides result in a red, yellow-brown coloration and manganese oxides are used for pink purple, brown or even black coloration.

As it was mentioned above, the sand that was used, many times contained impurities like iron oxides, which gave the glass a greenish hue. For that reason, glassmakers used *decolorizers*. The most common decolorizers were **Antimony (Sb)** and **Manganese (Mn)** oxides.

However, **Antimony (Sb)** and **Lead (Pb)** were also used as glass *opacifiers*, their addition making the glass to lose its transparency. It was caused by crystals inclusions inside the glass matrix which have reflective properties (Vogel, 1994). Opacifiers could also color the glass; for example the combination of antimony and lead could give a yellow untransparent glass, or antimony and calcium could result in a white opacified glass. Opacification could also be achieved by low melting temperatures, which create air bubbles inside the glass body (Stern & Schlick-Nolte, 1994).

3.3. Technology Production and Decoration of Glass

3.3.1. Beads

One of the initial forms of man-made glass objects are the glass beads. They have a lengthwise perforation for stringing on a chain. Glass beads were manufactured by various techniques. They could be mould pressed, cast, drawn and ('wire') wound. Beads were considered to be a valuable trade commodity in Neolithic societies. This probably occurred due to the fact that beads have a small size and are very durable objects, so their transportation and usage was widespread.

Beads were primarily used for personal adornment. They were also used for religious purposes and as a way to reflect the status of the wearer. In Egypt, for example, they were an important indicator of palatial affiliations. Tutankhamen's tomb was found to contain thousands of polychrome and monochrome beads of various materials. The objects were sewed on collars, bracelets, necklaces and even in a pair of sandals. The usage of the beads in this case was both for adornment and as a social status indicator (Lucas & Harris, 1962). In the Greek region, beads that were found in the Mycenaean tombs, were used as jewelry in male but mostly in female tombs. Examining the wall paintings in the Aegean, there are depictions of beads on necklaces, earrings and as hair accessories. (Ingram, 2005).

Furthermore, the religious character of beads was signified through their usage as amulets. In Egypt and around the Mediterranean, varieties of eye shaped beads have been found. The usage of the eye as a shape was a way to protect the wearer of the "bad eye" (bad luck), even nowadays.

3.3.1.1. Production Technology of the Beads:

The production process of the beads include many different techniques, the most significant as hereinafter described. The most common technique is the ***rod forming / winding technique***; in this technique, a mass of hot molten glass is continuously pulled and heated to form a bead around a metal rod (known as a mandrel) (Ignatiadou & Antonaras, 2008). The temperature of the heated glass was approximately 800- 1050 C°. The edge of the metal rod was frequently cone shaped, in order to facilitate the technician to remove the glass bead. A layer of calcite or clay, was often applied at the edge for the mandrel, making the detachment of the bead safer. Finally, the technician placed the object at a cooling place. (Henderson, 2000)

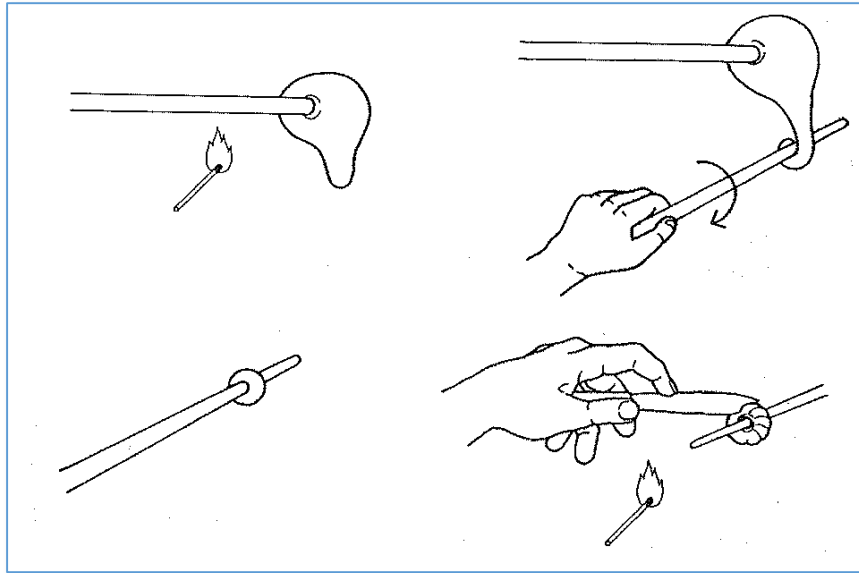


Figure 3.1 The rod forming technique

Some beads are also formed and decorated using the *drawing technique*. This technique and the winding technique are similar processes. The glassmaker used a mandrel to draw glass out of a viscous pool, in which the molten mass was attached. Then, long canes of glass were formed, using a second rod for continuous pulling and simultaneous heating. The canes were cut lengthwise into pieces of the desired size, and finally polished to yield the beads. Drawing was also applied as a decoration procedure.

Another technique that has been practiced, mostly in Mycenaean glass production, is the *mould pressing* technique. A blank of heated glass was pushed into a mould and formed in a hexagonal, square or biconical (with flat ends) shaped bead. According to Küçükerman, the formation of the beads using a mould can be distinguished in different techniques. A heated glass mass can be folded and pressed into the cast or two different heated glass layers can be pressed along the cast. (Kiiciikerman, 1995). The two techniques are shown in Figure 3.2 The two ways of mould pressing technique, for the bead formation..

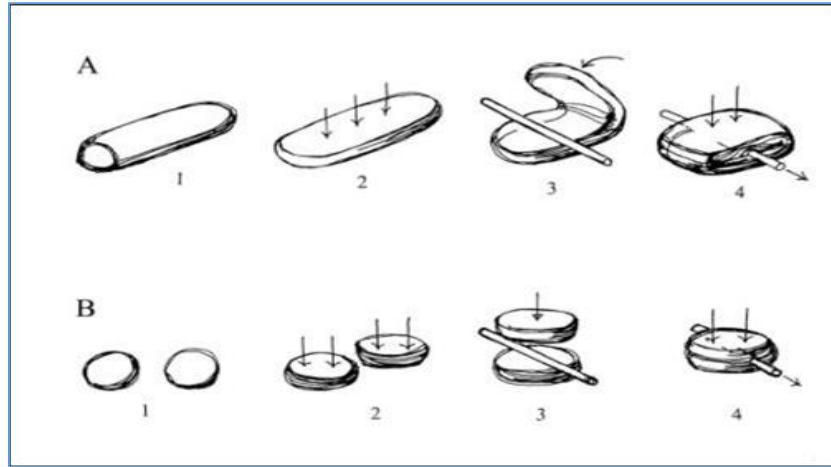


Figure 3.2 The two ways of mould pressing technique, for the bead formation

Glass beads could be *cast* as well. A mould is also used in this technique, so the results often appear similar to those of mould pressing technique. The casting technique can be achieved in two ways; by filling a mould with crushed glass and heating in a furnace until the fusion is completed, or by pouring molten glass into a mould. (See Figure 3.3)

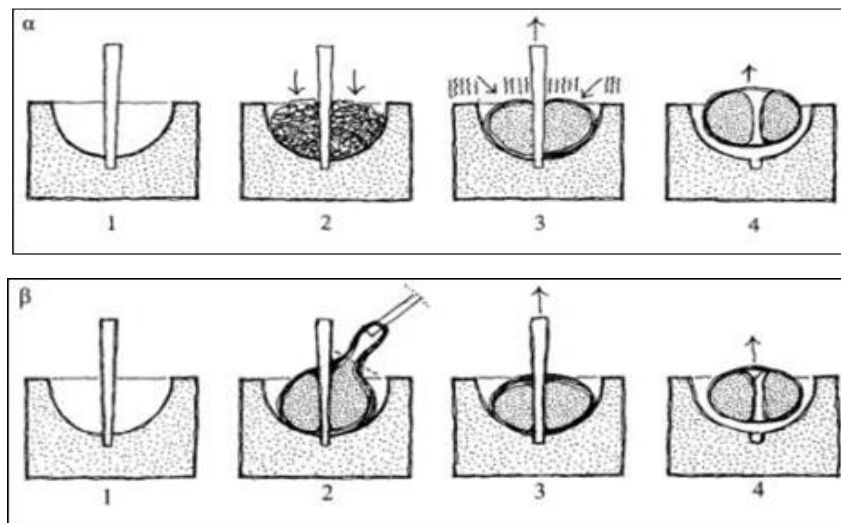


Figure 3.3 The two ways of filling the mould, above with crushed glass, below by pouring molten glass

To summarize, the methods that were commonly applied in glass bead production are the following: i) rod forming / winding, ii) drawing, iii) mould pressing and iv) casting technique (which were mentioned above). Other methods that were applied are: v) **folding** the glass around a core, vi) **perforating** with a mandril, and vii) **blowing** and drilling through solid glass. In figure some of the methods are shown. (Davinson, 2003).

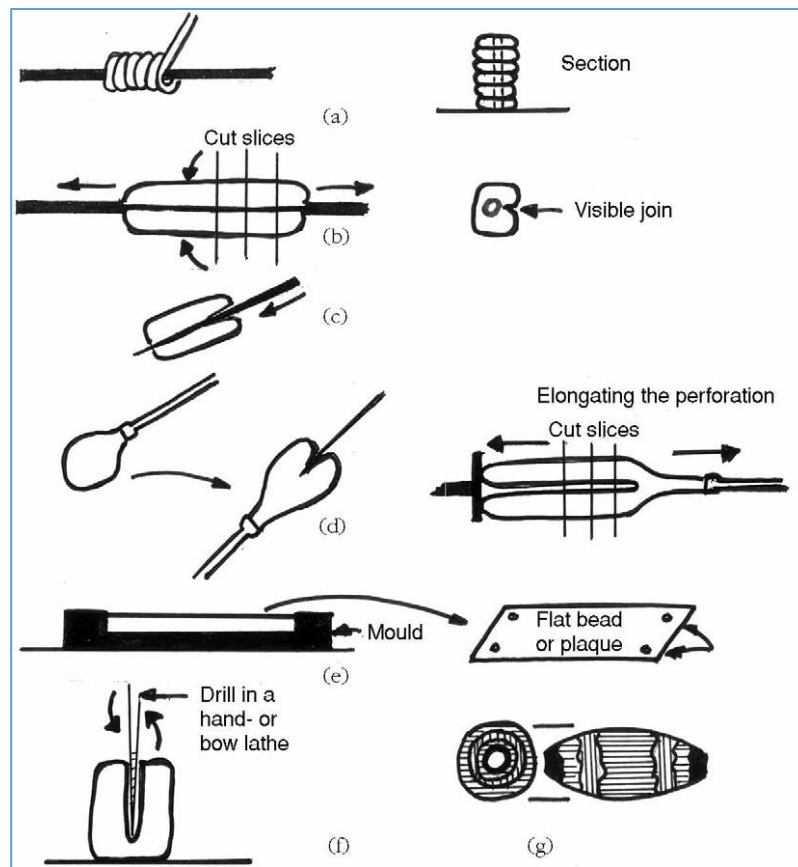


Figure 3.4 Techniques of bead making: (a) threading soft glass around a wire; (b) folding soft glass around a wire; (c) perforating a lump of soft glass; (d) perforating and drawing out a lump of glass; (e) fusing powdered glass in an open mould and drilling holes through the corners; (f) drilling through a cold lump of glass; (g) forming a mosaic glass bead. (Davinson, 2003)

3.3.1.2. Decoration techniques of the beads:

The beads can be found in a variety of shapes but mostly are round, cylindrical and disk shaped. Motifs of rosettes, ivy and spirals were relief patterns at the beads surface. Colored canes and threads were used to create decorative patterns such as stripes, spots, circles, zig-zags, chevrons and eye beads. The same manufacturing techniques as well as a combination of them were applied by the glassworkers to achieve these patterns.

Shapes and relief patterns were formed by the glass makers at the hot processing when beads were wound, drawn or fold formed or by giving the mould the demanded shape. Some relief patterns were achieved by tooling the soft glass. (Davinson, 2003)

A common combination of techniques that was used for the production of colorful beads is the drawing- folding method. Using the drawing technique, colored glass threads from different colored pieces are created and melted as one glass piece. The multicolored glass eventually melted and folded, providing a colorful bead, decorated with draws and circles. (Triantafyllidis, 1998) Another method for decoration was by rolling the initial bead in a semi molten different colored glass or dipping it in a viscous pool. A blowtorch was probably used as an auxiliary tool for a more detailed result. (Lierke, 1992)

3.3.2. Core Formed Vessels

Core forming technique appeared in Mesopotamia (modern day Iraq and a part of Syria), 3500 years before, and a little bit later in Egypt. At the end of the Archaic period, a great development of the core form vessels production occurred in the Greek region. This method continued to be applied throughout the Hellenistic period, but was extinct since the mouth blowing glass appeared.

Core form production in Greece was similar to the Late Bronze Age method in Egypt, although they had some differences. (Kontou, et al., 1995) .The local production's vessels were inspired by the attic pottery and, as a result, glass miniatures like alabastron, aryballos, amphorisk and oinochoe were produced. Their size was not very large (about 7 and 12 cm in height), and they were used as cosmetics containers like oils, perfumes and ointments.

3.3.2.1. *Production Technology of the Vessels*

The initial stage of the core form process was the creation of the core. The glass maker prepared a core, mixture of clay, sand and plant material (possibly by dung) and attached it to a metal rod. The function of the core was to form the cavity on the inside of the vessels. After the attachment the core was dried, so it could maintain its shape. Using the rod as a handle, the core was either dipped in a crucible of molten glass or wound with threads of molten glass and marvered (rolled in a flat surface) on a flat stone surface. Another theory about the formation of the body was that the glassmaker applied crushed glass on the core and simultaneously heated it. This theory though has not been proved yet (Stern & Schlick-Nolte, 1994).

A thread or threads of different colored glass were wound around the glass body in a spiral shape, embedded to create the decoration and marvered again. Then mouth, foot and handles

were formed and the vessel cooled down in an annealing oven. During the final stage, the rod was removed from the core and scraped out, creating the cavity inside the vessel.

Most of the core formed vessels display decoration of zig-zags, swags and trails. The most common colors that were used are yellow and white decoration on blue glass body. Monochrome objects manufactured with this technique were found but are very rare. (the author at this chapter used as literature source the Corning Museum videos of Core Formed Vessel Production). (Corning Museum of Glass, n.d.)

3.4. Corrosion of Glass

Although glass is considered to be a very durable material, the corrosion process is unavoidable (Ζαχαριάς & Οικονόμου, 2010). The two primary factors we have to take into consideration about glass corrosion, is the chemical composition of the artifact and the environment in which is exposed (Davison 2003).

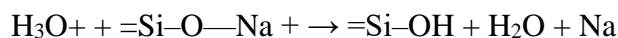
Composition

The microstructure of glasses can be described as a complex network having silica as the network former and sodium, potassium and calcium as the network modifiers. The network modifiers were usually added to reduce the melting temperature. The dissolution of alkalis depends on the amount of silica present in the glass f ; the higher amount the more stable the glass is. Studies have shown that below 66mol% silica (SiO_2), the glass is more vulnerable to corrosion process. This happens because at this percentage every silicon atom is associated with an alkali ion. The addition of sodium and potassium breaks the bonds between silica and oxygen so it helps reducing the melting temperature, but also affects the stability of the glass. On the other hand, the addition of calcium increases the durability of the material. Calcium present around 10% w.t. contributes in binding the alkali into the glass matrix. However, if the amount of calcium is higher than 15mol%, it leads to a silica-rich layer on the surface. The existence of small quantities of aluminum or phosphorus block the leaching process, immobilize the alkali ions and lead to a more stable glass (Jackson, et al., 2012).

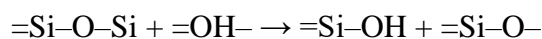
Environment

The amount of water in the environment that the glass is exposed to is very crucial for the deterioration. Two major processes occur due to this factor; the de-alkalization (leaching

process) and the network dissolution. The negatively charged alkali and metal cations are free to move around within the glass network, from one space to another. In a wet environment, they are extracted from the glass by water, to form a sodium or potassium hydroxide solution. Since the electrical neutrality of the glass must be maintained, hydronium ions (H_3O^+) from the water exchange positively charged hydrogen ions (protons) for the alkali ions leaching from the glass network. This process results in a hydrated silica-rich surface layer, sometimes referred to as a gel layer (Davinson, 2003).



The water of the attacking solution will usually be either slightly acidic or alkaline depending on the soil or the atmospheric conditions. Under alkaline conditions, the oxygen bridges of the glass network itself may be broken down and the silica dissolved. This reaction is strongly pH dependent. The rate of alkali leaching from glass in a buffered system at a pH of less than 9 is constant and independent of pH.



The temperature of the reaction can also affect the type of reaction and the rate. Again, this depends upon the pH of the substrate and the composition of the initial glass. In alkali solutions and at warmer temperatures, more silica is lost in a glass that contains potash and low calcium, so the glass is depleted in alkali and silica. In acidic solutions, the glass will lose alkali but much of the silica will remain.

Dulling

Dulling is one of the simplest effects; it describes the condition of glass which has lost its original clarity and transparency. It can occur due to the presence of scratches, abrasion or stains. The affected object stops being transparent. (Davinson, 2003)

Iridescence

Iridescence describes the multiple layers of glass that appear on the surface of the objects. The layers give a colorful appearance at the surface caused by the light interference and the metal oxides concentration they contain. The colors observed at the surface are usually vivid iridescent like purple, gold and pink. If the iridescence is extended, formation of thick layers

appear which flakes away. At the final stage of the phenomenon the complete collapse of the object may happen.

Milky or enamel-like surfaces

In this kind of corrosion milky or enamel like spots appear on the surface. They appear as opaque white, light brown or mottled brownish- black deterioration products. This kind of spots appear first on the surface and approximately penetrate inside the matrix. In some cases the spots flake away as crystals and leave pits in the glass. Often these patches remain at the surface and form layers. The thickness, the color and the development of these layers depends on the progress of the corrosion. Due to leaching process the concentration of sodium or potassium values at the surface may occur low but the concentration of the oxides (iron, manganese, antimony), may be enriched. (Davinson, 2003)

Spontaneous cracking

As mentioned before, glass has the tendency to form a highly hydrated surface layer. This layer undergoes dehydration and shrinkage due to the temperature and humidity variations leading to a cracking net on the surface of the object. The cracks may penetrate deeper and allow moist or other deterioration factors pass in the glass. Often slight scratches on the surface subsequently lead to the formation of bigger and deeper cracking network due to this effect. The development of the fractures that formed reach the surface and break a small fragment of the object. (Davinson, 2003)

Pitting

Small holes can occur at the surface of the glass. These pits can be categorized in four groups depending on their size; 0,2 mm, 0,5- 2 mm, 2- 4mm and above 4mm. These pits appear on the surface of the glass when a corrosion layer is lost. They have round shape because of the water droplets that weathered the glass at the specific area. This corrosion effect isn't fully explained yet. (Davinson, 2003)

Mn- Browning

Due to leaching affect, Mn oxides create black- brown stains in the glass. This phenomenon doesn't occur on the surface of the glass but it develops between the leached layers.

The oxygen through the leaching process oxidizes the magnesium traces of the glass and forms dendritic stains between the corroded layers. These stains are usually brown opaque and affect the glass' transparency. The formation of the stains starts from the inner to the outer layers and occupies the lamellar voids that have been formed. (Schalm, et al., 2011)

Discoloration

Glass objects that have been buried may have a blackened layer on the surface. The coloring ions, like iron, manganese or copper, leach out of the glass and are oxidized. This phenomenon alters the color of the crust that is formed on the object's surface. The change of color depends on the kind of the ion that is oxidized. Iron and manganese ions cause a darkening effect to crusts, black or dark brown, but copper ions cause green colored stains. (Schalm, et al., 2011)

Bio corrosion

Microorganisms do not affect the glass directly. They cannot get fed from the glass itself. Although when they appear in high humidity environments they tend to develop near the buried objects. The areas near the microorganisms occur to have extensive corrosion, due the humidity these organisms deposit. Some organisms even exude NH_3 , which affects positively the deterioration process. (Davinson, 2003)

3.5. Archaeological and Historic Background and the Material Studied

3.5.1. The Region

Thebes is located in the central mainland of Greece and belongs to Boeotia prefecture, Greece. In the ancient times Boeotia had a significant role since it was in a strategic position at the Gulf of Corinth. Ancient Boeotia boundaries did not have important differences to modern boundaries. In the north, it bordered with Opuntian Locris - though in ancient times it included a small region of Locris – in the south with Megaris and in southeast with Attica. The western side bordered with Phocis and had its coastline across the Gulf of Korinth and northeast across the Gulf of Euboea (see Figure 3.5) Thebes nowadays is the largest city of the county even if it is not the capital.



Figure 3.5 Map of the ancient Boeotia

The human activity at the area is dated since palaeolithic period until the end of antiquity. Settlements and excavated potteries testify the usage of the area in the Neolithic period. In the Early Bronze Age (3200/3000- 2000 BC) two of the most important cities at the ancient times, Thebes (south Boeotia) and Orchomenos (northwest Boeotia), were established. Interactions of the natives with citizens of Evvoia and Cyclades developed through the seaways. Around 2100/2000-1600BC production of Minyan pottery and cemeteries filled with gold offerings, evidence the development of the county. (Οικονόμου, 2012)

During the Middle Hellenic period Thebes accomplished to be the most important city of Boeotia. A great palace was built at the citadel of Kadmia, symbol of wealth and power. Also cemeteries of that period were found in the surrounding hills, as well. Around the 13th century, the city probably was destroyed. Excavations at the palace remains, showing that the damage was likely caused by an invasion. Since 12th century BC until the end of Geometric period the region was abandoned and lacks any archaeological remains. In the Archaic period, the whole Boeotia and especially Thebes faced economic and cultural growth. The Temple of Ismenian Apollo was build and the tombs of cemeteries, are loaded with pottery, figurines and jewelry. (Οικονόμου, 2012)

During the Persian Wars, Thebes and other Boeotian cities, except Plataeis and Thespians, allied to Persians. After the Greek victory Thebes got punished for its betrayal and its influence got limited. It even lost its leadership at the Boeotian Federation. In these dark times, Pindaros, a

remarkable ancient Theban poet, got recognized. Thebes tried many times to make a comeback to its previous power and succeeded in it after the end of Peloponnesian War, when Athenians were defeated by Spartans. This did not last long, as Sparta, former ally of Thebes, conquered the city on 382 BC and demolished the Boeotian Federation. Finally, in 371 BC, Thebes managed to win the crucial battle at Leuctra and regained its former prestige and power.

In the second half of 4th century BC Macedonians headed by Philip the 2nd, arrived from the north and expanded to Boeotia. Thebes was destroyed by Alexander the Great on 336 BC, when Thebans rioted after Philip's death. The city was rebuilt by Cassandros, a Macedonian king, at the end of 4th century BC and conquered in the 3rd century BC by Demetrius the Conqueror.

Finally, Thebes enters to Roman Empire in 197BC and the decadence of the city started. Romans destroyed many monuments and continued the desecration of the city until the end of Roman period. Boeotia and Thebes collapsed completely during the Goths' invasions in the end of 3rd and 4th century A.D. (Οικονόμου, 2012)

3.5.2. The Material Studied

The collection of glass artifacts, studied in this work, consists of colored glass beads and fragments of core-formed vessels. The beads were found in ancient burial sets, discovered during the construction overpass under railways in the road axis of Thebes-Mourikio. They are dated from Archaic to Hellenistic period (7th-2nd century B.C.), according to archaeological notes. The fragments of the vessels were excavated from an archaeological site in the city of Thebes and dated from Classical period (5th century B.C.).

4. Methods

4.1. Scanning Electron Microscopy / Energy-Dispersive X-Ray Spectroscopy (SEM/EDS)

A Scanning Electron Microscopy (SEM) provides information about the morphology and topography of solid surfaces. It is a microscopic technique which has a resolution better than an optical microscope. It uses a beam of high energy electrons which impinge at the examined area. The magnification of SEM ranging from 100 to 100,000 times, depending on the sample. A schematic figure of a SEM is shown in Figure 4.1.

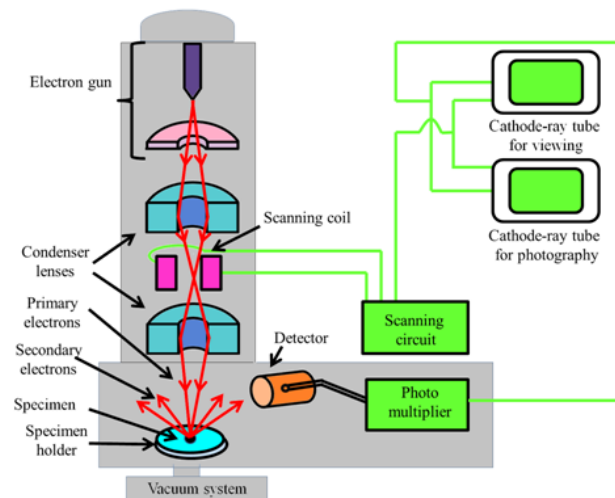


Figure 4.1 A simplified schematic diagram of a scanning electron microscope (Sharma, 2014)

In SEM, a scanning of the surface using highly focused electron beam, is taking place. The electron that is scattered from the sample gives an indication about the morphology of the surface. The scanning of the surface is repeated until the desired area of the surface is examined. The obtained signal of the backscattered and secondary electrons is converted to an image. The whole device is enclosed by a vacuum chamber. (Λυριτζής, 2007)

The SEM is coupled to an Energy-Dispersive X-ray Spectroscopy it is an analytical tool that is used for the elemental analysis of the examined sample. The interaction between the source of the X- ray excitation and the sample is translated to a spectrum where the characteristic peaks of the elements are determined. In Figure 4.2 the equipment that was used for the study is shown.

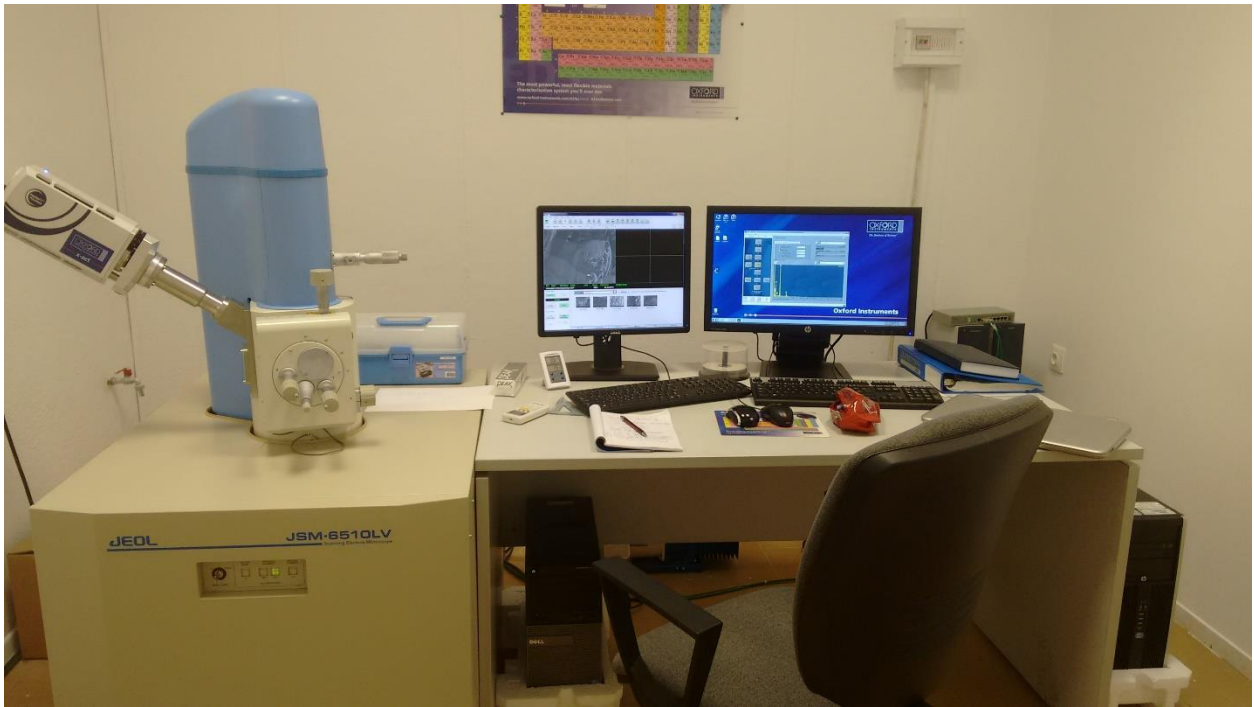


Figure 4.2 The SEM/EDS equipment of Laboratory of Archaeometry, which was used in this study. Photo taken at University of Peloponnese, Kalamata, Greece.

4.2. Ion Beam Analytical Techniques (RBS)

When an ion having a kinetic energy of the order of a few hundred keVs up to a few MeVs interacts with matter, it gradually loses energy by interacting mainly with the electrons of the target, but it can also interact (with a much lower probability) at the atomic or nuclear level with the target nuclei as well. The result of such interactions is the emission of characteristic radiation and/or light charged particles, which can – in principle – provide valuable information about the absolute concentration, as well as, depth distribution of the target nuclei. IBA techniques are in principle least destructive techniques, however, certain modifications to the samples can occur due to the so-called ‘beam effect’. Since a high-energy ion beam is bombarding the sample surface during the measurement, a considerable heat transfer occurs. Means of conducting the bombarded samples are considered, moreover the current is kept at the minimum acceptable level.

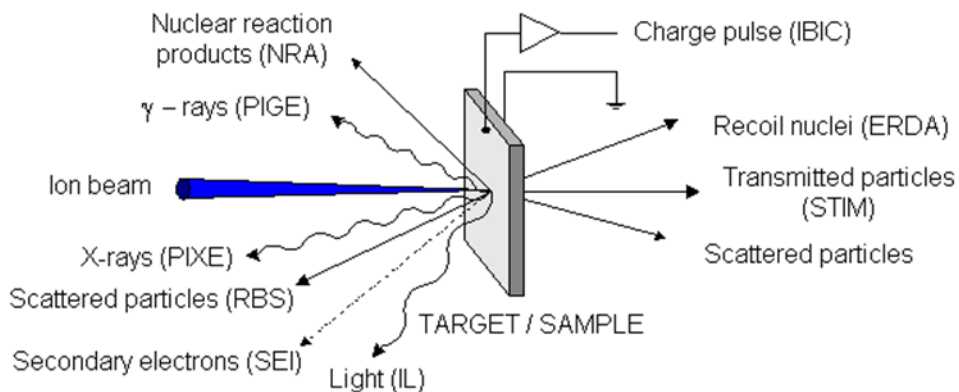


Figure 4.3 schematic figure of the analytical techniques an ion beam accelerator can apply.

In IBA analytical techniques the interactions of energetic ions with matter can permit off-line analysis of light elements in solids. Some of the most common applied techniques are:

- **PIXE** – Particle Induced X-ray Emission – using characteristic x-rays from atomic interactions.
- **PIGE** – Particle Induced Gamma-ray Emission- using γ -rays from nuclear reactions.
- **NRA** – Nuclear Reaction Analysis- using emitted light charged particles.
- **RBS-** (Rutherford Backscattering Spectroscopy) – use of elastic scattered particles at low energies.
- **EBS** – Elastic Backscattering Spectroscopy - implying non-Rutherford cross-sections, and
- **ERDA** – Elastic Recoil Detection Analysis - using the recoil target nuclei

Among IBA techniques, RBS, EBS, ERDA, PIGE (implementing strong, narrow resonances) and NRA are more commonly used for elemental depth profiling. An illustration of several typical IBA techniques is shown in Figure 4.3.

Depth Profiling using RBS

In RBS, The ions of the accelerator impinge on the material and they are back scattered. Is ideal for depth-profiling heavy elements on lighter substrates. The energy of the scattered projectile determine the mass of the target atom. The higher the Z of the matrix the higher the energy of backscattering. (Malmqvist 2004). RBS gives also depth profile of the material, the depth scale can be calculated by determining the energy loss of the incident ions before they

induce the elastic scattering and the energy loss of the scattered particles, and provide the depth profile for heavy or light elements, even for multilayered matrix. (Janssens 2014). RBS quantifies individual elements simultaneously, and can give a depth profile with a nanometer resolution.



Figure 4.4 The RBS setup at NSRC Democritos

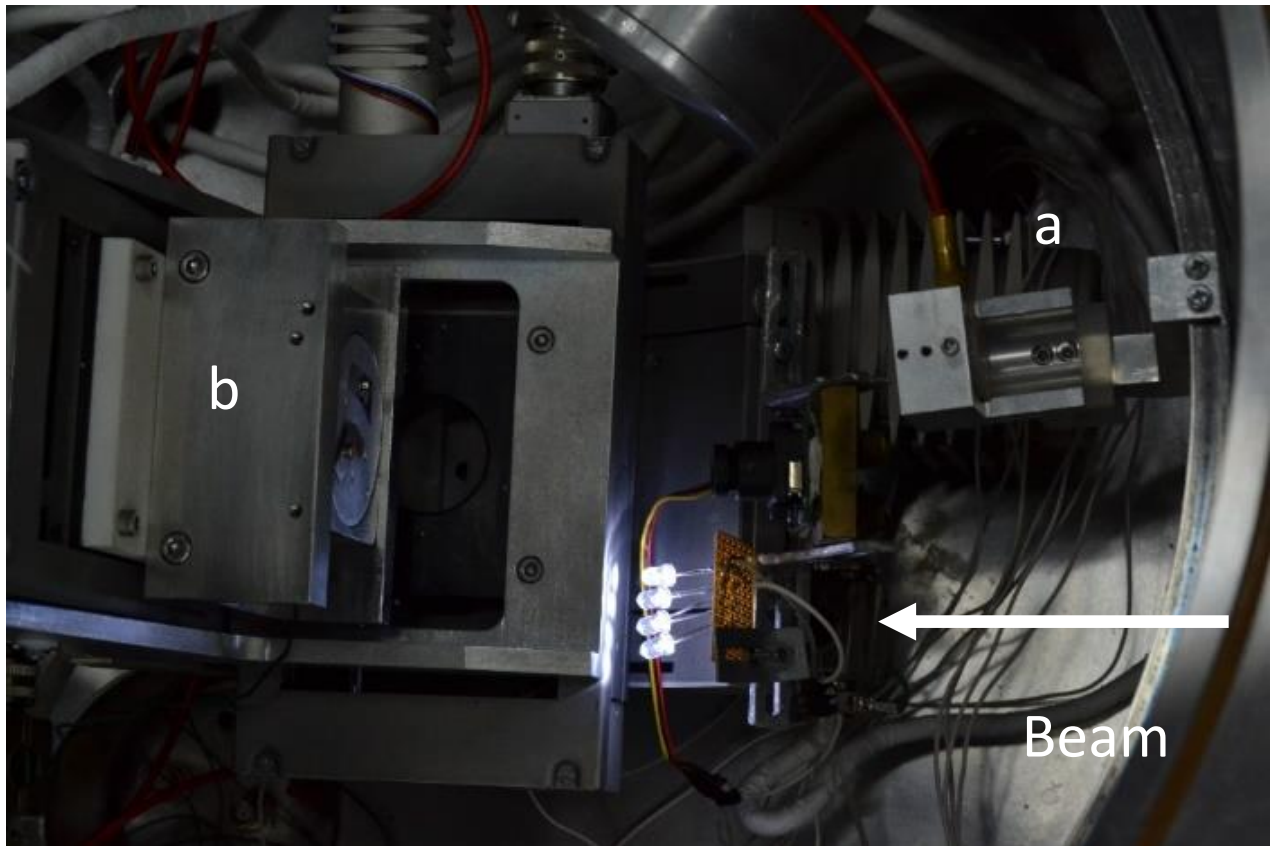


Figure 4.5 The special holder of the RBS

The RBS setup used for the measurements, at the Tandem Laboratory, is shown in Figure 4.4. The samples are mounted on a special holder (Figure 4.5 (b)), which is placed on a goniometer. The detector is positioned at backward angle with respect to the beam axis (Figure 4.5 (a)).

5. Experimental Part

5.1. Introduction

The aim of this work is the identification of corrosion mechanisms of colored glass beads and core-formed vessel fragments, originated from mainland Greece, Thebes. Although glass is considered to be a very durable material, the corrosion process is unavoidable. The two primary factors taken into consideration about glass corrosion, as it was mentioned and analyzed above, is the chemical composition of the object and the environment it was exposed to.

A combination of scientific analytical tools such as LED-OM, SEM/EDS, and Tandem Ion beam Accelerator were used to completely characterize the composition of the glass and to examine the corrosion processes. The examination of the samples was divided in two categories; the investigation of the surface modifications and the chemical characterization of the altered studied areas. The examination of the chemical composition of the collection was considered necessary, in order to compare the differences on pristine and corroded areas of the samples. Accomplished through the chemical composition analysis, an investigation of surface modifications patterns was also examined.

Finally a depth profiling examination of the corroded glass samples was carried out. The depth profiling was accomplished by line scanning at the SEM/EDS and by RBS technique using a Tandem Ion Beam Accelerator.

5.2. The samples

The collection under study consists of thirteen (13) beads and beads' fragments and three (3) fragments of core-formed vessels. The selected pieces are: two (2) fragments of blue beads, two (2) fragments of green beads, one (1) fragment and a whole (1) brown bead, two (2) fragments of black beads, , one (1) fragment and a whole of light blue bead – the whole is an eyed-bead-, two (2) fragments of transparent beads and a whole (1) white bead. Additionally the vessels samples consists of: one (1) blue body fragment with yellow and white decoration stripes, one (1) blue body fragment with yellow decoration stripes and one (1) blue body fragment with white decoration stripes.

Table 5.2.1 The list of the samples

| Sample | Coloration | Dating |
|---------------|-----------------------|-----------------------|
| T1 | Green | Archaic |
| T2 | Green | Archaic |
| T54 | White | Classical |
| T15 | Colorless | Archaic |
| T26 | Colorless Light Green | Late Archaic |
| T31 | Light Blue | Classical |
| T34 | Light Blue | Classical-Hellenistic |
| T11 | Dark Blue | Archaic |
| T50 | Dark Blue | Classical |
| T16 | Brown | Archaic |
| T45 | Brown | Hellenistic |
| T22 | Black | Archaic |
| T23 | Black | Archaic |
| Man 1 | Blue/Yellow | Hellenistic |
| Man 7 | Blue/Yellow/White | Hellenistic |
| Man 11 | Blue/ White | Hellenistic |

Sample Preparation

For the SEM analysis of the beads and bead fragments, the samples had already been polished, but not encased. So for this examination the fragments were not treated.

For the SEM analysis of the fragments, using the line scanning, sample preparation took place. The sample was cut out using a handle cutter. The samples were fastened in a plastic cast and encased with Caldo Fix- 2 Kit Resin and fixed in a heating oven for 2 hours. After that, using a polishing device 250 and different sand papers (180, 320, 800, 1200, 2000 and 4000) the resin was polished. Finally using polishing cloth MD-Dac 6µm, 3µm, 1 µm, the respective pastes DP-Paste M 6µm, 3µm, 1µm and DP Lubricant Blue, cooling and lubricating liquid the preparation was completed.

For the RBS technique the samples required no preparation. The samples that were decided to be analyzed using a Tandem Ion Beam Accelerator, were a group of heavily corroded bead fragments (brown group) and a group of slightly corroded samples (green group).

5.3. Macroscopic Examination

The collection that is studied in this work, is stored at the Laboratory of Archaeometry, University of Peloponnese, Kalamata. The initial collection that was given, consisted of twenty eight (28) glass pieces, from which the seventeen (17) were beads and bead fragments and eleven (11) were core-form vessel fragments.

Through macroscopic examination the glass samples of the beads divided in seven (7) groups based on the coloration: blue, light blue, brown, green, black, colorless-light colored and white. Since the body of the all the vessels' fragments was deep blue, they were categorized based on their decoration color in three (3) groups: yellow and white decoration, yellow decoration and white decoration.

Within the storage container iridescent dust and flaking of the altered areas was observed. The collapse of the glass corroded layers is considered to be due to a combination of dehydration of altered areas and physical stress. The deterioration degree was a determining factor for the final selection. Samples appeared, through macroscopic examination, highly corroded.

So the final examined collection consisted of thirteen (13) beads and beads' fragments and three (3) fragments of core-formed vessels. A table with additional information about the beads is shown on appendix.

During the examination and selection of the samples the photographic documentation was also carried out. A Canon EOS 600D camera, under natural light was used. A table with the photographic documentation of the samples is shown on appendix.

5.4. Microscopic Examination

A systematic examination and documentation of the decay degree of the fragments aimed to a more detailed investigation of the samples and their surface modifications. The microscopic examination carried out using a LED Optical Microscope Moritex combined to optical an Iscope computer software. The photographic documentation with LED-OM, initiated from lower x50 to

higher magnification x200. Magnification rate was depended to the interest some areas presented.

After the LED-OM examination the samples were categorized depending on their preservation state in three groups:

- Good Preservation State (cohesion on the surface, slightly corroded)
- Medium Preservation State (occurrence of corroded surface, cohesion on the surface)
- Heavily Corroded (friable samples, weathered crust flakes away)

Furthermore, microtopography examination of the surface modifications was also carried out using a Scanning Electron Microscope. For a comparative study, images from pristine glass and corroded areas were taken in order to be examined.

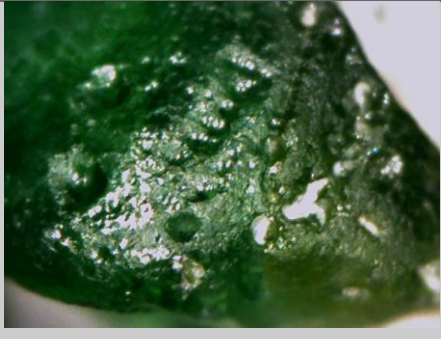

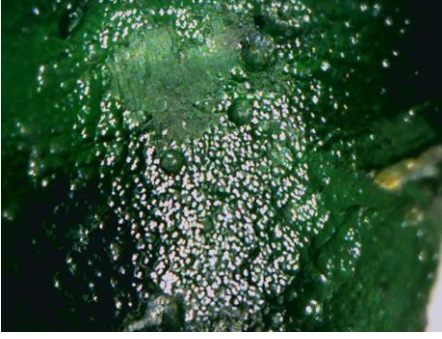

5.5. LED-OM Examination of the Beads

Green Samples

The green glass *samples T1 and T2* are dated back to the *archaic period* according to the archaeological notes. Both of the samples have extensive pitting on their surfaces. At the surface of **T1 sample** craters, pits and a linear pattern of pits is observed. The linear pattern of the pits was possibly formed upon manufacturing imperfections (lines) or caused by biocorrosion factors, which tend to create symmetric patterns at the surface. Under higher magnification (x200) the linear pattern that was observed, confirmed to be caused by technological lines than biocorrosion factors. The pits don't have the same size and are not symmetrical like those created by the microorganisms. On the **sample T2** craters and pits occur at the surface, too. The difference between the two samples is that the variation of the pitting size at sample T2 is bigger than in T1. Additionally, in sample T2, a small area of iridescence is observed. In **Error! Reference source not found.** images of the samples are shown.

A first assumption about the green samples is that except the extensive pitting both samples are in good preservation state. They do not present any color alterations on their surface or are friable. The chemical composition analysis will provide further information about the decay degree.

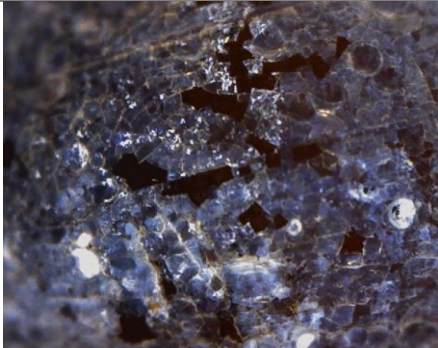
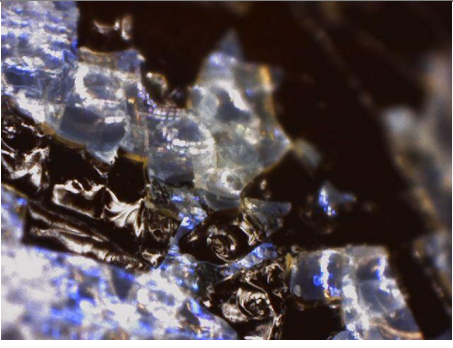
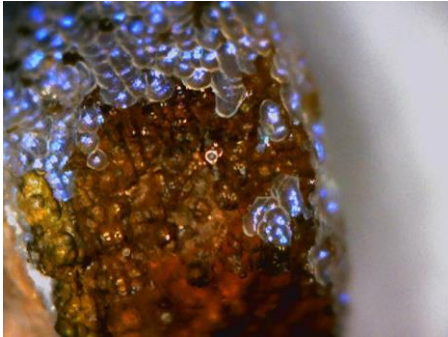
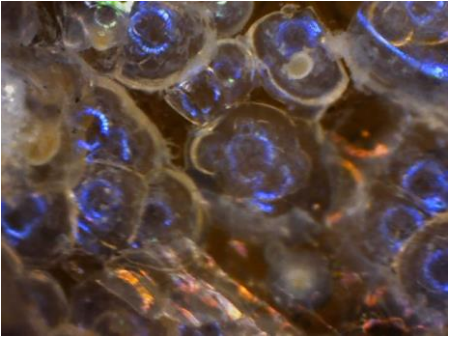
Table 5.4.1 LED Images of samples T1 and T2 under magnification x50 and x200

| Sample | Magnification X 50 | Magnification X 200 |
|--------|---|--|
| T1 |  |  |
| T2 |  |  |

Brown Samples

The samples T16 and T45 are dated back to the Archaic and Hellenistic period respectively. The samples are covered with intense iridescence nearly in the whole surface and show a white crust. The iridescent layers are thick and flake away. Underneath the iridescent and crust glass layer, a corroded surface, which has darker color (brown- black) is revealed. Pits and craters create a pattern of cracks on the outer surface. A variation of the color is also observed, the crust appear whiter near the edges of the sample. In the inner surface the iridescent layer is thicker and has lots of pits. The brown glass samples appear heavily corroded and friable, and are not in a good preservation state.

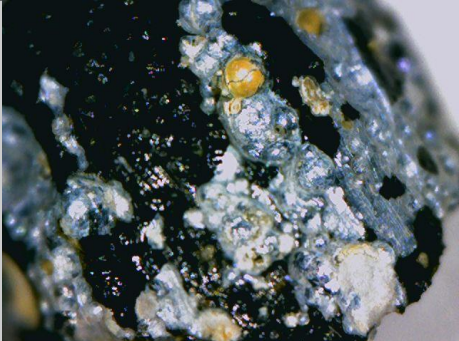
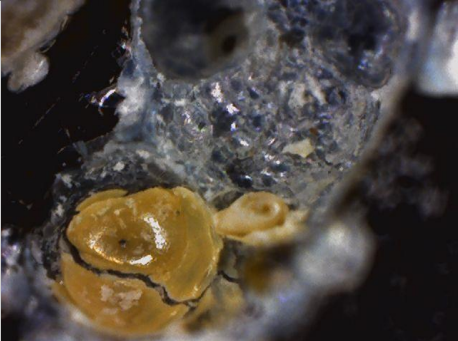
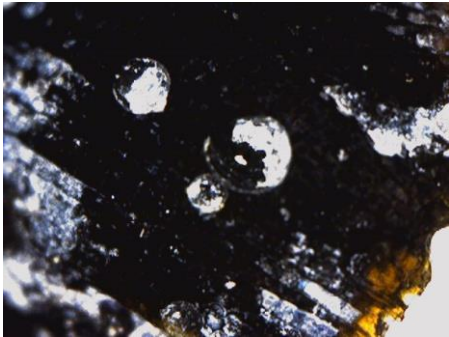

Table 5.4.2 LED Images of samples T16 and T45 under magnification x50 and x200.

| <i>Sample</i> | <i>Magnification X50</i> | <i>Magnification X200</i> |
|---------------|---|--|
| <i>T 16</i> |  |  |
| <i>T 45</i> |  |  |

Black Samples

The black samples T22 and T23 present a linear pattern on their surface, probably manufacturing evidence. Pits and craters cover the whole surface and the formation of the pitting follows the linear manufacturing pattern. A crust of iridescent layers occurs in the inner surface. Inside some craters, a colored crust is observed; it can be described as a semi opaque milky effect. The black samples appear to be in a medium preservation state.

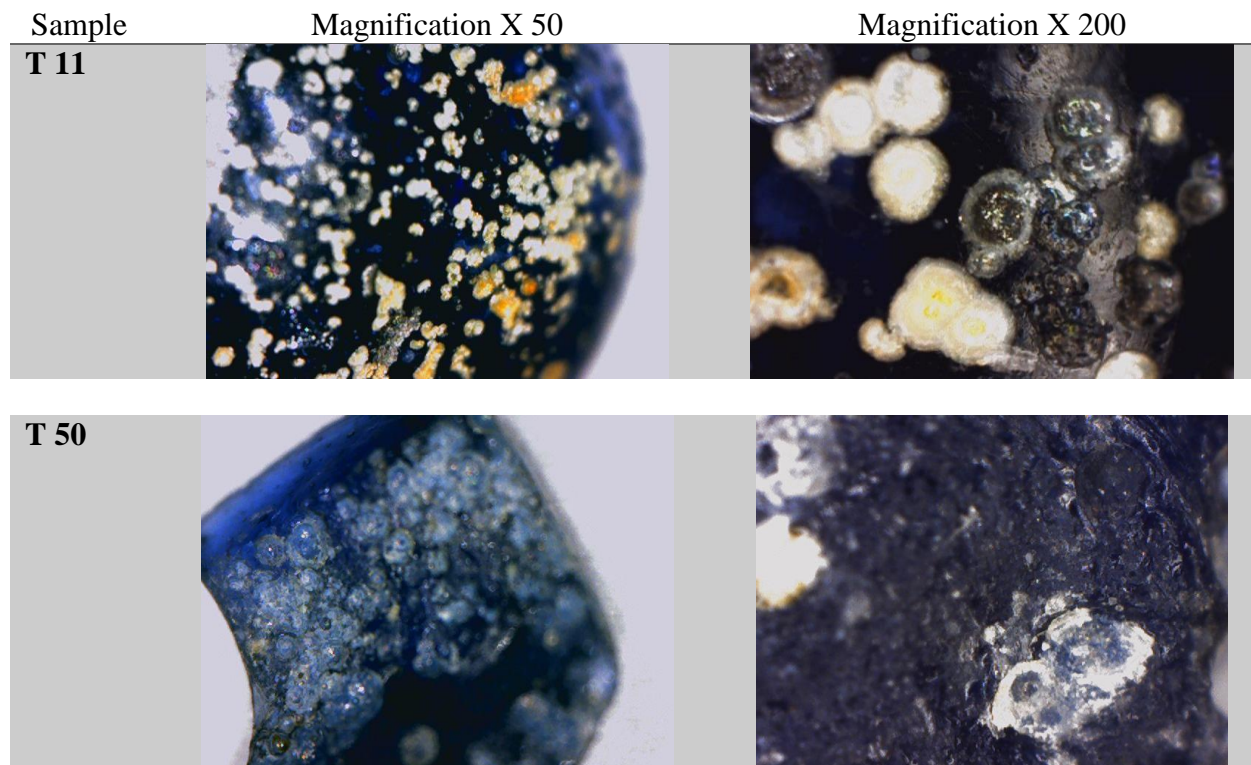
Table 5.4.3 Table 5.4.1 LED Images of samples T22 and T23 under magnification x50 and x200

| Sample | Magnification X 50 | Magnification X 200 |
|--------|---|--|
| T 22 |  |  |
| T 23 |  |  |

Blue Samples

The dark blue samples T 11 and T 50 present pitting on their whole surface. The pits have different diameters, and there is an increase in their frequency at the inner surface where the core meets the glass. Inside and around pits and craters lamination corrosion patterns are observed. The laminations layers present different colors like white and light brown. The surface of sample T50 is rougher in comparison to sample T11. The dark blue samples categorized in medium preservation state.

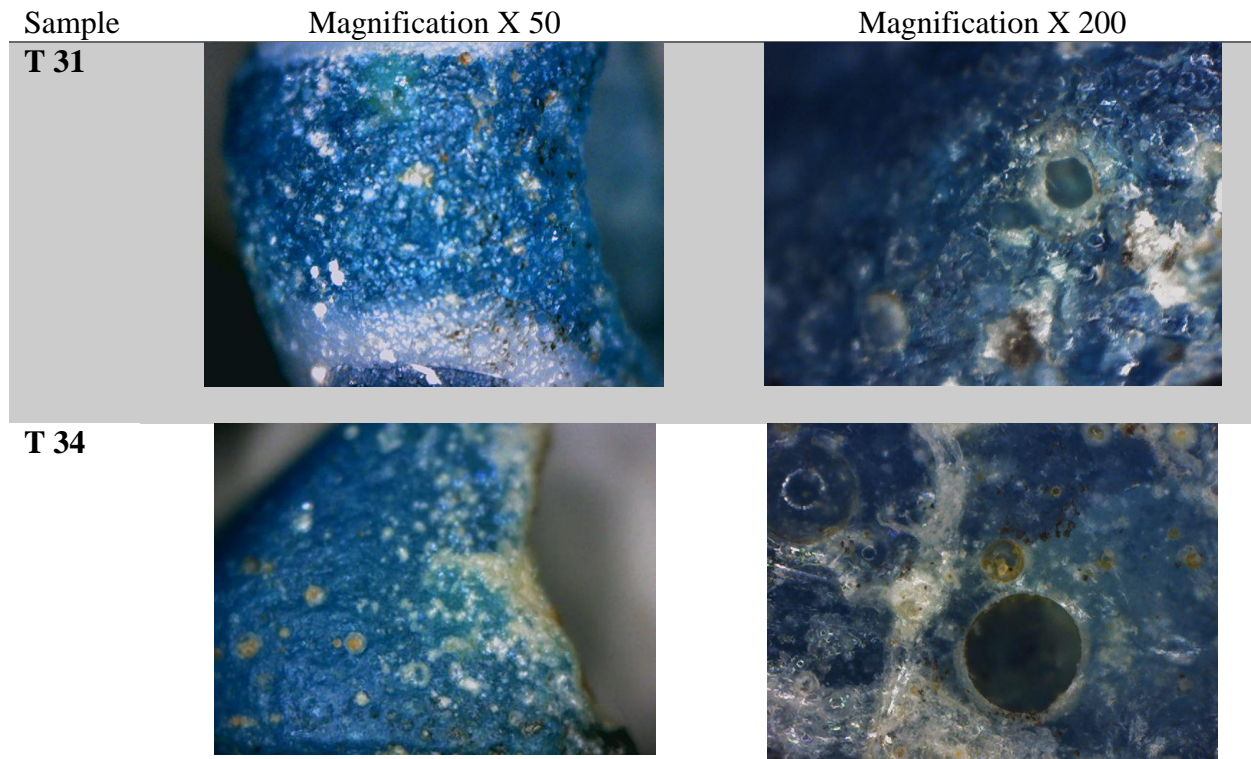
Table 5.4.4 LED Images of samples T11 and T50 under magnification x50 and x200



Light Blue Samples

Both light blue samples T31 and T34 present a roughness in their surface and a loss of solidity. Pitting and crater formation are the main corrosion patterns observed at the samples. Also at sample T34 a network of micro-cracks was noticed probably caused by physical stress. Color staining of black and dark brown color was also observed to both samples. The samples are categorized as heavily corroded.


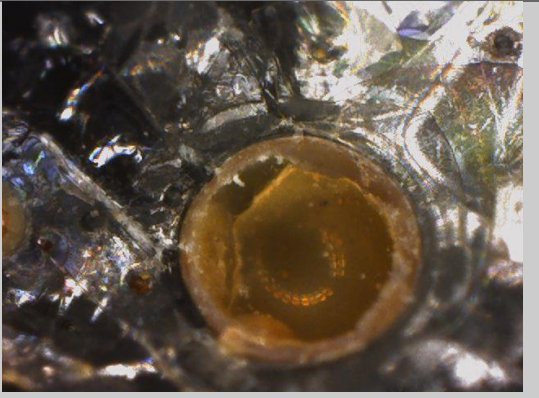

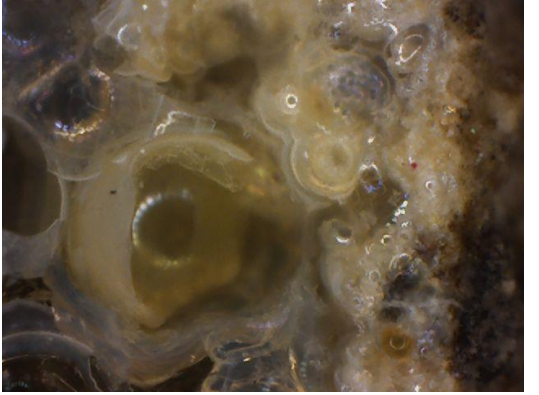
Table 5.4.5 LED Images of samples T31 and T34 under magnification x50 and x200



Colorless – Light Colored Green Samples

Sample T15 has an extensive pitting on its surface. The outer surface has an iridescent layer (vivid colors light blue, green, and pink). Pits create a pattern of cracks on the outer surface. A variation of color is also observed, the sample present whiter areas. In the inner surface the iridescent layer is thicker and has lots of pits. In some pits a semi opaque milky enamel like corrosion crust is noticed. At sample T 26 pits and craters are observed. It has lost its transparency in various areas because of milky enamel effect. Black staining is noticed as well. Both samples are categorized as heavily corroded.

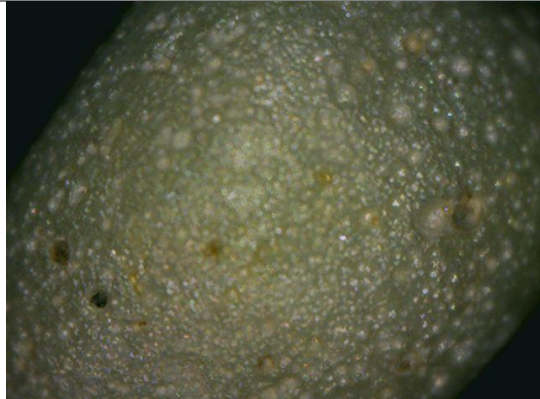
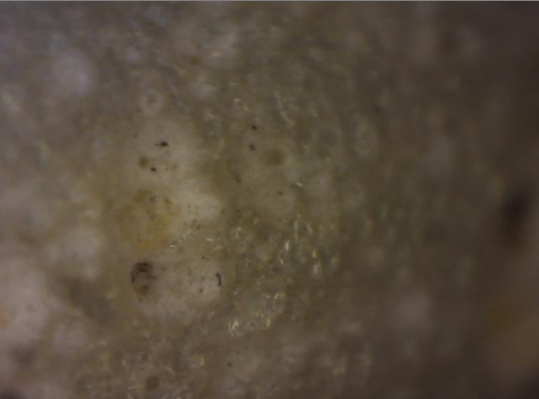
Table 5.4.6 LED Images of samples T15 and T26 under magnification x50 and x200

| Sample | Magnification X 50 | Magnification X 200 |
|-------------|--|---|
| T 15 |  |  |
| T 26 |  |  |

White sample

The white opacified sample is in good preservation state. It has not lost its coherence and its surface is even. Though small pits cover the surface, inside of some of these pits white spots and dark brown staining is noticed.

Table 5.4.7 LED Images of sample T 50 under magnification x50 and x200

| Sample | Magnification X 50 | Magnification X 200 |
|-------------|---|--|
| T 54 |  |  |

5.6. LED-OM Examination of Core Form Vessel Fragments

Yellow- White Decoration on blue body glass

The sample Man 7, is a blue body vessel fragment with yellow and white decoration trails. The blue body is coated by pits and in some areas iridescence is also observed. The surface can be characterized even without extreme surface modifications. However, the yellow decoration, which is covered by pits – of larger diameter -, has a rough, uneven surface. Dark staining is also noticed. White decoration trail is noticed to have an even surface but extensive pitting as well. Lamination was not observed at the white trail only close to the blue body. A silver corrosion layer is also adjacent partial to white trails. At sample Man 7 the area that is observed to be highly corroded is the yellow colored glass trail.

Yellow Decoration on blue body glass

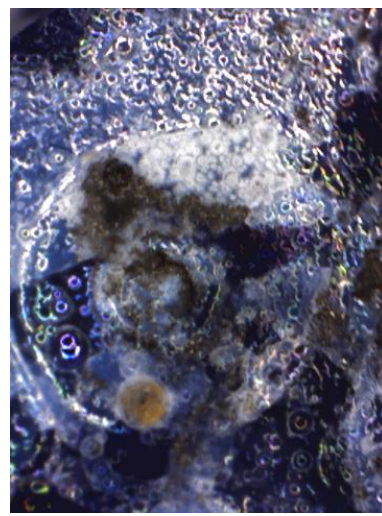
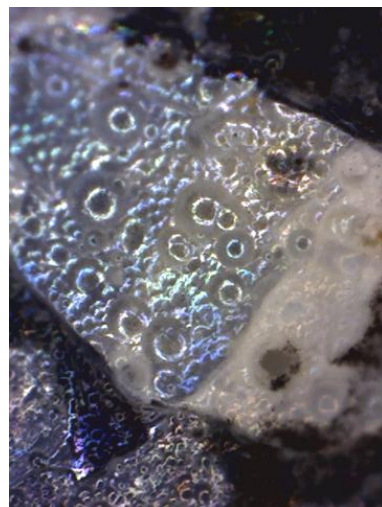
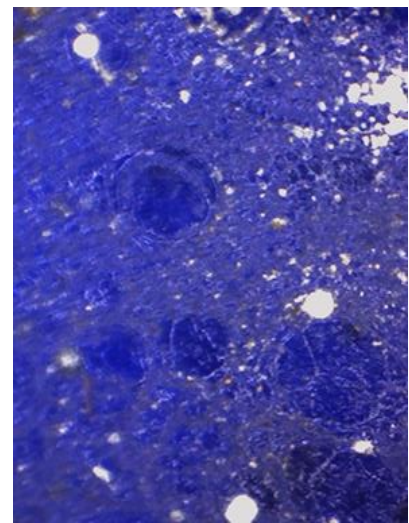
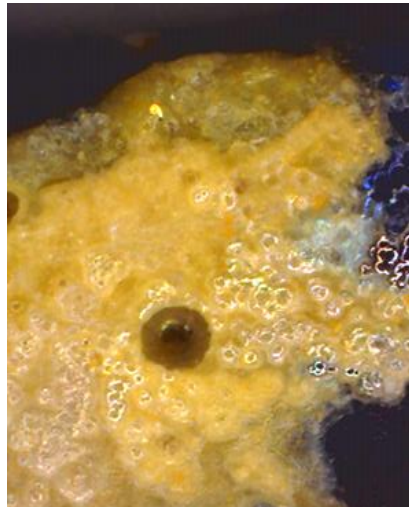
The surface modifications to sample Man 1 are likely similar to the sample Man 7. The blue glass body is covered with pits and iridescent layer, it is also observed that some areas have color alterations. Brown areas are observed and flakes have detached. Though again the yellow decoration is highly corroded in comparison to blue body. Craters and hollows are observed, and the iridescence is whole surface. The sample can be described as highly corroded.

Yellow Decoration on blue body glass

A blue body fragment decorated with white trails was also observed. The sample Man 11 is covered by craters, pits at the whole surface. A dark brown crust is also formed partial to the sample. An extensive iridescence layer is also observed. The pits at the white trail have larger diameter than at the blue body. The surface appears uneven and rough. The sample can be described as highly corroded with intense surface modifications.

To summarize, a variation is observed in the corrosion patterns that are formed, at the three different colored areas. The areas with the most intense surface modifications, are the white glass trails. In comparison, the white trails appear to have the same corrosion effects on their surface, but in sample Man 11 the alteration seems heavier. Pitting, hollows, lamination, crater formations and crusts are the observed alteration effects at the samples.

Magnification X 200



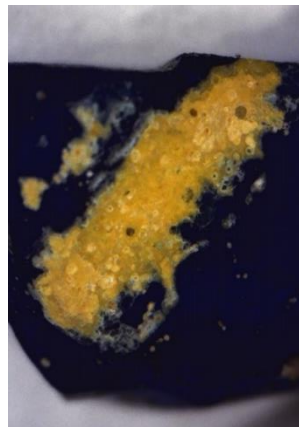
Magnification X 50

Sample

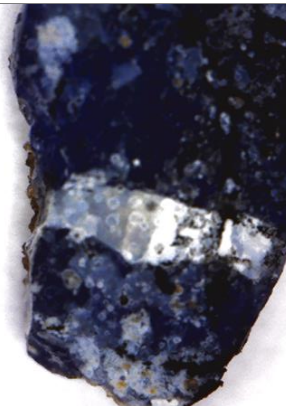
Man 7



Man1



Man11



5.7. Surface Analysis Using SEM-EDS

For a more detailed corrosion investigation, a Scanning Electron Microscopy coupled with EDS (Oxford Systems) provided the analytical data using the INKA software, was used in this study. The measurements took place at the Laboratory of Archaeometry at University of Peloponnese, Kalamata, Greece. The measurements were carried out using accelerating voltage, of 20 keV energy and a beam 40 spot size. The collection time for the measurements was 120 sec and the magnification for bulk analysis x300.

Bulk analysis from pristine glass and altered areas was carried out. The chemical characterization was a significant task in this study, assisting the examination of the corrosion processes and surface modifications. Corrosion patterns, microtopography and surface homogeneity were also studied thoroughly.

The bulk analysis of pristine glass areas from the beads and the vessels are shown in table 5.7.1

Table 5.7.1 The bulk analysis of the pristine glass areas from the beads and the vessels.

| Oxides | Beads mean value (wt. %) | Vessels mean value (wt. %) |
|--------------------------------|--------------------------|----------------------------|
| SiO ₂ | 72.75 | 71.69 |
| Na ₂ O | 13.15 | 17.48 |
| K ₂ O | 0.44 | 0.27 |
| CaO | 8.17 | 5.77 |
| MgO | 0.57 | 0.38 |
| Al ₂ O ₃ | 1.6 | 2.43 |
| SO ₃ | 0.46 | 0.4 |
| Cl | 1.16 | 1.43 |

The samples were analyzed and characterized in previous studies (Zaxarias Oikonomou) as a soda lime silica glasses. Natron was determined to be the main source of alkalis. The chemical elements that have been used as colorants at the studied material are cobalt, copper, antimony, iron and lead.

However, the results of the beads in this study, the values for soda lime silica glass are not the typical. The examined samples were already polished, but not encased in resin. Every glass bead had a polished area which was analyzed for the pristine glass chemical characterization. Since the samples were heavily corroded and not encased in resin, it is possible that the analysis include altered areas as well. For that reason the analysis of Sample T15, was removed.

The examination of the corrosion was focused in microtopography and chemical composition of the examined areas. The chemical composition analysis of polished and corroded areas will be compared as well. Some of the most common corrosion patterns observed through macroscopic and microscopic examination, are presented.

Pitting and Micropitting:

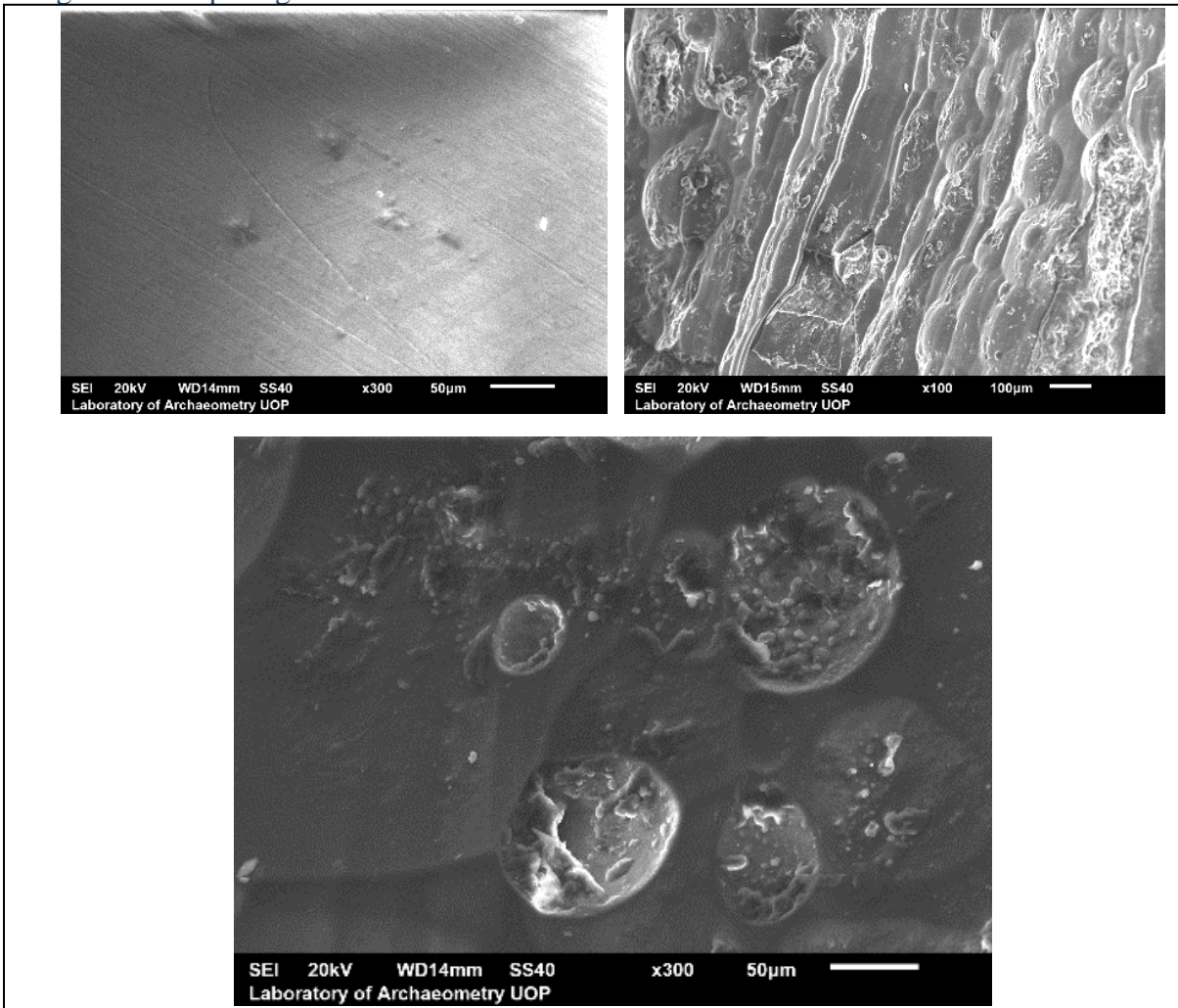


Figure 5.1 Different glass areas of sample T23 under x100 and x300 magnification

The most common corrosion pattern that was observed in the majority of the glass samples was pitting. In Figure 5.1 images from **Sample T23**, black colored bead, in different magnification are presented. The first image presents a pristine glass area of the sample under x300 magnification, the second and third image the altered area under x100 and x300 magnification respectively. Signs of pitting, micro and larger hemispheric cavities and hollows are clearly observed.

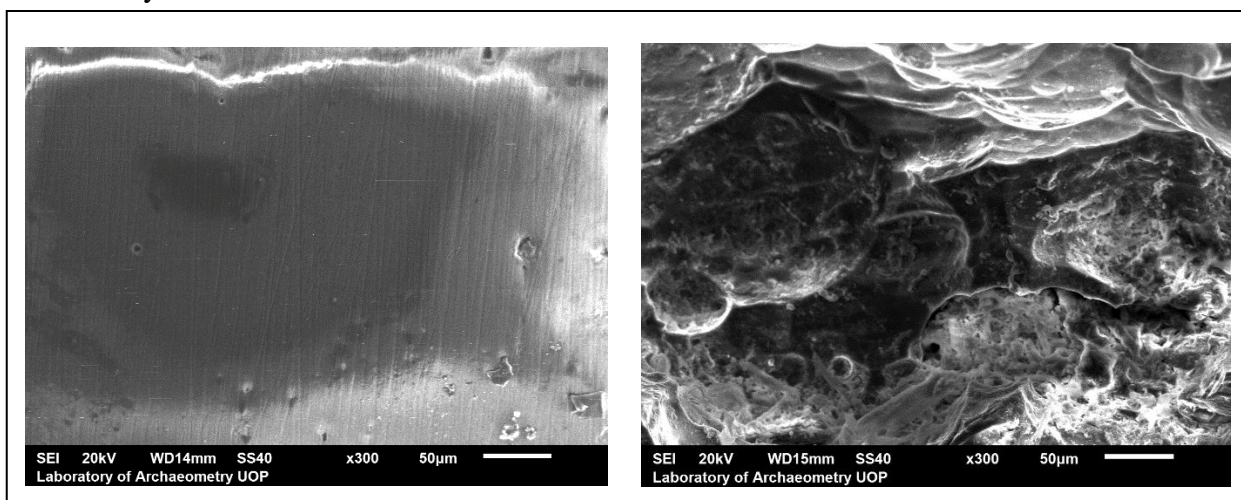


Figure 5.2 SEM images of sample T31, left the polished area right the corroded (magnification x300)

SEM images of **Sample T31**, a light blue glass bead, are shown in Fig. 5.2. For comparison purposes images taken from pristine and corroded glasses are presented. The first image was taken from a pristine glass area, the surface appear even and do not present and surface modifications. On the second image, captured under x300 magnification, the sample shows an uneven surface with a “spongy” texture probably caused by the extensive micropitting.

Table 5.7.2 Chemical composition of major oxides present on the pristine glass and the iridescent areas of sample T31 (determined by SEM/EDS, in wt%, normalised to 100%)

| S. T31 | Na ₂ O | MgO | Al ₂ O ₃ | SiO ₂ | SO ₃ | Cl | K ₂ O | CaO | Fe ₂ O ₃ | CuO |
|-----------------------|-------------------|------|--------------------------------|------------------|-----------------|------|------------------|------|--------------------------------|------|
| Polished Glass | 15.46 | 0.56 | 2.7 | 72.35 | 0.55 | 1.01 | 0.36 | 6.06 | 0.26 | 0.73 |
| σ | 0.14 | 0.1 | 0.16 | 0.71 | 0.12 | 0.12 | 0.03 | 0.08 | 0.09 | 0.62 |
| Corroded Glass | 7.03 | 2.52 | 6.04 | 70.04 | 1.77 | 1.26 | 3.03 | 6.35 | 1.2 | 0.79 |
| σ | 0.98 | 2.08 | 1.26 | 1.21 | 0.66 | 0.04 | 0.76 | 0.86 | 0.54 | 0.01 |

The chemical composition of sample T31, that was determined by SEM/EDS, is shown in Table 5.7.2.. Silica content of the polished area of the sample is 72.35 wt%, values of Na₂O and CaO 15.46 wt% and 6.35 wt% respectively. Due to alkalis loss the concentration of Na₂O presented a decrease of 50% at the corroded area, 7.03 wt%. Al₂O₃ values though increased at 6.04wt%, indication of an alumina- silica protective layer formation.

Lamination and Iridescence:

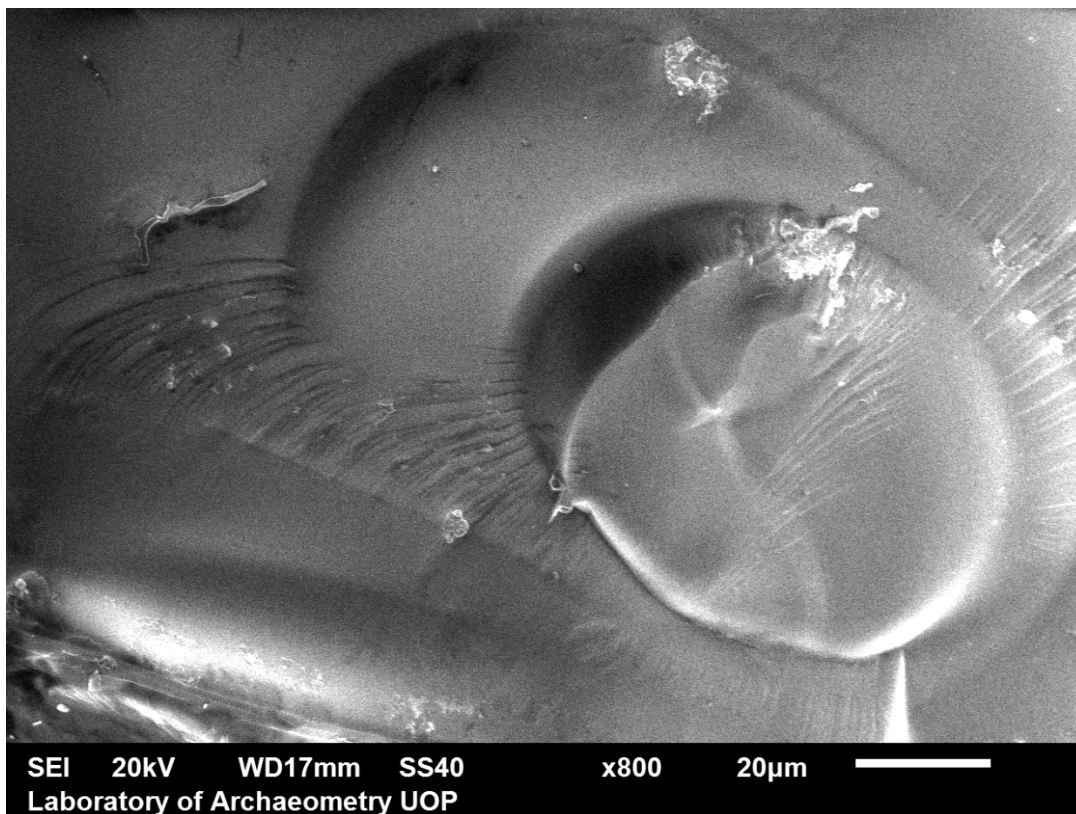


Figure 5.3 Lamination formation on initial stage

During the examination of Sample T16, an initial lamination formation was observed at the surface. The etching area is presented in Figure 5.3, the length of the engraved areas vary between 10 to 30µm.

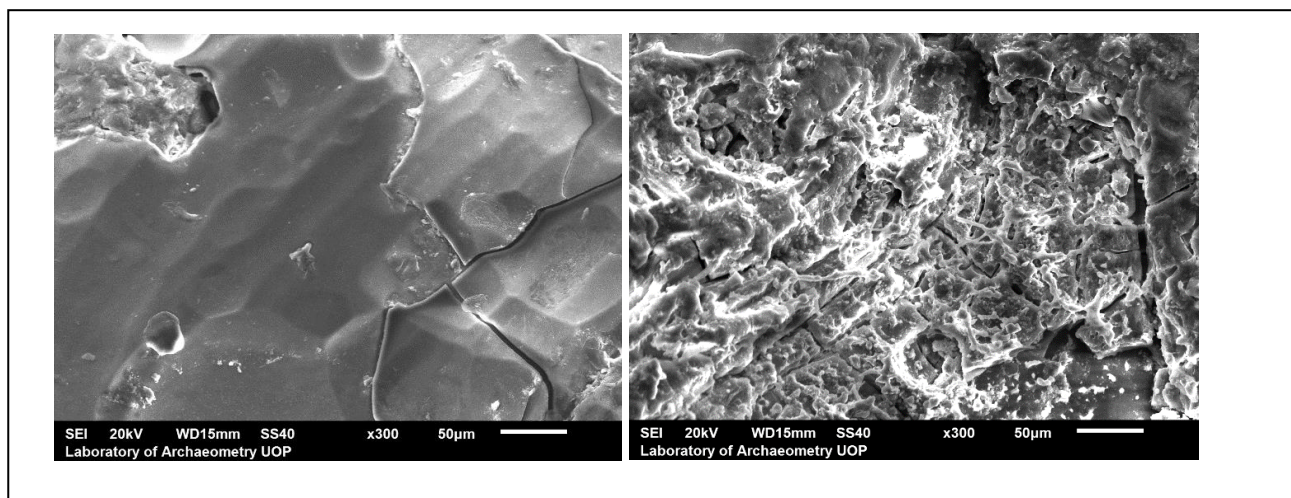


Figure 5.4 Initial iridescence phenomenon and crust formation of spongy texture

The images present the iridescence phenomenon on its initial phase (left) and a crust that was formed above the lamination (right). The crust is spongy and has developed both on the surface of the iridescent layers and on the voids of a microcracking network. The chemical analysis (table 21) resulted that the crust consists of CaO since the SiO₂ are taken probably from the background. A leaching out of the alkalis at the corroded area is also observed.

Table 5.7.3 Chemical composition of major oxides present on the pristine glass and the iridescent areas of sample T22 (determined by SEM/EDS, in wt%, normalised to 100%)

| Sample T22 | Na ₂ O | MgO | Al ₂ O ₃ | SiO ₂ | SO ₃ | Cl | K ₂ O | CaO | Fe ₂ O ₃ | Sb |
|-----------------------|-------------------|------|--------------------------------|------------------|-----------------|------|------------------|-------|--------------------------------|------|
| Pristine Glass | 13.16 | 0.57 | 0.64 | 73.25 | 0.27 | 1.45 | 0.17 | 8.66 | 1.84 | n.d. |
| σ | 1.51 | 0.03 | 0.28 | 0.63 | 0.26 | 0.21 | 0.17 | 0.62 | 2.34 | n.d. |
| Corroded Area | 8.04 | 0.78 | 0.82 | 75.3 | 0.49 | 1.54 | 0.41 | 8.88 | 0.84 | 0.66 |
| σ | 2.26 | 0.16 | 0.11 | 0.54 | 0.13 | 0 | 0.06 | 1.32 | 0.12 | 0.84 |
| Crust | 2.37 | 1.74 | 9.78 | 55.07 | 1.39 | 1.76 | 1.4 | 23.59 | 2.18 | n.d. |

Gel Layer Formation

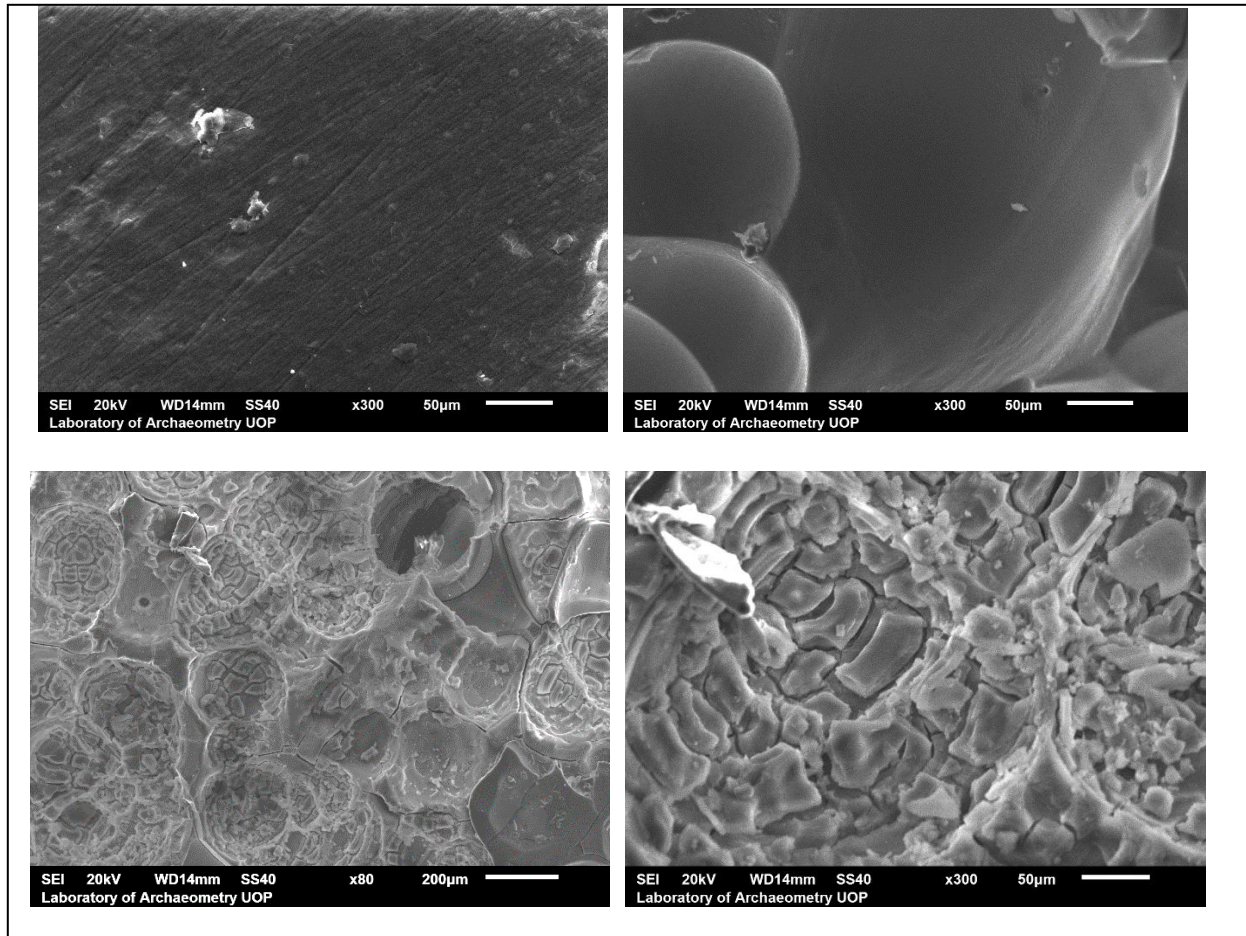


Figure 5.5 Top left image pristine glass area, Top right image round initial formation of hydrated silica rich layer, down left image crust formation and down right image flakes, craters and hollows at the crustation Sample T45

The formation of hydrated silica rich surface layer is a characteristic mechanism at the glass corrosion, for soda lime silica glasses. The under study areas belong to **Sample T45**, a brown bead, the shown images depict the pristine glass, a gel formation area and the alteration crust. The pristine glass present an even surface, without modifications. The second image present lamellae of sample, in granular structure. The alteration crust is not homogeneous, and is coated by thick flakes, craters and hollows.(Fig. 5.5)

The chemical composition of the three areas is presented on table (23). Corroded glass compared with pristine glass is poor on Na_2O and CaO but relatively enriched in SiO_2 , Al_2O_3 , and K_2O indicating a differentiated cation mobility. In general, in the gel layer and alteration crust, major elements reveal different behavior. In the gel layer, an enrichment in SiO_2 is evident, followed by a decrease towards the alteration crust. Values of Na_2O and Cl show a sharp fall in

both gel layer and corroded area, however CaO is constant at the gel layer and decrease at the alteration crust. Concentrations of Al₂O₃ showed an initial rise in the gel layers and a rapidly increase at the crust. K₂O concentration is relatively stable at the gel layer but showed an intense increase at the crust. SO₃ values present an increase on the corroded area but not detected at the gel layer.

Table 5.7.4 Chemical composition of major oxides present on the pristine glass and the corroded areas of sample T 45 (determined by SEM/EDS, in wt%, normalised to 100%)

| Sample T45 | Na₂O | MgO | Al₂O₃ | SiO₂ | SO₃ | Cl | K₂O | CaO | Fe₂O₃ |
|-----------------------|------------------------|------------|------------------------------------|------------------------|-----------------------|-----------|-----------------------|------------|------------------------------------|
| Pristine Glass | 15.45 | 0.79 | 1.89 | 72.11 | 0.69 | 1.25 | 0.74 | 6.66 | 0.44 |
| σ | 0.84 | 0.37 | 0.12 | 0.21 | 0.04 | 0.13 | 0.04 | 0.29 | 0.28 |
| Gel Layer Area | 4.65 | 0.71 | 3.82 | 81.61 | n.d. | 1.08 | 0.68 | 6.59 | 0.87 |
| Corroded Area | 2.16 | 2.35 | 10.54 | 75.88 | 1.55 | 1.58 | 5.3 | 0.6 | 0.36 |
| σ | 0.59 | 0.07 | 0.33 | 0.33 | 0.25 | 0.12 | 0.65 | 0.42 | 0.15 |

Semi-Opaque Milky Effect

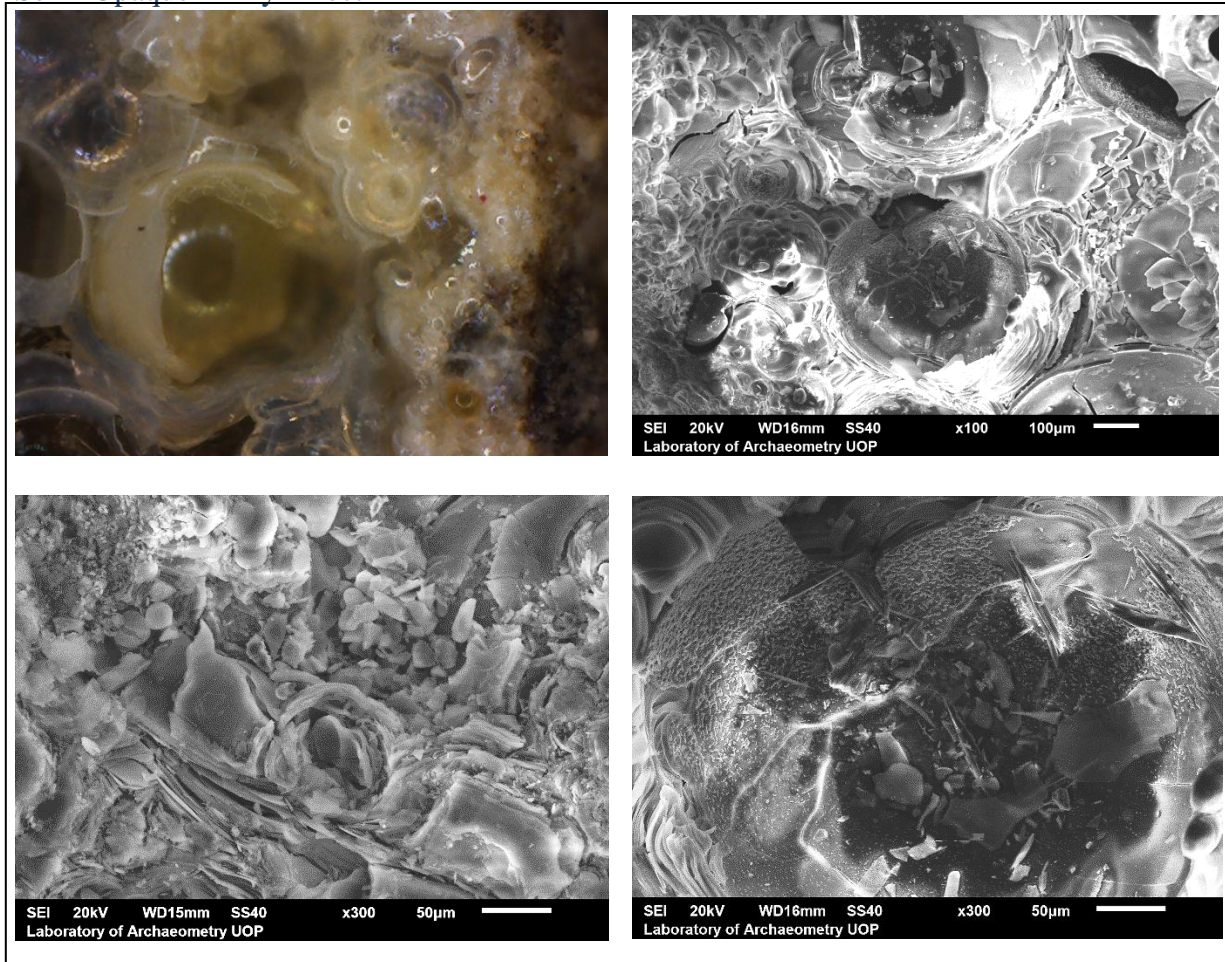


Figure 5.6 The semi opaque milky effect ,pits, lamellae, local crust

The semi-opaque milky effect, which was observed during macroscopic examination, is considered to be a combination of corrosion processes. The studied pattern is presented, at Figure (23) by LED- OM and SEM images. Concentric layers forming local crust, lamination, flakes and pits filled with thin glass layers are observed. The lamination layers were observed to have different thicknesses and sizes; microtopography is very interesting in this area.

Table 5.7.5 Chemical composition of major oxides present on the pristine glass and the corroded areas of sample T 26 (determined by SEM/EDS, in wt%, normalised to 100%)

| Sample | Na ₂ O | MgO | Al ₂ O ₃ | SiO ₂ | SO ₃ | Cl | K ₂ O | CaO | Ti | Fe ₂ O ₃ | Sb |
|-----------------------|-------------------|------|--------------------------------|------------------|-----------------|------|------------------|------|------|--------------------------------|------|
| T26 | | | | | | | | | | | |
| Pristine Glass | 15.34 | 0.51 | 2.29 | 71.49 | 0.46 | 1.01 | 0.83 | 7.13 | 0.27 | 0.25 | 0.9 |
| Corroded Area | 0.7 | 2.03 | 9.65 | 78.43 | 0.48 | 0.18 | 0.62 | 4.95 | 1.35 | 2.31 | 1.07 |

The Na₂O remained as a trace element and was almost leached out completely. The Fe₂O₃ increase attributed to the coloration of the surface, leached out and oxidized, coloring the glass with black, brown and light brown hues. The glass lost partial its transparency, due to multiply lamination layers and Fe staining.

5.8. Corrosion Depth Analysis

In order to verify how the corrosion mechanism behaved in different colored glasses a depth profiling analysis considered necessary. The corrosion depth analysis carried out by line scanning on the SEM as well as applying the RBS technique at a Tandem Ion Beam Accelerator.

5.8.1. Line Scanning measurements SEM-EDS

Using a SEM –EDS a line scanning examination was performed, at the core formed vessel fragments. The measurements were carried out using accelerating voltage, of 20 keV energy, a beam 40 spot size and WD 15. The collection time for the measurements was 300 sec and the magnification for the analysis x2000. The depth profiling of SiO₂, CaO, Na₂O and Al₂O₃, was acquired from the cross section of the examined glass areas, in an approximate depth of 30-35 μm.

As an example of the analysis, the results of Sample Man 7 are shown. The blue, yellow and white glass areas are presented below. The blue area that is observed at Figure 5.7 has lamination layers until 5μm. The values of silica increase dramatically in this area in contrast to sodium values that are relatively low. At this area a peak of aluminum is also observed. The values of calcium are increased in a very thin outer layer of the sample. The extreme variations of the values of the examined elements, stopped occurring near 8-10μm deep from the surface.

At the yellow area (Fig.5.8), the spectrum is showing an increase of silica values until 8 μ m. Silica values did stabilize near 10 μ m deep from the outer surface. On the other hand, sodium values stabilized a few microns deeper, at 13 μ m. The lack of sodium on the outer surface is an indication of the de alkalization mechanism. The aluminum spectrum shown a gradual increase until 5 μ m and some peaks at 6, 8 and 28 μ m from the edge, these peaks did not taken into consideration, because they were probably effect of the glass inhomogeneity. The values of calcium are increased near the edge. The overall stabilization of the examined elements, occurred near 15 μ m from the surface.

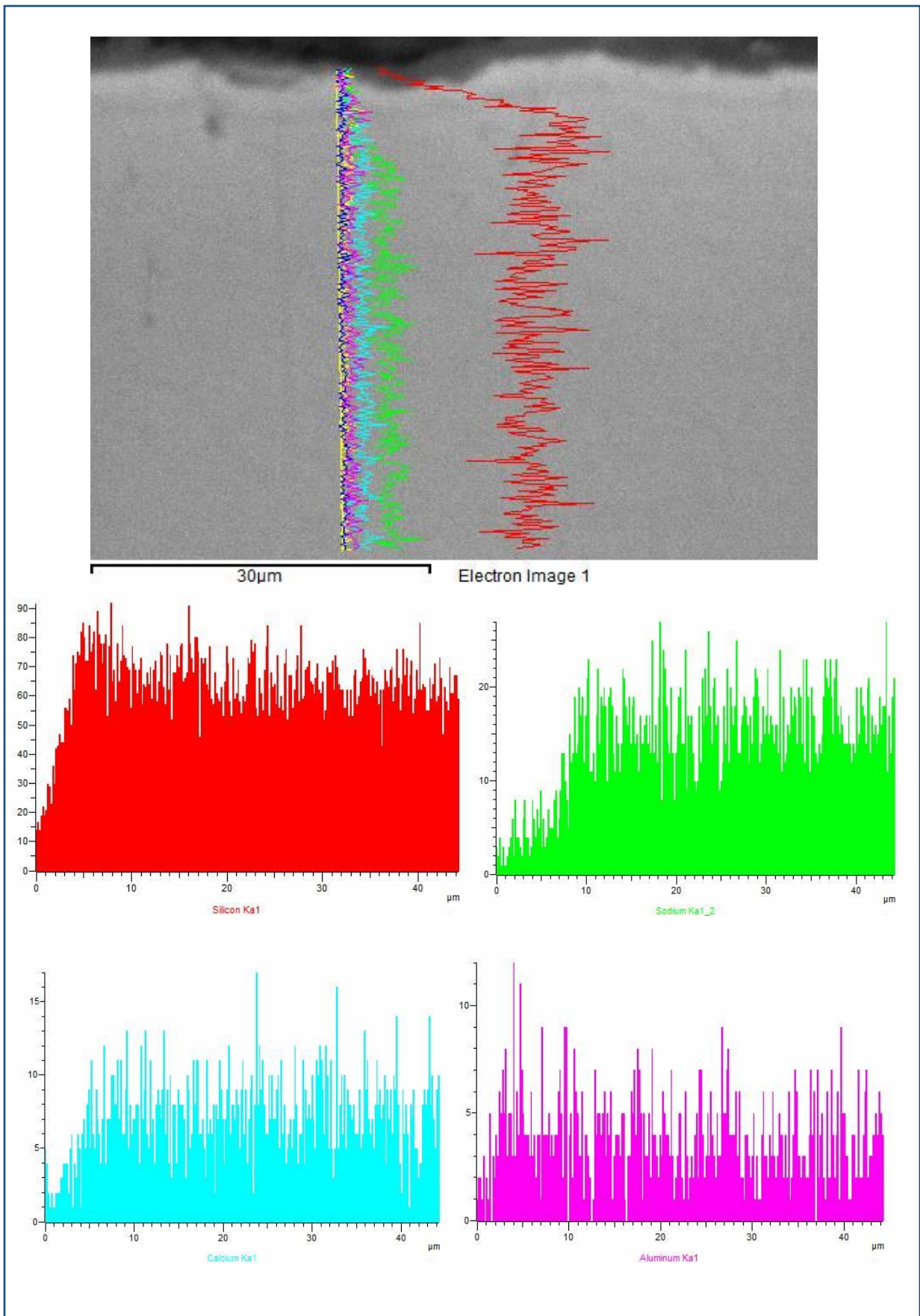
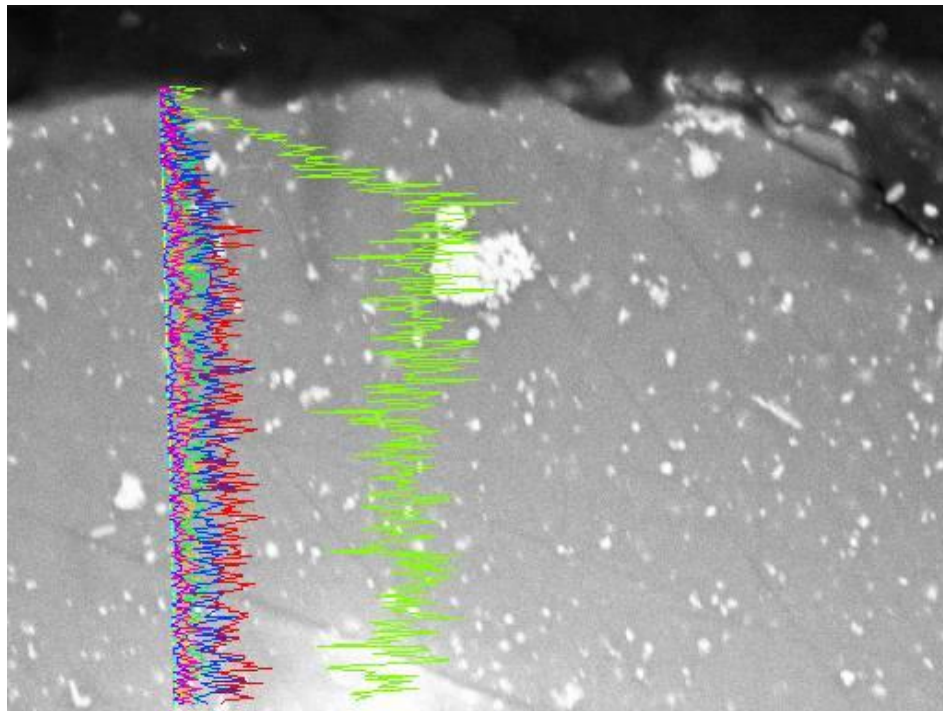
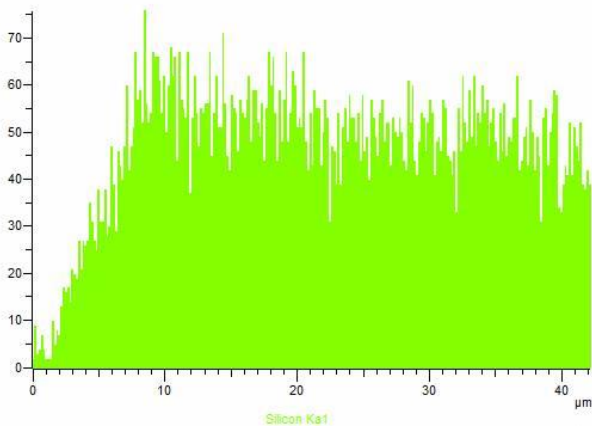


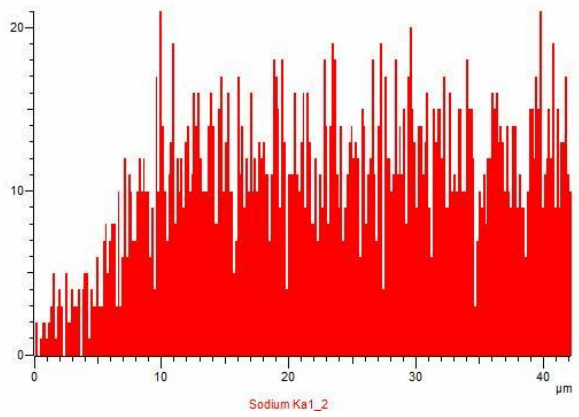
Figure 5.7 Line scanning Sample Man7 Blue area



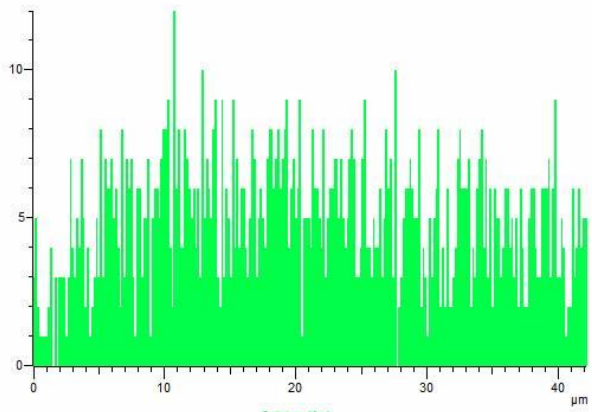
30µm Electron Image 1



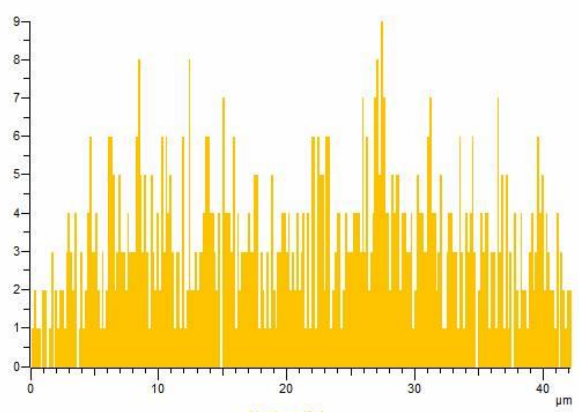
Silicon Ka1



Sodium Ka1_2



Calcium Ka1



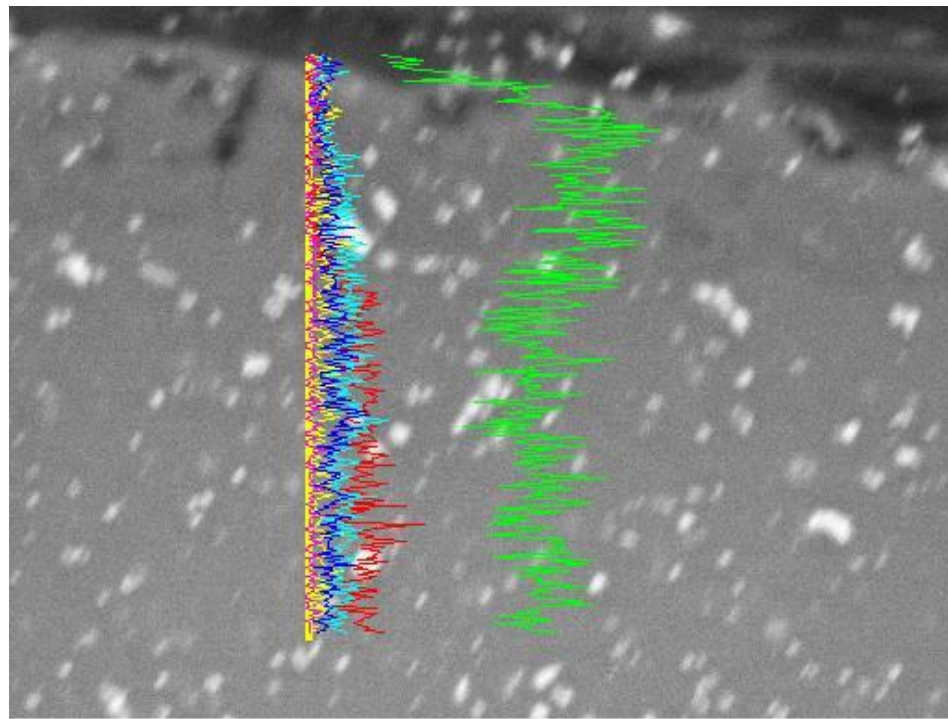
Aluminum Ka1

Figure 5.8 Line scanning Sample Man7 yellow area

For the white colored area, the study was focused on the outside edge of the fragment, on a zone of 40 μm . At the area of 15 μm was observed a layer with low concentration of alkalis and high values of silica and aluminum. On a zone of 3 μm a layer was formed, having high concentration of calcium but in a zone between 3- 7 μm the values of calcium dramatically decrease. The overall corrosion layer approximately pause at 30 μm deep from the surface.

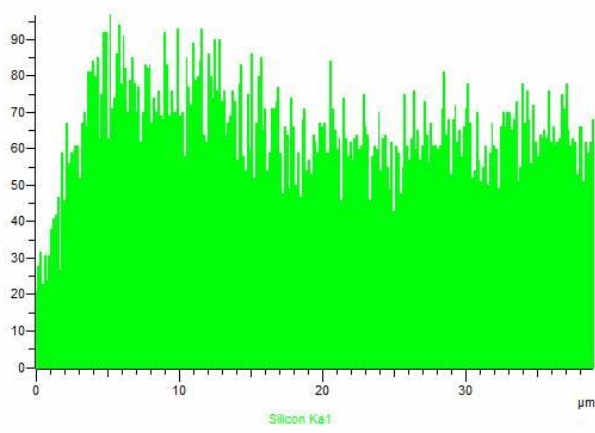
Investigating the three colored areas, from the same glass fragments, it is noticed that the corrosion zones did not have the same thickness. The corrosion phenomenon penetrated deeper on the white examined area than the yellow and blue. The white and blue areas were observed to have similar alkali loss and corrosion depth.

The obtained data from samples Man 1 and Man 11 are presented at the appendix.

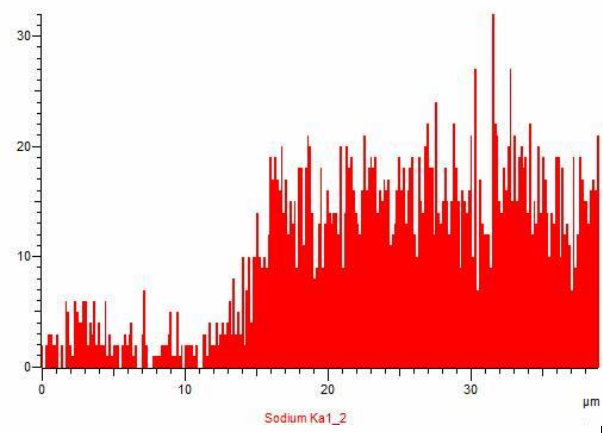


30µm

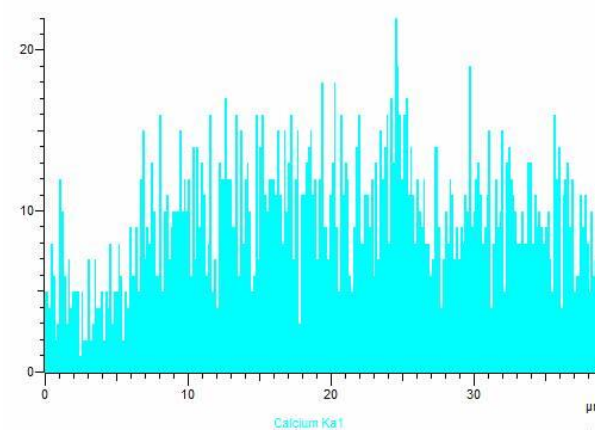
Electron Image 1



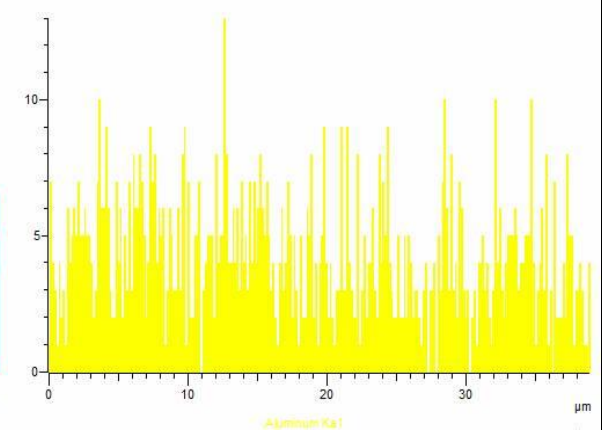
Silicon Ka1



Sodium Ka1_2



Calcium Ka1



Aluminum Ka1

Figure 5.9 5.10 Line scanning Sample Man7 white area

5.8.2. RBS Ion Beam Analysis

The Rutherford Backscattering Spectroscopy (RBS) experiment was performed at the Tandem Accelerator of Institute of Nuclear and Particle Physics National, National Center of Scientific research, “Demokritos”, Athens, Greece. The measurements were carried out using a deuteron beam, of 1.35 MeV energy. The beam spot had a diameter of $\approx 3\text{mm}$ and the detector was placed at 170° with respect to the beam. The calibration of the setup was performed, using a Standard Glass Sample with nominal composition of SiO_2 72%, 12% CaO , 14% Na_2O and 2% Al_2O_3 . The analysis of the obtained spectra, was carried out using the SIMNRA software. In this program, the user defines the experimental conditions and by assuming a layered target the code simulates the expected spectrum. By multiple iterations and fine tuning of the chemical composition of the examined samples the simulated spectrum is then fitted to the experimental one.

The obtained data were categorized into two groups according to the coloration of the target. Samples of green (2) and brown (2) glass bead fragments were examined. The depth profiling of SiO_2 , CaO , Na_2O and Al_2O_3 , was acquired from corroded bulk areas, in an approximate depth of $5\mu\text{m}$. The concentrations of the aforementioned elements with respect to the intensity are presented in the following figures

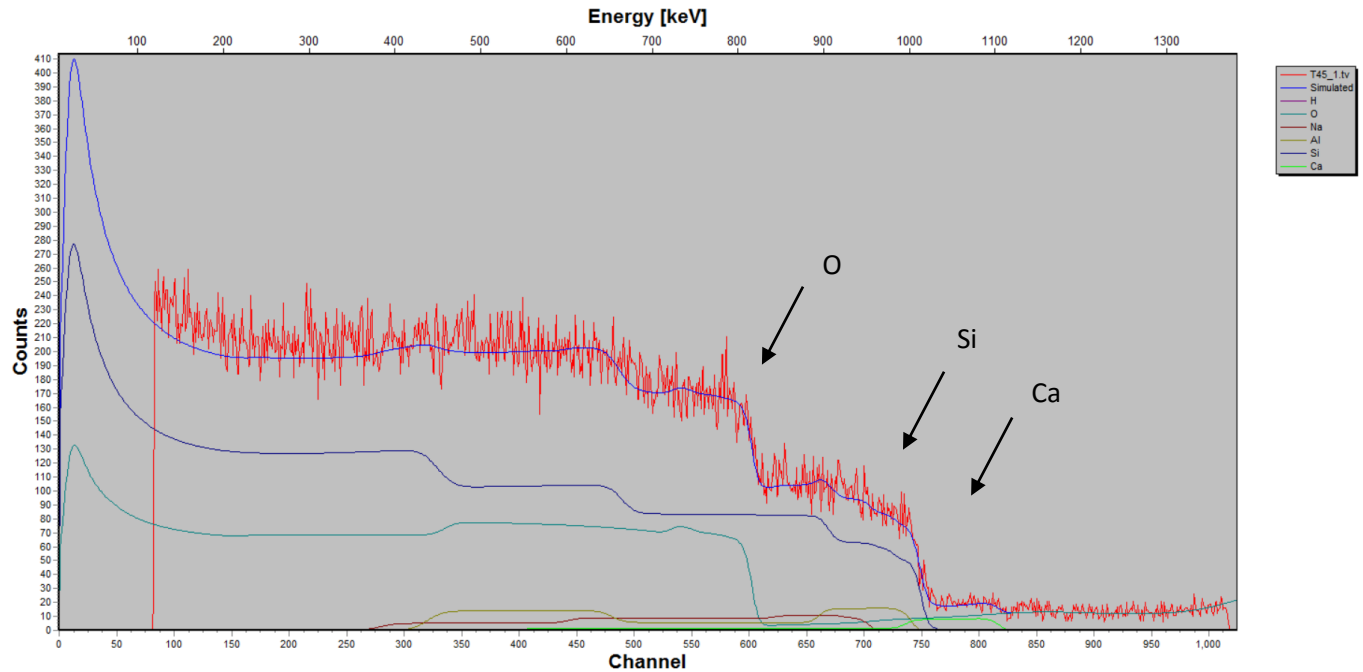


Figure 5.11 RBS Analysis of Sample T45, the red line represent the experimental and the blue the simulated spectrum respectively.

As an example, the analysis of sample T45 is presented in Figure 5.11. The red line represents the experimental spectrum and the blue line the simulated one, as it was calculated by the SIMNRA software. The bulk analysis of the sample was taken into account for the identification of the chemical elements. In order to understand the shape of the spectrum, one has to take into account that, a higher energy at the spectrum corresponds to the heavier element and to deeper penetration analysis. Observing from right to the left, the chemical elements are detected. The contribution of each element to the total spectrum is shown in the legend of the figure with different color lines.

Layers of different chemical compositions have formed in order to reproduce the experimental spectrum. The Table 5.8.1 summarizes the composition of the different layers, corresponding to the depth profile of the examined sample.

Table 5.8.1 Depth profiling, chemical compositional analysis of Sample T45. (Atomic Concentration of the oxides at %)

| Sample T 45 layer | 1 | 2 | 3 | 4 | 5 | 6 |
|---|------|------|------|------|-------|------|
| Thickness(10^{15} at/cm ²) | 1400 | 1500 | 1500 | 3600 | 13500 | 9500 |
| SiO ₂ | 60 | 57 | 59 | 62 | 79 | 80 |
| Na ₂ O | 17 | 17 | 18 | 17 | 14 | 7 |
| CaO | 4 | 5 | 4 | 4 | 1 | 1 |
| Al ₂ O ₃ | 19 | 21 | 19 | 18 | 6 | 13 |

The values of SiO₂ vary between 60-80 at%, Na₂O values between 18-7 at%, CaO values between 5-4 at% and Al₂O₃ values between 21-6 at%. It is observed that the Na₂O, CaO Al₂O₃ and are in higher concentration at the outer layers in contrast to SiO₂ which present an increase at the inner layers.

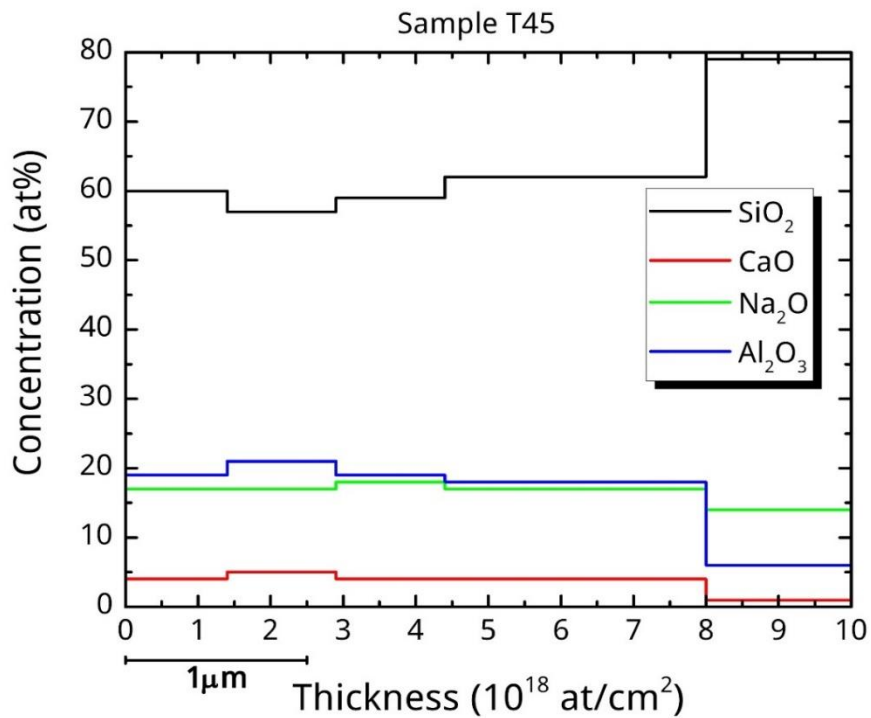


Figure 5.12 Concentration graph of sample T45

It is also observed that the fifth layer is the thicker, occurring near 3.07 μm from the surface. (Fig. 5.12)

The same procedure was followed for the analysis of all the samples measured by the RBS technique. The results of all the RBS measurements are presented in the following tables.

Brown Glass Group:

Table 5.8.2 Depth profiling, chemical compositional analysis of Sample T16. (Atomic Concentration of the oxides at %)

| Sample T16 layer | 1 | 2 | 3 | 4 | 5 |
|---|------|------|------|------|-------|
| Thickness(10^{15} at/cm ²) | 1400 | 1500 | 1500 | 3300 | 15000 |
| SiO ₂ | 59 | 60 | 53 | 63 | 67 |
| Na ₂ O | 15 | 15 | 23 | 15 | 15 |
| CaO | 10 | 6 | 6 | 8 | 1 |
| Al ₂ O ₃ | 16 | 19 | 17 | 14 | 18 |

Green Glass Group:

Table 5.8.3 Depth profiling, chemical compositional analysis of Sample T2. (Atomic Concentration of the oxides at %)

| Sample T 2 layer | 1 | 2 | 3 | 4 | 5 |
|---|------|------|------|------|------|
| Thickness(10^{15} at/cm ²) | 1400 | 1500 | 1300 | 3300 | 1400 |
| SiO ₂ | 65 | 66 | 60 | 65 | 69 |
| Na ₂ O | 23 | 18 | 22 | 19 | 14 |
| CaO | 5 | 10 | 15 | 13 | 14 |
| Al ₂ O ₃ | 7 | 7 | 4 | 4 | 3 |

Table 5.8.4 Depth profiling, chemical compositional analysis of Sample T1. (Atomic Concentration of the oxides at %)

| Sample T 1 layer | 1 | 2 | 3 | 4 | 5 |
|---|------|------|------|------|------|
| Thickness(10^{15} at/cm ²) | 1400 | 1500 | 1300 | 3300 | 1400 |
| SiO ₂ | 65 | 66 | 60 | 65 | 69 |
| Na ₂ O | 23 | 18 | 22 | 19 | 14 |
| CaO | 5 | 10 | 15 | 13 | 14 |
| Al ₂ O ₃ | 7 | 7 | 4 | 4 | 3 |

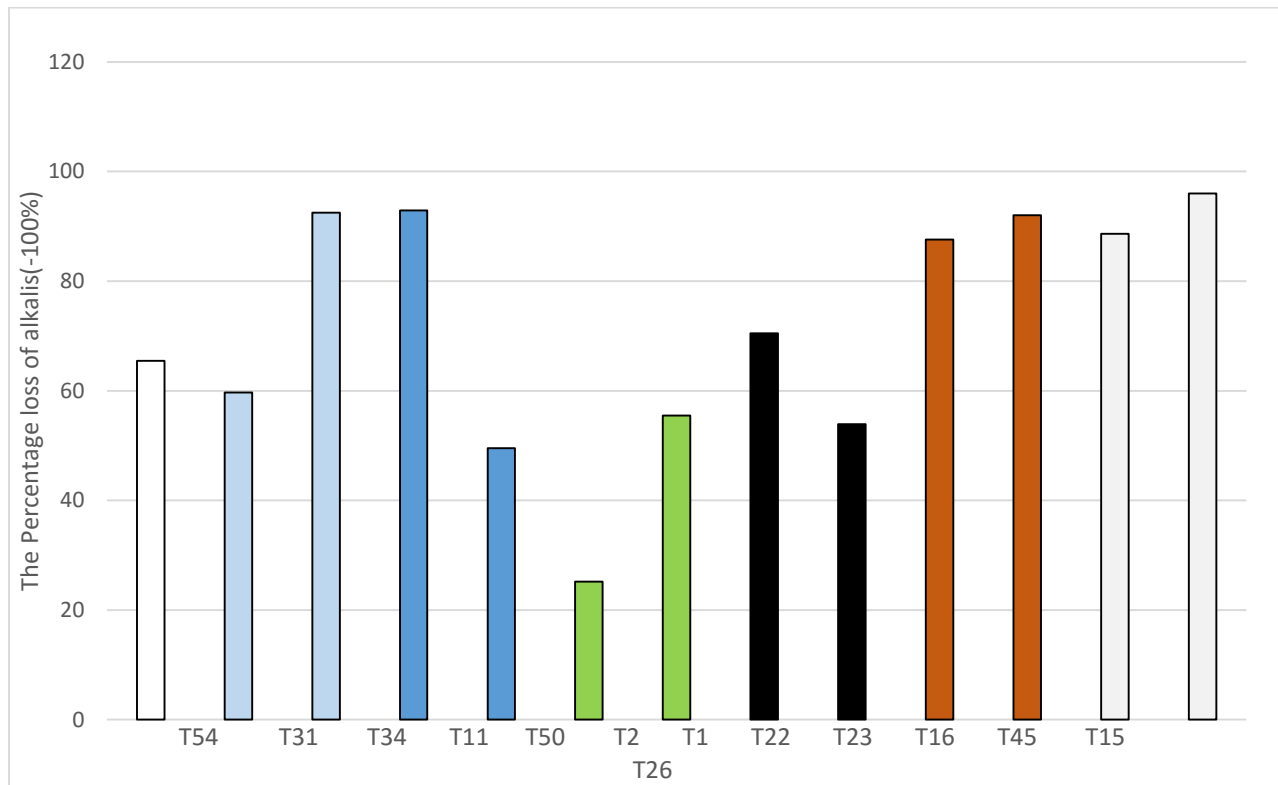
6. Discussion:

The deterioration rate of the glass objects is based on their chemical composition, the manufacturing process and the environment they were exposed to. The soda lime silica glasses are considered as highly resistant to corrosion mechanism. (El-Shamy & Douglas, 1972). A comparison of the weathered glass samples was carried out, in order to obtain information about the corrosion mechanism. Since the dealkalization, was the only determined corrosion process that was remarked in this study, a comparison of the alkalis behavior considered necessary.

The Alkalis Loss

The main alkali in both beads and vessels was sodium. It is known that sodium glasses have shown strong chemical resistance in comparison to potassium rich glasses. The difference of the Na_2O on the pristine glass to the corroded was calculated. It was mentioned above, that the polished areas of the glass beads, did not result the pristine glass values, so the mean Na_2O value was defined as literature research result. As a mean value of sodium for the equation, the value 17.43wt% was selected. The selected number was the mean value of bulk analysis from previous study, which focused on technology and provenance examination of the samples. (Zacharias, et al., 2008) (Oikonomou, et al., 2012) . For the glass beads the Table 5.8.1 shows the groups and the alkali loss percentage.

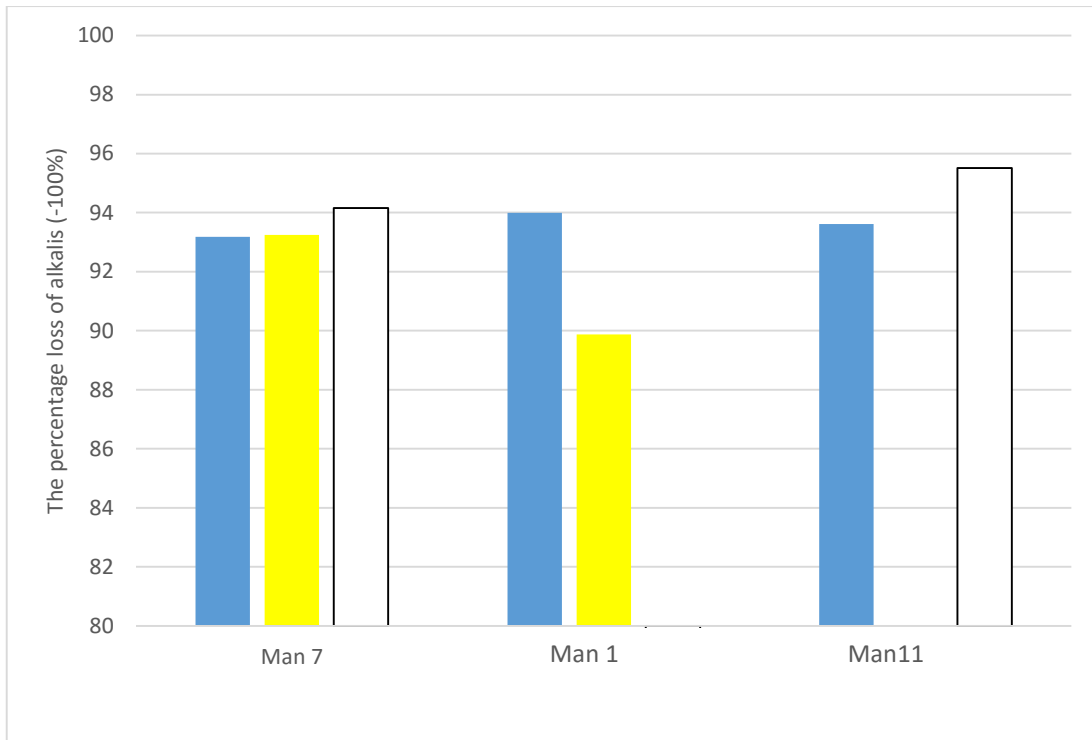
Table 5.8.1 The percentage loss of alkalis of the beads. The seven color groups are presented: white, light blue, blue, green, black, brown, colorless samples



It is observed that the group which was more durable at the buried environment was the green sample's group. The black group considered to be the second more durable. These two glass groups, had shown the mildest surface modifications. The glass groups that had the higher loss of alkalis where the brown samples and the colorless. For the dark blue, light blue and white we do not have a clear statement.

For the core formed vessels the Table 5.8.2, shows the groups and the alkali loss percentage. It is clear that the percentage of the alkalis loss is higher at the white colored glasses exceeded the 94%. For the blue colored areas the percentage ranges between 92-94%, for the yellow colored trails the percentage ranges between 90-94%.

Table 5.8.2 The percentage loss of alkalis of the core formed vessels. Samples Man 7, Man 1 and Man11 for blue, white and yellow colored glass areas



Comparing the two tables (6.1, 6.2), it is observed that the core formed vessels have a higher percentage to alkalis lost compared to glass beads. Glass beads have a mean percentage of 71.48% and vessels of 93.37%. This variation it is possible due to two purposes the chemical composition and the manufacturing technique.

The silica content of a glass is one of the most crucial factors for the deterioration process (El-Shamy, 1973a). In this case, the chemical composition the wt. % of silica does not have a large variation between the two examined groups, for the beads the mean value is 72.75wt% and for vessels 71.69 wt. %. So the difference of the corrosion rate is not be dependent of the silica content in this study.

The calcium oxide considered to be a stabilizer and up to 10%mol reduces soda extraction. The molar percentage of beads and vessels is 8.87% and 6.27% respectively (the molar percentages were calculated by the author). The difference between the calcium oxide concentrations is an indicator for the variation of the alkali loss between the two groups. The vessels which have lower calcium concentrations, are more likely to absorb water by the surface layers and corrode, than the beads. (Jackson, et al., 2012)

Manufacturing Effect

The differences in technology production is very crucial, for the deterioration rate. For the beads three different surfaces patterns are observed: for glass waste samples - uneven surfaces, for the beads - craft even surfaces and colored fused surfaces forming ridges and valleys. For the vessels the decorative glass trails are also forming ridges and valleys at the surface (Semenov, et al., 1972).

When a glass appear to have an uneven surface, occurring valleys and the ridges, the exposure area to the corrosion factors is larger than to an even surface. Observing a cross section SEM photography of Sample Man 11, the lamination thickness at the edge of the white decoration trail is 5 times thicker than at the blue body.

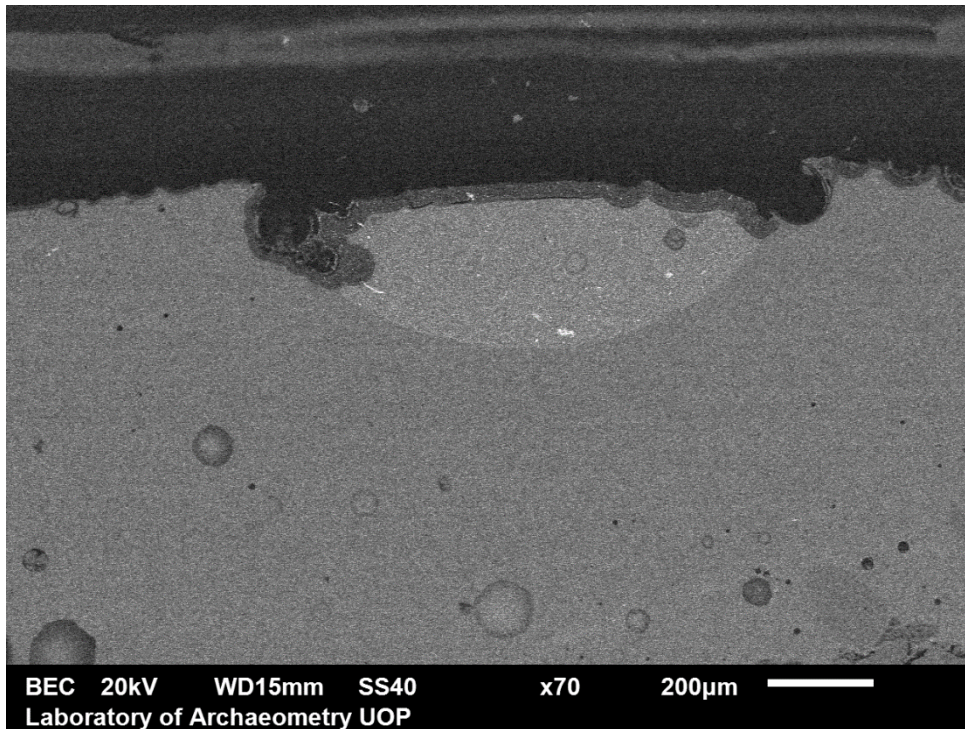


Figure 6.1 SEM-BSE image of sample Man 11. Lamellae 50 µm thick at the decoration edge.

According to Hench and Clark (1978, p. 91), the corrosion rate was accelerated logarithmically in glasses with a greater surface area. Experiments to ground glasses (Jackson, et al., 2012) showed that the alkalis loss was heavier in uneven surfaces. In this study, the glass waste samples, had the most corroded surfaces. The alkali loss of the glass waste endorse the

hypothesis that surface unevenness accelerate the decay rate. For the same reason the light blue samples present highly corroded surfaces.

The colorants

The inhomogeneity of the glass is another factor that affects the corrosion mechanism. Bubbles, caused by reheating of the object, cords, stones and crystallization leave their mark at the corrosion process (Adams, 1984). The burial environment, in this case, combined to the impurities of the glass contributed to the corrosion mechanism. It is observed that the introduction of antimony at the bulk, form crystallites that might be sources of local strain. (Yuryeva & Yurev, 2014). The network of micro-cracking allow to moisture to penetrate to deeper layers of glass and to accelerate the de alkalization. (Cagno, et al., 2011)

Taking into consideration the addition of calcium antimonite and the uneven topography, it is probably that is the case for the white glass trails corrosion mechanism. The same effect occur also to the yellow glass trails which have been colored with lead. (Palamara, et al., 2015)

Corrosion Depth Analysis

During macroscopic and microscopic examination the green sample T2 categorized at good preservation state group. However, during the examination using SEM/EDS tool it was found that the sample present micro pitting and light iridescence patterns. In figure 5.14 the corroded areas are presented under LED-OM and SEM images.

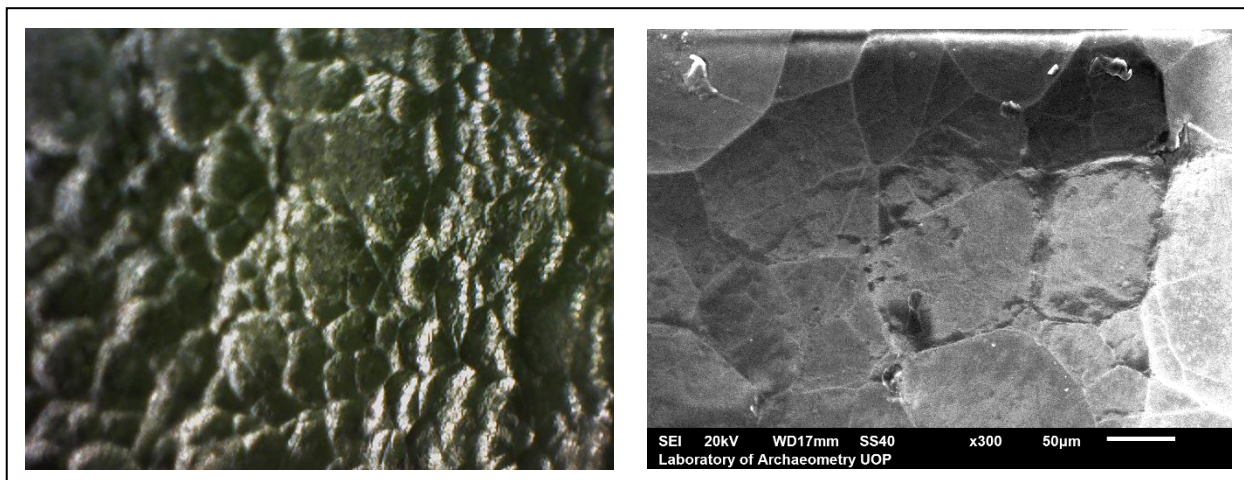


Figure 6.2 Micropitting and light iridescence patterns under LED-OM and SEM

The chemical concentration of the area is shown in table (6.3). According to EDS analysis the sample is considered slightly corroded.

Table 5.8.3c Chemical composition of major oxides present on the corroded area of sample T2 (determined by SEM/EDS, in wt. %, normalized to 100%)

| Sample T2 | Na ₂ O | MgO | Al ₂ O ₃ | SiO ₂ | SO ₃ | Cl | K ₂ O | CaO | Fe ₂ O ₃ |
|---------------|-------------------|------|--------------------------------|------------------|-----------------|------|------------------|------|--------------------------------|
| Corroded Area | 15.45 | 0.79 | 1.89 | 72.11 | 0.69 | 1.25 | 0.74 | 6.66 | 0.44 |
| σ | 0.24 | 0.23 | 0.07 | 0.57 | 0.14 | 0.1 | 0.21 | 0.69 | 0.3 |

The examination of the sample using the RBS technique revealed a variation of Na₂O, in different layers. Observing the Figure a concentration profile of the sample, it is clear that the deterioration evidence occur around 3-3.5 μm deep from the surface. The table (6.4) shown the Na₂O values. This variation of the alkalis indicates, the leaching out corrosion mechanism in initial stage.

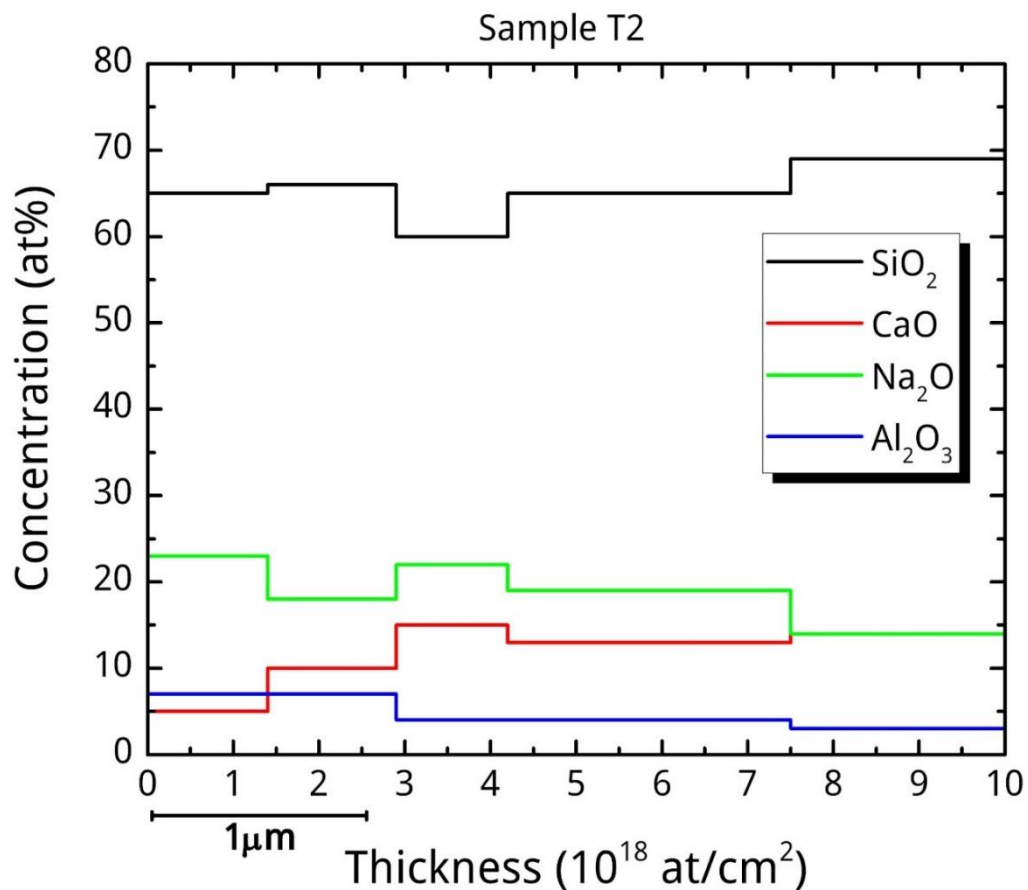


Figure 6.3 RBS Graph of sample T2

Table 5.8.4 Na₂O values determined by RBS

| Sample T 2 layer | 1 | 2 | 3 | 4 | 5 |
|---|------|------|------|------|------|
| Thickness (10 ¹⁵ at/cm ²) | 1400 | 1500 | 1300 | 3300 | 1400 |
| Na ₂ O | 23 | 18 | 22 | 19 | 14 |

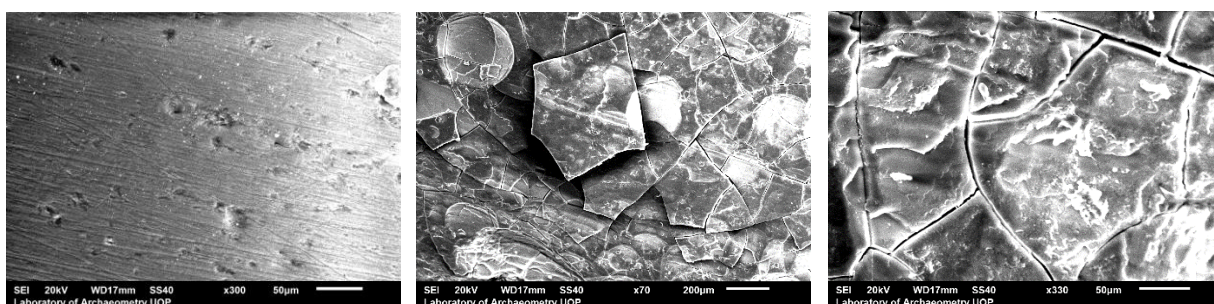


Figure 6.4 sample T16 images of SEM showing pristine and corroded areas (x 70, x 330)

Iridescence was the most common corrosion pattern that was detected at the collection. SEM images of **Sample T16**, a brown glass bead, are shown in Fig 5.16 For comparison purposes images taken from pristine and corroded glasses are presented. The first image was taken from a pristine glass area, the surface appear even and do not present and surface modifications. On the second and third image, captured under x70 and x330 magnification respectively, the sample shown surface high iridescent and extensively flaky. The flakes overlay each other at the area under study and during the image capturing continuous flake away.

Table 5.8.5 Chemical composition of major oxides present on the pristine glass and the iridescent areas of sample T16 (determined by SEM/EDS, in wt. %, normalized to 100%)

| Sample | Na ₂ O | MgO | Al ₂ O ₃ | SiO ₂ | SO ₃ | Cl | K ₂ O | CaO | Fe ₂ O ₃ |
|-----------------------|-------------------|------|--------------------------------|------------------|-----------------|------|------------------|------|--------------------------------|
| T16 | | | | | | | | | |
| Polished Glass | 10.54 | 0.69 | 1.88 | 74.22 | 0.21 | 1.65 | 0.44 | 9.78 | 0.59 |
| σ | 0.84 | 0.37 | 0.12 | 0.21 | 0.04 | 0.13 | 0.04 | 0.29 | 0.28 |
| Corroded Glass | 2.16 | 2.35 | 10.54 | 75.88 | 0.36 | 1.55 | 1.58 | 5.3 | 0.6 |
| σ | 0.59 | 0.07 | 0.33 | 0.33 | 0.15 | 0.25 | 0.12 | 0.65 | 0.42 |

The chemical composition of sample T16, that was determined by SEM/EDS, is shown on table 6.5. Silica content of the pristine glass of the sample 74.22wt%, values of Na₂O and CaO wt10.54% and wt9.75% respectively. Due to alkalis loss the concentration of Na₂O at the iridescent area dramatically decreased to 2.16 wt. %, Al₂O₃ values though increased at 10.54 wt%. An alumina- silica protective layer was formed, a typical type III corrosion surface formation. (Hench & Clark, 1978)

Examining the altered area using RBS technique (table 6.6) it is observed that the CaO at the first layer has 10 at% value. At the second layer and deeper to the studied area the CaO is decreased and valued 8-1 at%. The variation of the CaO confirmed the hypothesis of the formation of Type III surface. (Hench & Clark, 1978)

Table 5.8.6 Sample T 16 Ca profile with RBS

| Sample T16 layer | 1 | 2 | 3 | 4 | 5 |
|---|------|------|------|------|-------|
| Thickness (10 ¹⁵ at/cm ²) | 1400 | 1500 | 1500 | 3300 | 15000 |
| CaO | 10 | 6 | 6 | 8 | 1 |

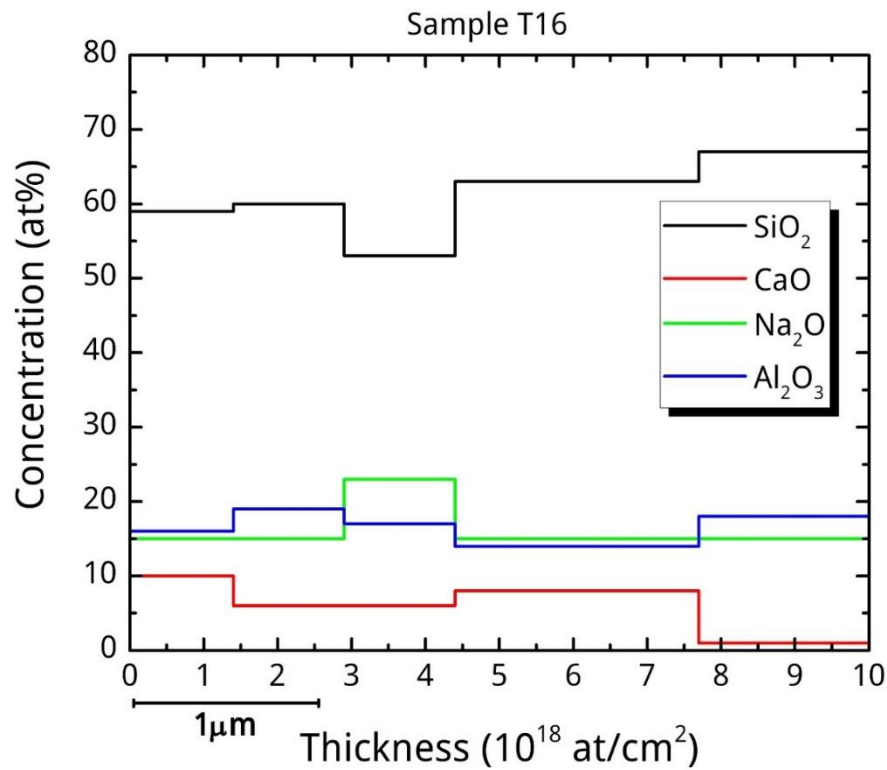


Figure 6.5 RBS Graph showing the concentration profile of sample T16

The Corrosion Patterns

Pitting is the corrosion pattern that was identified to the all examined samples, in this study. Even the lightly corroded green bead's samples, had pitting on their surface. Excessive pitting and crater formation was observed at the colorless glass samples and to the white and yellow decoration trails of the vessel samples. It was observed that the pitting most of the cases was formed in a pattern following the crafting lines of the object.

Iridescence was another corrosion pattern that was determined. The existence of thin flakes of few nanometers for the light corroded samples to thick flakes of 1µm was observed at the study. The vivid coloration that occurred was due to the iron oxidation. The mean value of iron at the polished glass was 0.68 wt. % and at the corroded areas was 1.33 wt. %.

The thickness of the *laminated* layers was associated to the alkalis loss and to technology production of the sample. For uneven surfaces the layers were thicker in comparison to surfaces without valleys or ridges. The *milky semi - opaque effect* that was observed was due to multiple layers, each of few dozen nanometers in thickness. Similar morphologies have been reported by Salviuolo, in a study of soda lime silica glass dated at early medieval. (2004, p. 301)

The polymerization of the glass in initial stage can be followed at longer leaching times, forming a hydrated silica-rich surface layer (Lynch, et al., 2007) . Sometimes it is referred as a gel layer. It was noticed in many of the samples. The hydrated silica layer was observed mostly at the vessels, though in some beads occurred under the iridescent layers. The formation of the gel layer is indication of an environment of high humidity. (Hench & Clark, 1978)

The Burial Environment

Soil from the excavation was not available for analysis, although the contamination of the samples from organic residues was taken into account. The beads have been buried among abundant layers of organic ashes from burnt bones (Palamara, et al., 2015).The presence of SO₃ has resulted in the inner – pristine and outer- corroded glass area of the beads. Since the samples have been buried inside a tomb, the development from outer to inner glass layers of SO₃, is an indication of contamination probably by organic residues. (Reiche, et al., 1999).

Natron which was the main ingredient both for vessels and beads, contains a small quantity of sodium sulfate. It is possible that the presence of sulfur at the samples, is resulted by natron addition and augmented by organic residues contamination.

7. Conclusions

In this study a collection consists of thirteen (13) colored beads and beads' fragments and three (3) fragments of core-formed vessels, was examined. The samples dated from Archaic to Hellenistic period and originated from mainland Greece, Thebes. The analytical methods that were applied are SEM- EDS, RBS and LED-OM.

Glass is a complex material and the corrosion mechanisms that occurred are even more complicated. Aim of this research is the observation of the corrosion patterns and its association to the complex interaction of composition, glass structure and exposure environment. The corrosion patterns that observed at this study are: iridescence, pitting and micro pitting, crust formation, craters, hollows, micro cracking network and semi-opaque effect caused by lamination.

The basic corrosion mechanism that was observed was the de alkalization. The concentration of calcium oxide influenced the alkali leaching. The molar percentage closer to 10% reduce the corrosion mechanism. The surface modifications caused by different shaping technologies also influenced the rate and extent of glass surface degradation. The lack of sleek surface increases the deterioration rate.

Using different analytical tools the corrosion depth for the vessels was determined to be around 15-20 μm and for slightly corroded glass beads around 5 μm . Clear statement for the colorant effect on the corrosion process did not result. A hypothesis that the addition of antimony in the glass, affect the homogeneity of the material and increase the deterioration rate was also stated. The hypothesis was based only to white trails and colorless beads, for yellow trails did not present strong correlations. Further studies need to done to ascertain if the hypothesis was indeed the case.

The development of the hydrated silica layer in the surface of the samples, is an indication of exposure to highly moisture environment. Evidence of sulfur oxides in higher

concentrations at the outer surface, is possible due to the contamination of the glass by organic residues.

Bibliography

- Ζαχαριάς, Ν. & Οικονόμου, Α., 2010. Γυαλιά: Η Φυσικοχημεία και η Παθολογία τους. In: Ν. Ζ. Ιωάννης Λυριτζής, ed. *ΑΡΧΑΙΟΛΟΓΙΚΑ*. Αθήνα: Εκδόσεις Παπαζήση,, pp. 123-143.
- Adams, P. B., 1984. Glass Corrosion. *Journal of Non-Crystalline Solids*, 64(4), pp. 193-205.
- Brill, R. H., 1992. Chemical analyses of some glasses from Frattesina. *Journal of Glass Studies* 34, pp. 11-22.
- Cagno, S. et al., 2011. Evaluation of manganese-bodies removal in historical stained glass windows via SR-m-XANES/XRF and SR-m-CT. *Anal. At. Spectrom*, Volume 26, p. 2442–2451.
- Corning Museum of Glass, n.d. *Corning Museum of Glass*. [Online]
Available at: <http://www.cmog.org/video/core-formed-vase-technique>
- Davinson, S., 2003. *Conservation and Restoration of Glass*. London: Butterworth Heinmann.
- Doremus, R. H., 1994. Chemical durability: Reaction of water with glass. *Glass Science* , pp. 215-240.
- El-Shamy, T. M., 1973a. The chemical durability of Na₂O–CaO–SiO₂ glasses. *Physics and Chemistry of Glasses*, Volume 14, pp. 1-5.
- El-Shamy, T. M. & Douglas, R. W., 1972. Kinetics of the reaction of water with glass. *Glass Technology*, p. 77–80.
- Freestone, I. C., 1991. Looking into glass. In: S. Bowman, ed. *Science and the Past*. London: British Museum Press, pp. 37-56.
- Hench, L. & Clark, D. E., 1978. Physical chemistry of glass surfaces. *Journal of Non-Crystalline Solids*, Volume 28, p. 83–105.
- Henderson, J., 2000. *The science and archaeology of materials: on investigation of inorganic materials*. 1st ed. London: Routledge.
- Ignatiadou, D. & Antonaras, A., 2008. *A Greek- English, English- Greek Dictionary*. 1st ed. Thessaloniki: Center of Greek Language.
- Ingram, R. S., 2005. *Faience and Glass Beads from the Late Bronze Age Shipwreck at Uluburn, Texas*: Texas A&M University.
- Jackson, C. M., Greenfield, D. & Howie, L. A., 2012. An assessment of compositional and morphological changes in model archaeological glasses in acid burial matrix. *Archaeometry*, Volume 54, p. 489–507.
- Kiicikerman, O., 1995. Anatolian glass beads: the final traces of three millennia of glassmaking in the Mediterranean region.. *Studies in Technology and Culture*, Volume 2, pp. 97 - 102.

- Kontou, H. K., Kotzamanh, D. D. & Lampropoulos, B., 1995. *Γυαλί, Τεχνολογία και Διαβρωση*. Athens: Independent.
- Lambert, J. B., 1997. *Traces of the Past: unravelling the secrets of archaeology through chemistry*. Massachusetts: helix Books / Addison-Wesley.
- Lierke, R., 1992. Early history of Lampwork-Some facts, findings and theories. Teil 2: Fire or flame; Lampworking techniques in antiquity. *Glastechnische Berichte*, Volume 65, pp. 331-348.
- Lucas, A. & Harris, J. R., 1962. *Ancient Egyptian Materials and Industries*. 4th Edition ed. London.: s.n.
- Lynch, M. E., Folz, D. C. & Clark, D. E., 2007. Use of FTIR reflectance spectroscopy to monitor corrosion mechanisms on glass surfaces. *Journal of Non- Crystalline Solids*, Volume 353, pp. 2667-2674.
- Oikonomou, A., Beltsios, K. & Zacharias, N., 2012. *Analytical and technological study of an ancient glass collection from Thebes, Greece: An overall assessment*. Thessaloniki, s.n., pp. 75-80.
- Palamara, E. et al., 2015. *Spectroscopic Study of a Historical Glass Collection from Thebes, Greece, by Raman and IR*. United Kingdom, British Archaeological Reports Ltd.
- Reiche, I. et al., 1999. Trace element composition of archaeological bones and postmortem alteration in the burial environment. *Nuclear Instruments and Methods in Physics Research*, 150(B), pp. 656-662.
- Salviulo, G., Silvestri, A., Molin, G. & Bertocello, R., 2004. An archaeometric study of the bulk and surface weathering characteristics of Early Medieval (5th–7th century) glass from the Po valley, northern Italy. *Journal of Archaeological Science*, Volume 31, p. 295–306.
- Sayre, E. & Smith, R., 1965. Compositional Categories of Ancient Glass. *SCIENCE, VOL. 133*, pp. 1824-1826.
- Schalm, O. et al., 2011. manganese staining of archaeological glass: the characterization of Mn rich inclusions in leaches layers and a hypothesis of its formation. *Archaeometry*, Volume 53, pp. 103-122.
- Semenov, N. I., Paplauskas, A. B. & Ryabov, V., 1972. Effect of surface microstructure on the strength of glass. *Glass Technology*, 13(6), p. 171–5.
- Sharma, A. K., 2014. NPTEL. [Online]
Available at: <http://nptel.ac.in/courses/102103047/module6/lec34/1.html>
[Accessed 16 October 2014].
- Stern, M. E. & Schlick-Nolte, B., 1994. Early Glass of the Ancient World 1600BC- AD 50. *Ostfildern: Verlag Gerd Hatje.*, p. 20.
- Triantafyllidis, P., 1998. *Τα γυάλινα αντικείμενα από την Μινώα Αμοργού. Συμβολή στη μελέτη της υαλοουργίας στις Κυκλάδες κατά την Ελληνιστική και Ρωμαϊκή περίοδο*, Ioannina: s.n.
- Voggel, W., 1994. *Glass Chemistry*. Second Edition ed. Berlin: Springer-Verlag..
- Yuryeva, T. V. & Yurev, V. A., 2014. Degradation and destruction of historical blue green glass beads: A study using microspectroscopy of light transmission. *Journal of optics*, Volume 16, pp. 1-7.

Zacharias, N. et al., 2008. Solid-state luminescence for the optical examination of archaeological glass beads. *Optical Materials*, Volume 30, pp. 1127-1133.

Zacharias, N., 2015. *Lecture*. Kalamata: University of Peloponnese.

Λυριντζής, Ι., 2007. *Φυσικές επιστήμες στην αρχαιολογία*. δεύτερη ed. Αθήνα: τυπωθήτω.

Οικονόμου, Α., 2012. *Μελέτη αρχαίων υάλων και εφουαλωμάτων του ελλαδικού χώρου*, Ιωάννινα: s.n.

8. Appendix

8.1. The Analytical Data of the Beads

Table 8.1.1 EDS compositional analysis of major elements of green glass beads. The standard deviation (σ) is presented for each sample n.d.: not determined.

| Sample | Na ₂ O | MgO | Al ₂ O ₃ | SiO ₂ | SO ₃ | Cl ₂ O | K ₂ O | CaO | Fe ₂ O ₃ |
|-------------|-------------------|------|--------------------------------|------------------|-----------------|-------------------|------------------|-------|--------------------------------|
| T1 polished | 12.81 | 0.58 | 0.36 | 73.32 | 0.35 | 0.99 | 0.14 | 10.64 | 0.82 |
| σ | 0.53 | 0.12 | 0.02 | 0.47 | 0.21 | 0.1 | 0.13 | 0.33 | 0.16 |
| T1 corroded | 7.76 | 0.46 | 1.69 | 70 | 0.68 | 1.62 | 1.16 | 14.4 | 2.24 |
| σ | 2.14 | 0.08 | 1.53 | 3.57 | 0.66 | 0.5 | 0.45 | 1.77 | 1.82 |
| T2 polished | 12.55 | 0.42 | 0.46 | 73.6 | 1.06 | 0.18 | 10.51 | 0.97 | 0.25 |
| σ | 0.27 | 0.19 | 0.23 | 0.51 | 0.09 | 0.08 | 0.38 | 0.18 | 0.17 |
| T2 corroded | 13.04 | 0.51 | 0.73 | 73.86 | 0.5 | 1.02 | 0.44 | 9.08 | 0.81 |
| σ | 0.24 | 0.23 | 0.07 | 0.57 | 0.14 | 0.1 | 0.21 | 0.69 | 0.3 |

Table 8.1.2 EDS compositional analysis of major elements of dark blue glass beads. The standard deviation (σ) is presented for each sample n.d.: not determined

| Sample | Na ₂ O | MgO | Al ₂ O ₃ | SiO ₂ | SO ₃ | Cl ₂ O | K ₂ O | CaO | MnO | Fe ₂ O ₃ | CoO | CuO |
|---------------|-------------------|------|--------------------------------|------------------|-----------------|-------------------|------------------|------|------|--------------------------------|------|------|
| T11 polished | 13.63 | 0.55 | 2.25 | 73.39 | 0.41 | 1.31 | 0.46 | 7.29 | n.d. | 0.51 | 0.21 | n.d. |
| σ | 0.65 | 0.11 | 0.05 | 0.43 | 0.21 | 0.19 | 0.08 | 0.16 | - | 0.05 | 0.17 | - |
| T11 corroded | 3.24 | 0.9 | 3.84 | 78.87 | 0.74 | 1.40 | 1.1 | 2.45 | n.d. | 7.98 | 0.45 | n.d. |
| σ | 0.27 | 0.18 | 0.3 | 1.57 | 0.48 | 0.49 | 0.33 | 0.3 | - | 0.45 | 0.3 | - |
| T50 polished | 16.29 | 0.88 | 1.98 | 75.23 | n.d. | 0.84 | n.d. | 3.53 | 0.14 | 0.24 | n.d. | n.d. |
| σ | 0.43 | 0.41 | 0.07 | 2.18 | - | 0.12 | 0.93 | - | 0.2 | 0.23 | - | - |
| T 50 corroded | 8.8 | 0.94 | 3.72 | 73.6 | 0.59 | 1.56 | 1.01 | 6.92 | n.d. | 1.92 | n.d. | 1.09 |
| σ | 3.23 | 0.84 | 3.29 | 1.76 | 0.1 | 0.22 | 0.61 | 2.2 | - | 0.41 | - | 0.49 |

Table 8.1.3 EDS compositional analysis of major elements of light blue glass beads. The standard deviation (σ) is presented for each sample n.d.: not determined

| Sample | Na ₂ O | MgO | Al ₂ O ₃ | SiO ₂ | SO ₃ | Cl ₂ O | K ₂ O | CaO | TiO ₂ | Fe ₂ O ₃ | CoO | CuO | Sb |
|---------------------|-------------------|------|--------------------------------|------------------|-----------------|-------------------|------------------|------|------------------|--------------------------------|------|------|------|
| T31 polished | 15.46 | 0.56 | 2.7 | 72.35 | 0.55 | 1.01 | 0.36 | 6.06 | n.d. | 0.26 | n.d. | 0.73 | n.d. |
| σ | 0.14 | 0.1 | 0.16 | 0.71 | 0.12 | 0.12 | 0.03 | 0.08 | - | 0.09 | - | 0.62 | - |
| T31 corroded | 7.03 | 2.52 | 6.04 | 70.04 | 1.77 | 1.26 | 3.03 | 6.35 | n.d. | 1.2 | n.d. | 0.79 | n.d. |
| σ | 0.98 | 2.08 | 1.26 | 1.21 | 0.66 | 0.04 | 0.76 | 0.86 | - | 0.54 | - | 0.01 | - |
| T11 polished | 12.15 | 0.52 | 1.8 | 71.79 | 0.67 | 1.04 | 0.44 | 7.78 | 0.23 | 0.32 | 0.28 | 1.67 | 1.59 |
| σ | 0.74 | 0.13 | 0.33 | 0.51 | 0.05 | 0.1 | 0.09 | 0.39 | 0.11 | 0.08 | 0.04 | 0.27 | 0.36 |
| T11 corroded | 1.31 | 3.62 | 3.86 | 81.4 | 0.82 | 0.61 | 0.88 | 2.83 | 0.25 | 0.59 | n.d. | 2.71 | 1.27 |
| σ | 0.24 | 1.15 | 0.06 | 0.08 | 0.46 | 0.02 | 0.06 | 0.04 | 0.24 | 0.38 | - | 0.59 | 0.71 |

Table 8.1.4 EDS compositional analysis of major elements of colorless glass beads. The standard deviation (σ) is presented for each sample n.d.: not determined

| Sample | Na ₂ O | MgO | Al ₂ O ₃ | SiO ₂ | SO ₃ | Cl ₂ O | K ₂ O | CaO | TiO ₂ | Fe ₂ O ₃ | Sb |
|---------------------|-------------------|------|--------------------------------|------------------|-----------------|-------------------|------------------|------|------------------|--------------------------------|------|
| T15 polished | 0.88 | 0.49 | 2.8 | 82.99 | n.d. | 0.58 | 1.32 | 8.74 | n.d. | 0.54 | 1.65 |
| σ | 0.17 | 0.21 | 0.27 | 1.55 | - | 0.09 | 0.09 | 0.94 | - | 0.24 | 0.54 |
| T15 corroded | 1.98 | 2.33 | 4.24 | 80.87 | n.d. | 0.67 | 2.32 | 4.74 | n.d. | 0.7 | 2.15 |
| σ | 0.39 | 0.61 | 0.87 | 7.54 | - | 0.29 | 0.93 | 4.75 | - | 0.34 | 2.01 |
| T26 polished | 15.34 | 0.51 | 2.29 | 71.49 | 0.46 | 1.01 | 0.83 | 7.13 | 0.27 | 0.25 | 0.9 |
| σ | 0.2 | 0.07 | 0.21 | 0.26 | 0.15 | 0.17 | 0.21 | 0.21 | 0.13 | 0.05 | 0.04 |
| T26 corroded | 0.7 | 2.03 | 9.65 | 78.43 | 0.48 | 0.18 | 0.62 | 4.95 | 1.35 | 2.31 | n.d. |
| σ | 0.2 | 0.28 | 1.9 | 2.83 | 0.15 | 0.08 | 0.23 | 0.48 | 0.7 | 1.13 | - |

Table 8.1.5 EDS compositional analysis of major elements of brown glass beads. The standard deviation (σ) is presented for each sample n.d.: not determined

| Sample | Na ₂ O | MgO | Al ₂ O ₃ | SiO ₂ | SO ₃ | Cl ₂ O | K ₂ O | CaO | Fe ₂ O ₃ |
|---------------------|-------------------|------|--------------------------------|------------------|-----------------|-------------------|------------------|------|--------------------------------|
| T16 polished | 10.54 | 0.69 | 1.88 | 74.22 | 0.21 | 1.65 | 0.44 | 9.78 | 0.59 |
| σ | 0.84 | 0.37 | 0.12 | 0.21 | 0.04 | 0.13 | 0.04 | 0.29 | 0.28 |
| T16 corroded | 2.16 | 2.35 | 10.54 | 75.88 | n.d. | 1.55 | 1.58 | 5.3 | 0.9 |
| σ | 0.59 | 0.07 | 0.33 | 0.33 | - | 0.25 | 0.12 | 0.65 | 0.42 |
| T45 polished | 15.45 | 0.79 | 1.89 | 72.11 | 0.69 | 1.25 | 0.74 | 6.66 | 0.44 |
| σ | 0.4 | 0.15 | 0.08 | 0.23 | 0.36 | 0.07 | 0.3 | 0.13 | 0.2 |
| T45 corroded | 1.39 | 2.4 | 11.81 | 79.27 | n.d. | 0.15. | 0.39 | 3.72 | 0.80 |
| σ | 0.17 | 0.34 | 0.59 | 0.55 | - | 0.12 | 0.07 | 0.27 | 0.4 |

Table 8.1.6 EDS compositional analysis of major elements of black glass beads. The standard deviation (σ) is presented for each sample n.d.: not determined

| Sample | Na ₂ O | MgO | Al ₂ O ₃ | SiO ₂ | SO ₃ | Cl ₂ O | K ₂ O | CaO | Fe ₂ O ₃ |
|---------------------|-------------------|------|--------------------------------|------------------|-----------------|-------------------|------------------|-------|--------------------------------|
| T22 polished | 13.16 | 0.57 | 0.64 | 73.25 | 0.27 | 1.45 | 0.17 | 8.66 | 1.84 |
| σ | 1.51 | 0.03 | 0.28 | 0.63 | 0.26 | 0.21 | 0.17 | 0.62 | 0.03 |
| T16 corroded | 9.04 | 0.78 | 0.82 | 75.3 | 0.49 | 1.54 | 0.41 | 8.88 | 0.37 |
| σ | 2.26 | 0.16 | 0.11 | 0.54 | 0.13 | 0 | 0.06 | 1.32 | 0.12 |
| T45 polished | 13.36 | 0.51 | 0.79 | 72.43 | 0.41 | 1.16 | 0.19 | 9.04 | 2.07 |
| σ | 0.79 | 0.15 | 0.14 | 0.29 | 0.11 | 0.03 | 0.09 | 0.26 | 0.19 |
| T45 corroded | 4.95 | 1.94 | 3.03 | 69.88 | 0.98 | 1.31 | 1.26 | 13.65 | 2.21 |
| σ | 2.17 | 1.57 | 2.21 | 9.75 | 0.51 | 0.15 | 0.57 | 5.45 | 0.55 |

Table 8.1.77EDS compositional analysis of major elements the white glass bead. The standard deviation (σ) is presented for each sample n.d.: not determined

| Sample | Na ₂ O | MgO | Al ₂ O ₃ | SiO ₂ | SO ₃ | Cl ₂ O | K ₂ O | CaO | Fe ₂ O ₃ | Sb |
|----------------------------|-------------------|------|--------------------------------|------------------|-----------------|-------------------|------------------|-------|--------------------------------|------|
| T54 polished | 8.04 | 0.29 | 2.11 | 69.87 | 0.62 | 1.16 | 0.86 | 10.94 | n.d. | 6.09 |
| σ | 1.03 | 0.08 | 0.39 | 0.74 | 0.41 | 0.16 | 0.12 | 0.69 | - | 0.26 |
| T54 corroded | 6.02 | 1.63 | 6.58 | 68.84 | 1.16 | 1.84 | 2.12 | 8.48 | 0.6 | 2.78 |
| σ | 2.6 | 0.23 | 0.01 | 3 | 0.5 | 1 | 1.22 | 2.89 | 0.06 | 0.32 |

8.2. The Analytical Data of The Core Formed Vessels

Table 8.2.1Table 8. EDS compositional analysis of major elements of the blue glass areas of core formed vessels.n.d. not determined

| Sample | Na ₂ O | MgO | Al ₂ O ₃ | SiO ₂ | SO ₃ | Cl ₂ O | K ₂ O | CaO | Fe ₂ O ₃ | Sb |
|------------------------|-------------------|------|--------------------------------|------------------|-----------------|-------------------|------------------|------|--------------------------------|------|
| Man 1 Pristine | 19.63 | 0.47 | 2.15 | 65.78 | 0.5 | 0.83 | 0.27 | 7.4 | 0.43 | 2.62 |
| Man 1 corroded | 0.54 | 2.14 | 0.38 | 3.34 | 0.36 | 1.11 | 0.85 | 1.06 | 0.85 | n.d. |
| Man 7 Pristine | 17.19 | 0.33 | 2.50 | 73.22 | n.d. | 1.56 | 0.21 | 5.00 | n.d. | n.d |
| Man 7 corroded | 1.12 | 1 | 3.81 | 82.49 | n.d. | 0.89 | 1.03 | 6.05 | n.d. | 6.05 |
| Man 11 Pristine | 7.76 | 0.42 | 2.36 | 70.16 | 0.40 | 1.29 | 0.32 | 6.54 | 0.76 | n.d. |
| Man 11 corroded | 1.26 | 0.82 | 2.83 | 87.11 | n.d. | 1.04 | 1.42 | 5.53 | n.d. | n.d. |

Table 8.2.2 1Table 8. EDS compositional analysis of major elements of the yellow glass areas of core formed vessels.n.d. not determined

| Sample | Na ₂ O | MgO | Al ₂ O ₃ | SiO ₂ | Cl ₂ O | K ₂ O | CaO | Fe ₂ O ₃ | Sb | Pb |
|-----------------------|-------------------|------|--------------------------------|------------------|-------------------|------------------|------|--------------------------------|-------|-------|
| Man 1 pristine | 16.66 | 0.69 | 1.00 | 59.94 | 0.69 | 0.32 | 3.80 | n.d. | 2.22 | 14.67 |
| Man 1 corroded | 1.77 | 0.71 | 6.60 | 69.22 | 1.28 | 3.98 | 2.85 | 2.82 | 4.14 | 6.63 |
| Man 7 pristine | 17.42 | 0.60 | 1.61 | 60.52 | 0.62 | 0.28 | 4.55 | n.d. | 14.40 | 17.42 |
| Man 7 corroded | 0.89 | 1.06 | 3.61 | 75.19 | 1.06 | 1.24 | 2.72 | 2.4 | 7.93 | 3.92 |

Table 8.2.3 EDS compositional analysis of major elements of the white glass areas of core formed vessels.n.d. not determined

| Sample | Na ₂ O | MgO | Al ₂ O ₃ | SiO ₂ | SO ₃ | Cl ₂ O | K ₂ O | CaO | Fe ₂ O ₃ | Sb |
|--------------------|-------------------|------|--------------------------------|------------------|-----------------|-------------------|------------------|------|--------------------------------|-------|
| Man 7 pristine | 17.47 | n.d | 2.40 | 64.80 | 0.97 | 1.30 | 0.36 | 6.90 | 0.55 | 5.25 |
| Man 7 corroded | 0.36 | 1.2 | 3.11 | 79.03 | n.d. | n.d. | 0.75 | 3.7 | n.d. | 11.85 |
| Man11 pristine | 17.67 | 0.54 | 1.32 | 64.80 | 0.61 | 1.74 | 0.36 | 7.17 | 0.50 | 5.55 |
| Man 11 corroded | 0.83 | 0.56 | 6.87 | 69.84 | n.d. | | 2.49 | 4.59 | | 14.83 |

8.3. Line Scanning Data

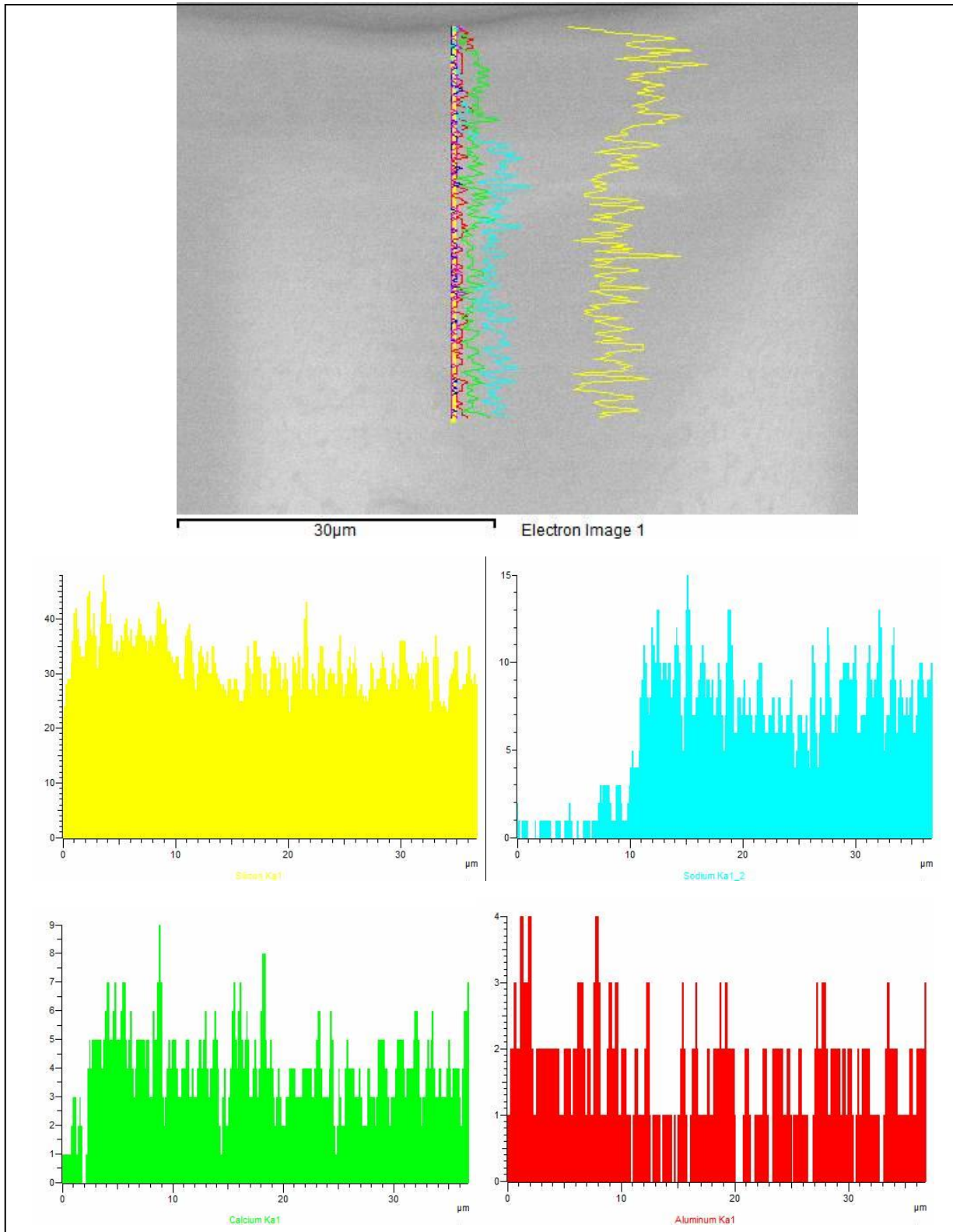
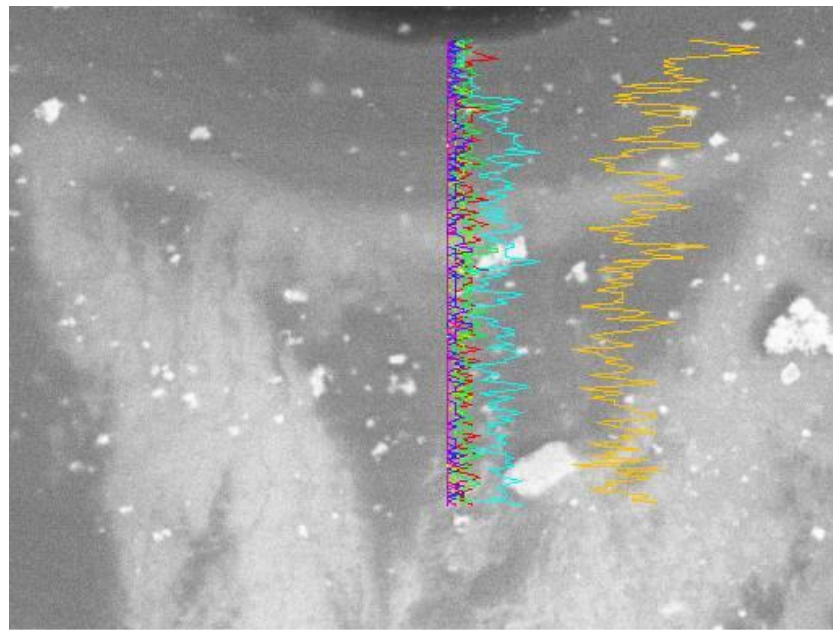
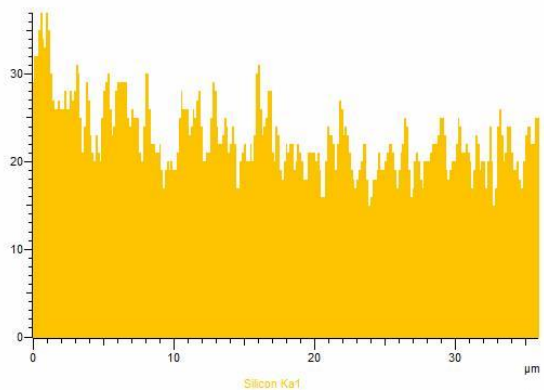


Figure 8.1Man 1 Blue area line scanning

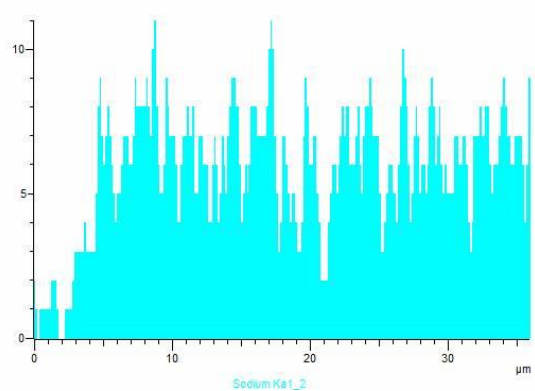


30µm

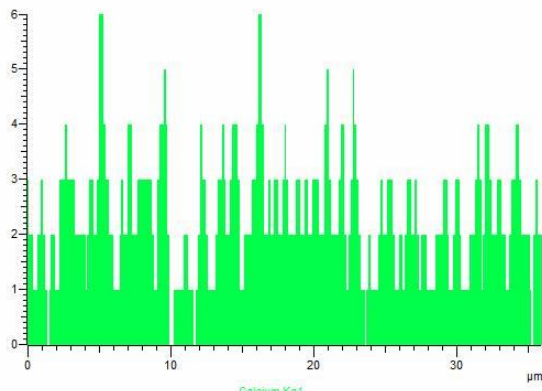
Electron Image 1



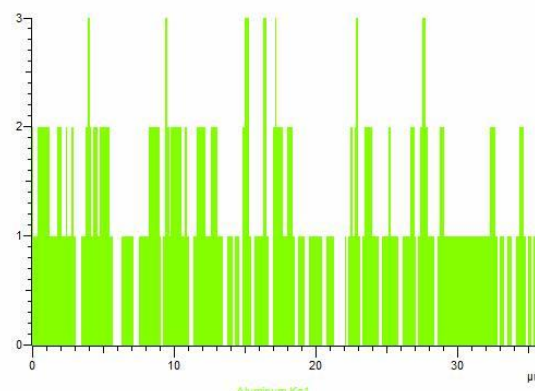
Silicon Ka1



Sodium Ka1_2



Calcium Ka1



Aluminum Ka1

Figure 8.2 Man 1 yellow area line scanning

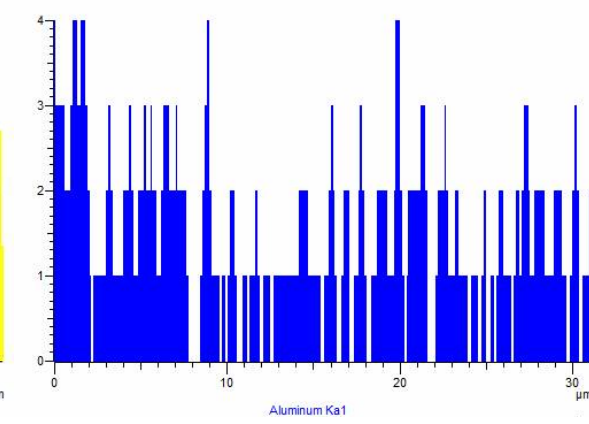
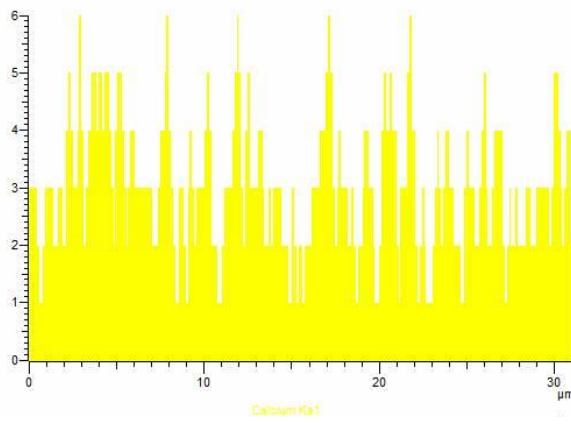
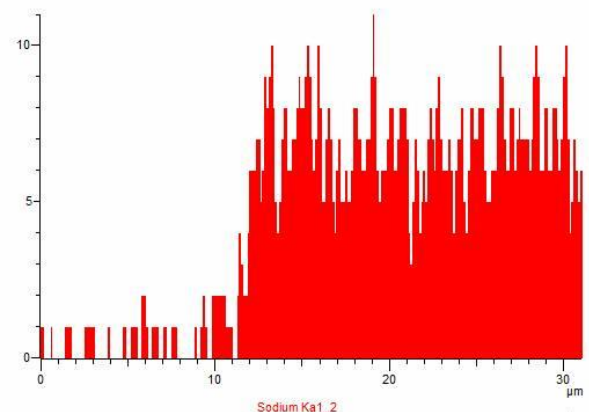
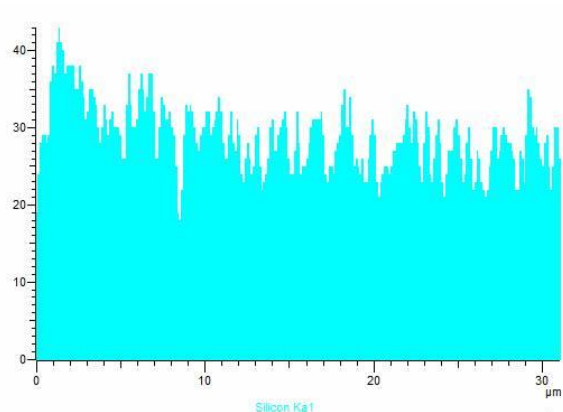
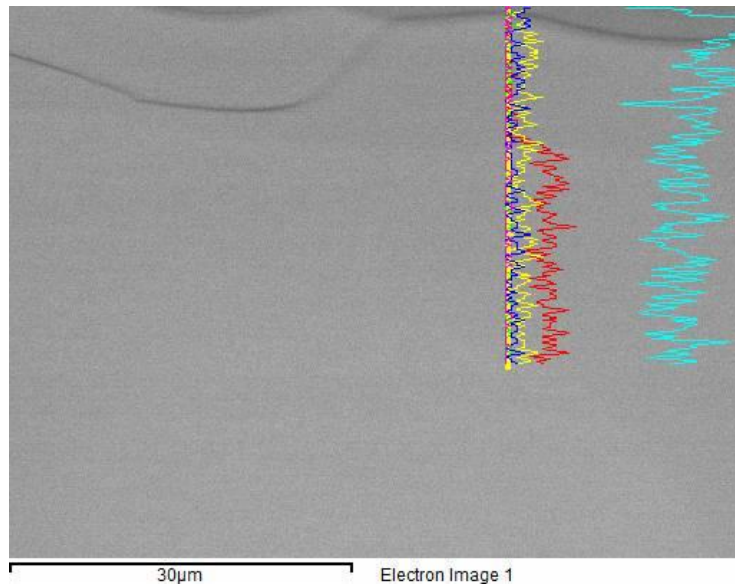
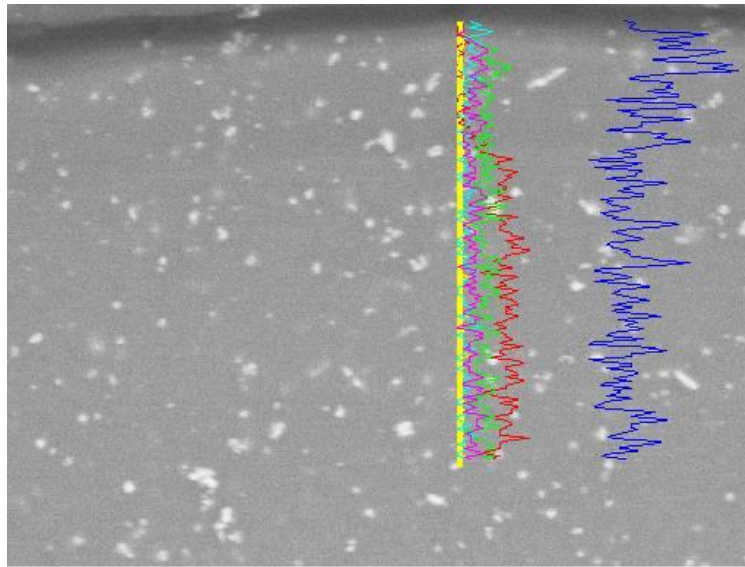
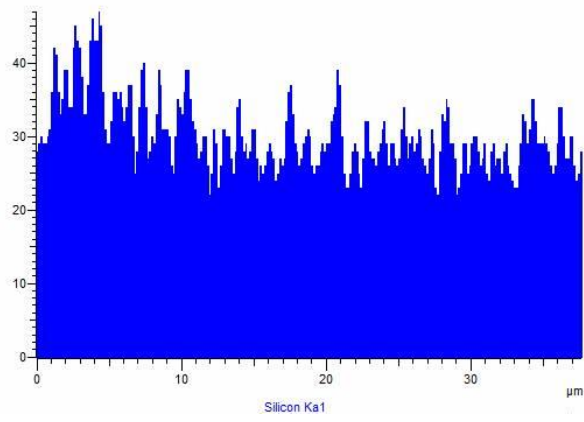


Figure 8.3Man 11 blue area line scanning

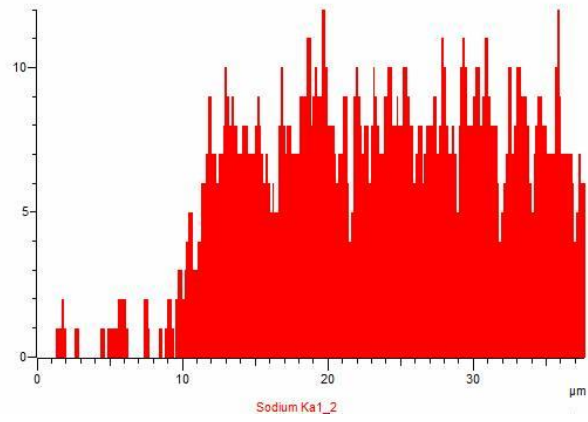


30µm

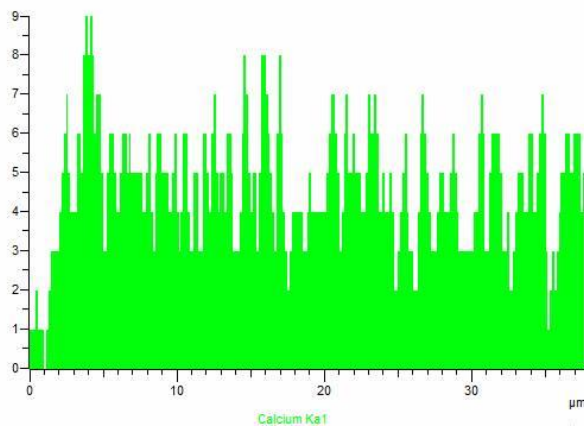
Electron Image 1



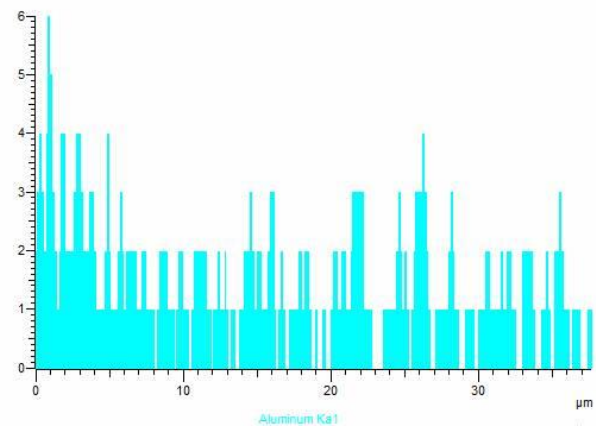
Silicon Ka1



Sodium Ka1_2



Calcium Ka1



Aluminum Ka1

Figure 8.4 Figure 8.3 Man 11 white area line scanning

8.4. Graphs of Concentration profiles by RBS

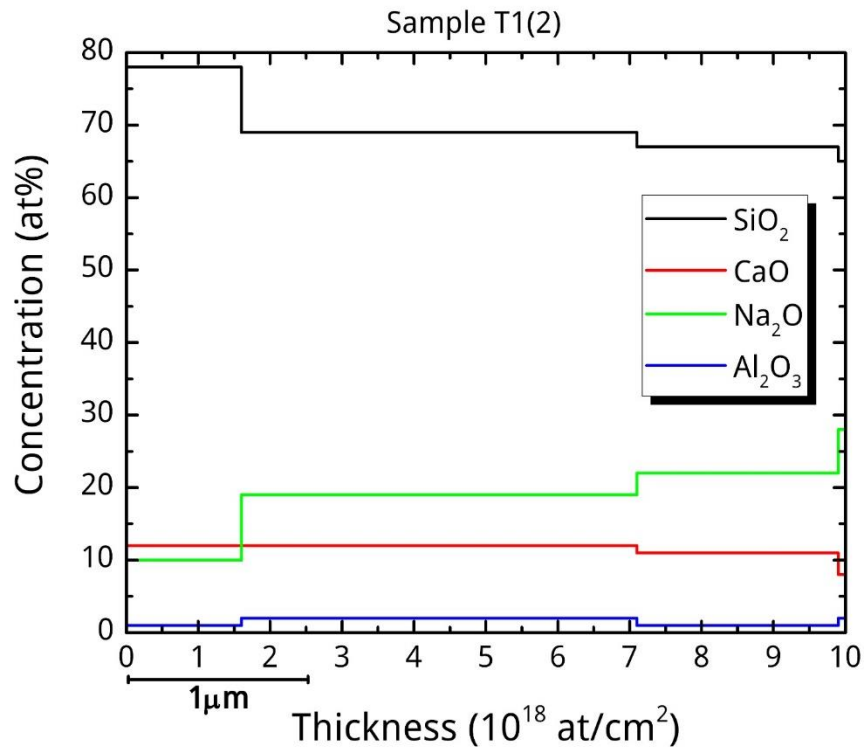


Figure 8.5 Concentration profile for sample T1 by RBS

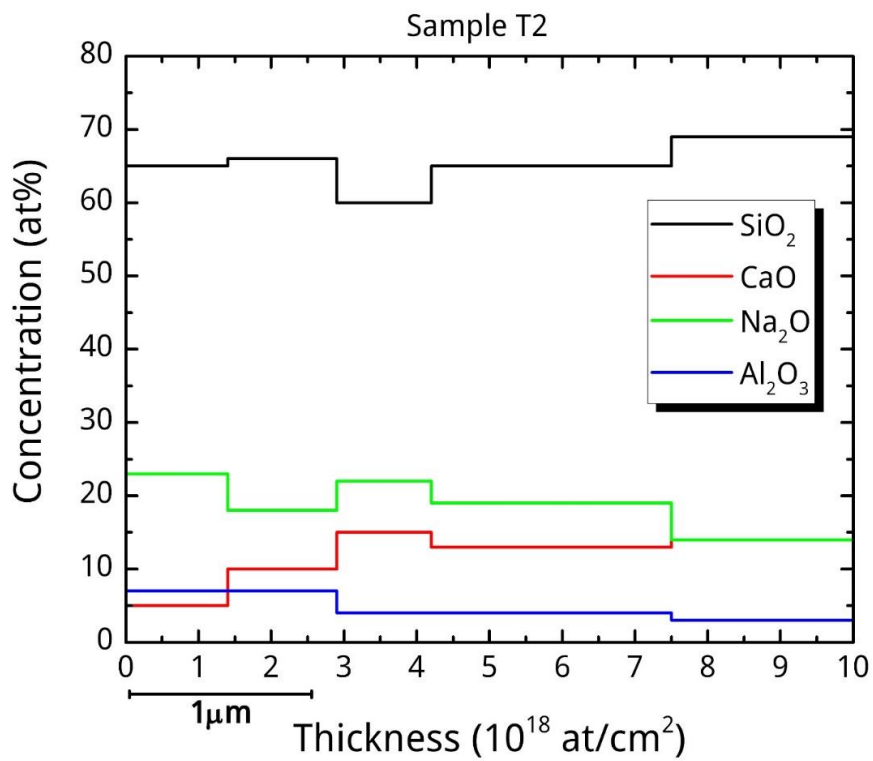


Figure 8.6 Concentration profile for sample T2 by RBS

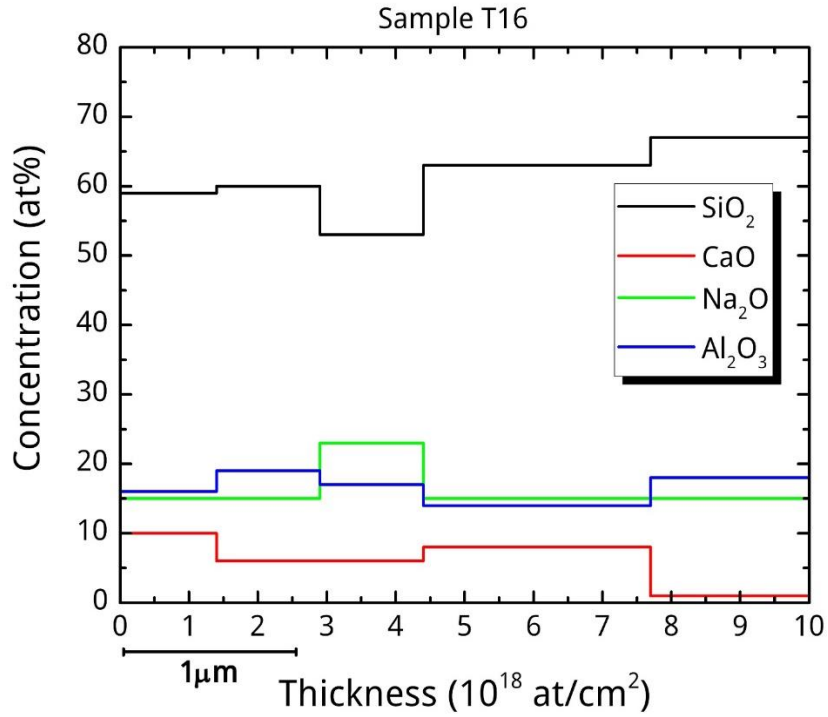


Figure 8.7 Concentration profile for sample T16 by RBS

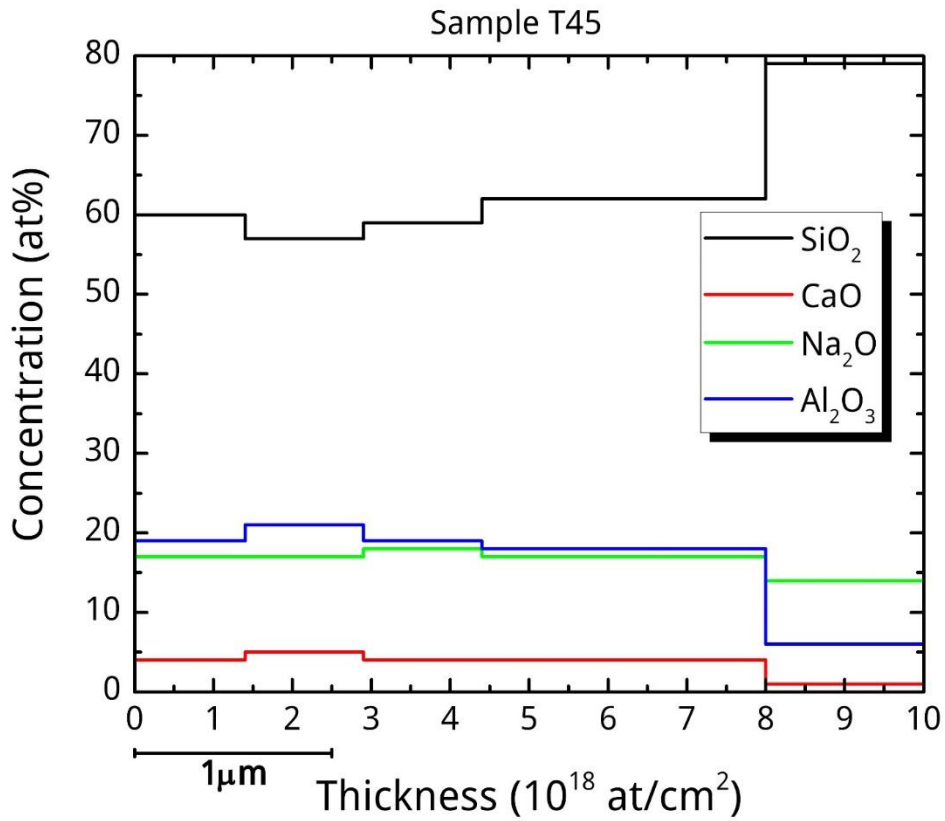


Figure 8.8 Concentration profile for sample T45 by RBS